DEVELOPMENT OF SUPRAMOLECULAR STRUCTURED
BENZOXAZINE DIMERS AND THEIR POTENTIAL APPLICATIONS

Miss Choltirosn Sutapin

A Dissertation Submitted in Partial Fulfillment of the Requirements
for the Degree of Doctor of Philosophy Program in Nanoscience and Technology
(Interdisciplinary Program)
Graduate School
Chulalongkorn University
Academic Year 2016
Copyright of Chulalongkorn University

การพัฒนาโครงสร้างซุปปราโมเลกุลเบนซอกซาซีนไดเมอร์และการนำไปประยุกต์ใช้

นางสาวชลธิรศน์ สุเทปิน

วิทยานิพนธ์นี้เป็นส่วนหนึ่งของการศึกษาตามหลักสูตรปริญญาวิทยาศาสตรดุษฎีบัณฑิต
สาขาวิชาวิทยาศาสตร์นาโนและเทคโนโลยี (สหสาขาวิชา)
บัณฑิตวิทยาลัย จุฬาลงกรณ์มหาวิทยาลัย
ปีการศึกษา 2559

Thesis Title   DEVELOPMENT OF SUPRAMOLECULAR STRUCTUREDBENZOXAZINE DIMERS AND THEIR POTENTIAL APPLICATIONS

By   Miss Choltirosn Sutapin

Field of Study   Nanoscience and Technology

Thesis Advisor   Professor Suwabun Chirachanchai, Ph.D.

Accepted by the Graduate School, Chulalongkorn University in Partial Fulfillment of the Requirements for the Doctoral Degree

.... Dean of the Graduate School
(Associate Professor Sunait Chutintaranond, Ph.D.)

THESIS COMMITTEE

.... Chairman
(Associate Professor Vudhichai Parasuk, Ph.D.)

.... Thesis Advisor
(Professor Suwabun Chirachanchai, Ph.D.)

.... Examiner
(Ratthapol Rangkupan, Ph.D.)

.... Examiner
(Associate Professor Voravee Hoven, Ph.D.)

.... External Examiner
(Associate Professor Apirat Laobuthee, Ph.D.)

.... External Examiner
(Associate Professor Yun Yan, Ph.D.)

ชลธิรศน์ สุเทปิน : การพัฒนาโครงสร้างซุปปราโมเลกุลเบนซอกซาซีนไดเมอร์และการนำไป
ประยุกต์ใช้ (DEVELOPMENT OF SUPRAMOLECULAR STRUCTUREDBENZOXAZINE
DIMERS AND THEIR POTENTIAL APPLICATIONS) อ.ที่ปรึกษาวิทยานิพนธ์หลัก: สุวบุญ
จิรชาญชัย, 102 หน้า.

วิทยานิพนธ์ฉบับนี้มุ่งเน้นไปที่การออกแบบและการพัฒนาโครงสร้างเบนซอกซาซีนไดเมอร์เพื่อการ
นำไปประยุกต์ใช้ โดยในส่วนแรกโมเลกุลเบนซอกซาซีนไดเมอร์ถูกเตรียมด้วยวิธีการที่ง่ายและมีความจำเพาะ
ผ่านการเปิดวงเบนซอกซาซีน โมเลกุลเบนซอกซาซีนไดเมอร์เหล่านี้ทำหน้าที่ทั้งเป็นตัวเร่งและตัวริเริ่มปฏิกิริยา
ในพอลิเมอไรเซชั่นแบบเปิดวงแลคไทด์ ไฮดรอกซิลของเบนซอกซาซีนไดเมอร์ถูกกระตุ้นด้วยตัวเร่งปฏิกิริยา
อินทรีย์เพื่อเป็นสารริเริ่ม การปรับเปลี่ยนหมู่เมทิลีนทำให้สามารถบ่งชี้ลิแกนด์ที่ใช้งานได้ดีในการเกิด
สารประกอบเชิงซ้อนกับแอลคิลหรือแอลคอกไซด์อะลูมิเนียม สารประกอบเชิงซ้อนนี้ได้รับการพิสูจน์ทราบถึง
การเป็นตัวเร่งปฏิกิริยาในพอลิเมอไรเซชันแบบเปิดวงแลคไทด์ พอลิแลคไทด์ถูกพอลิเมอไรด้วยดัชนีการกระจาย
ตัวที่แคบและควบคุมน้ำหนักโมเลกุลได้ดี ในส่วนที่สองเป็นครั้งแรกในการแสดงฟิล์มพอลิแลคติกแอซิดที่เปลี่ยน
สีตามอุณหภูมิ ด้วยการสร้างเบนซอกซาซีนสีแขนจากเพ็นตะอีริทริทอล ตามด้วยการเปิดวงแลคไทด์ที่ถูกประตุ้
นด้วยตัวเร่งปฏิกิริยาอินทรีย์ จากนั้นคอนจูเกชัน ไดอะเซทิลีนเพื่อให้ได้พอลิแลคติกแอซิดแปดแขนที่ถูกคอนจูเกท
ด้วยไดอะเซทิลีน การผสมกับเม็ดเรซินพอลิแลคติกแอซิดตามด้วยการหล่อแบบตัวทำละลายนำไปสู่ฟิล์มเปลี่ยนสี
ตามอุณหภูมิที่สามารถย้อนกลับได้ ในการศึกษาเปรียบเทียบพบว่าไดอะเซทิลีนและพอลิแลคติกแอซิดที่ถูกคอนจู
เกทด้วยไดอะเซทิลีนแบบเส้นตรง สี่แขน และหลายแขน ไม่แสดงสมบัติเปลี่ยนสีดังกล่าว การวิเคราะห์โครงสร้าง
จุลภาคบ่งชี้โครงสร้างสมมาตรแปดแขนควบคุมการเรียงตัวของพอลิไดอะเซทิลีนในเมทริกซ์พอลิแลคติคแอซิด
ขณะร้อนและเย็น นำไปสู่การเคลื่อนตัวของสายโซ่พอลิแลคติคแอซิดและพอลิไดอะเซทิลีนที่ต่ำ จากงานทั้งสอง
ชิ้นนี้ทำให้สามารถกล่าวได้ว่าเบนซอกซาซีนไดเมอร์เป็นหนึ่งในตัวเลือกสำหรับสังเคราะห์รูปดาวหรือแขนพอลิ
แลคไทด์ ในส่วนสุดท้ายงานวิจัยครอบคลุมถึงกระบวนการที่เหมาะสม เป็นมิตรต่อสิ่งแวดล้อม และง่ายเพื่อ
สังเคราะห์เบนซิมิดาโซลผ่านการปิดวงระหว่างอนุพันธ์แอลดีไฮด์และฟีนิลีนไดเอมีนภายใต้การลดแรงดัน
กระบวนการสังเคราะห์นี้ไม่เพียงแต่ให้เบนซิมิดาโซลที่ผลผลิตสูงแต่การเลือกแอลดีไฮด์และฟีนิลีนไดเอมีนที่มี
หมู่ฟังก์ชันที่พร้อมเกิดปฏิกิริยา นำไปสู่สารตั้งต้นสำหรับการสังเคราะห์เบนซอกซาซีนไดเมอร์แบบใหม่ที่
ตอบสนองต่อค่าความเป็นกรด-ด่าง และการเปล่งแสงหลากหลายสี

สาขาวิชา   วิทยาศาสตร์นาโนและเทคโนโลยี   ลายมือชื่อนิสิต _____

ปีการศึกษา 2559   ลายมือชื่อ อ.ที่ปรึกษาหลัก _____

5487839420 : MAJOR NANOSCIENCE AND TECHNOLOGY

KEYWORDS: BENZOXAZINE DIMER / LACTIDE RING-OPENING POLYMERIZATION / DIACETYLENE / METAL-LIGAND COMPLEX / INITIATOR / THERMOCHROMIC / FREE-STANDING FILM / BENZIMIDAZOLE / PH-SENSITIVE FLUORESCENT / MULTICOLOR EMISSION

CHOLTIROSN SUTAPIN: DEVELOPMENT OF SUPRAMOLECULAR STRUCTUREDBENZOXAZINE DIMERS AND THEIR POTENTIAL APPLICATIONS. ADVISOR: PROF. SUWABUN CHIRACHANCHAI, Ph.D., 102 pp.

The present work focuses on molecular design and development of benzoxazine dimer structures for their potential applications. In the first part, a series of *N,N*-bis(2-hydroxybenzyl) alkylamine, so called benzoxazine dimers, are prepared via a simple and selective ring-opening reaction of benzoxazines with the yield as high as 90%. These compounds perform dual functions as initiator and catalyst for ring-opening polymerization of lactide. Two hydroxyl groups of benzoxazine dimers are initiated by organocatalyst to be initiator. By simply varying methylene bridge, very active ligands for alkyl/alkoxide aluminium complex formation can be clarified. Metal-ligand complexes are proved to be catalysts in ring-opening polymerization of lactide. Polylactides obtained are polymerized with narrow polydispersity index and well controlled molecular weight. In the second part, for the first time, a thermochromic free-standing poly(L-lactic acid) film is studies. By simply constructing tetra-branched benzoxazine dimers from pentaerythritol followed by L-lactide ring opening polymerization initiated by organocatalyst as well as the conjugation with diacetylene at terminal, a precise eight-armed poly(L-lactide) conjugated diacetylene can be obtained. The blend with poly(L-lactic acid) followed by solution casting leads to the thermochromic free-standing film. The comparative studies declare that bulk diacetylene and other linear-, four- and multi-armed poly(L-lactide) terminated polydiacetylene do not show thermochromic property. The microstructure analysis indicates the symmetric eight-armed structure controls the packing of polydiacetylene in poly(L-lactic acid) matrix upon heating and cooling. From these two works, the benzoxazine dimers can be noticed to be one of the choices for decorating star and/or multi-branched polylactide. In the final part, the work covers a convenient, environmentally friendly, and simple procedure to obtain benzimidazoles through the cyclization between aldehyde and phenylenediamine derivatives under reduced pressure. This synthesis pathway not only gives the benzimidazoles with high yield from the mild condition but also the selection of benzaldehyde and phenylenediamine with reactive functional group leads to the precursor for synthesis a new class of benzoxazine dimer with pH-sensitive fluorescent intensity and multichromatic emissions.

Field of Study: Nanoscience and Technology	Student's Signature	_____
Academic Year: 2016	Advisor's Signature	_____

ACKNOWLEDGEMENTS

CONTENTS

CHAPTER I
INTRODUCTION

Benzoxazines are new class of phenolic-type thermoset resin which conventional benzoxazine monomers are synthesized from phenol derivatives, primary amine derivatives and formaldehyde in either solution or melted state to form the oxazine ring through the Mannich reaction. Conventionally, benzoxazine monomers are polymerized to polybenzoxazine by thermal curing at high temperature at 170°C to 190°C without any curing agents or catalysts.[1] Because of the advantages of polybenzoxazine over traditional phenolic resin, such as no release volatiles during curing process, good mechanical properties, high thermal stability and flexibility in molecular design development in both academic research and industrial production is still received much attention and the many unique polybenzoxazine have been reported.

For the past decade, Chirachanchai *et al*.[2] have proposed benzoxazine derivatives which simply produced by Mannich reaction of phenols, formaldehyde, and amines. They focused on self-termination of *N,N*-bis(2-hydroxybenzyl) alkylamine derivatives, so-called benzoxazine dimers, from a single ring-opening of para-substituted benzoxazine monomers. The unique structures under inter- and intra-molecular hydrogen bonds at the phenols and aza linkage leading to stable asymmetric structures.[2-3] They also demonstrated the macrocyclization of benzoxazine dimers in high yield (above 80%) without by-products in the simple and effective conditions.[4] In fact, chemical structures of ring-opened benzoxazines are resemble to aza-calixarene which is a derivative of calixarenes with aza-ethylene linkage that has the molecular properties of ions capture. The evidences that the benzoxazine dimers and macrocycles show host-guest inclusion based on molecular assembly with several metal ions through the studies by single crystal analysis not only confirm the supramolecular chemistry of benzoxazine dimers, but also related to the role of specific hydrogen bond network of benzoxazine dimers.[3, 5-6]

The present work shows another unique phenomenon based on reactive -OH group and supramolecular chemistry of benzoxazine dimer. This leads us to propose simple and selective approach to prepare benzoxazine dimers with high yields (80-90%) for ROP of LA (Chapter III). The work clarifies how the benzoxazine dimers provide

active ligands for metal-ligand complex catalysts and initiators to initiate ROP of lactide. The constructing benzoxazine dimers is also the points to be considered. It is a challenge to us to propose other benzoxazine dimer structures including the potential properties. In Chapter VI, tetra-branched benzoxazine dimers was synthesized from pentaerythritol core. A precise eight-armed poly(L-lactide) conjugated diacetylene can be obtained from polymerization of lactide on tetra-branched benzoxazine dimers as well as the conjugation with diacetylene at terminal. The blend and solution casting lead to free-standing PLA film. The topochemical polymerization by UV irradiation in film form is performed. The success of the work should bring us to another novel type of reversible thermochromic free-standing film. In addition, by simply changing monophenol- to diphenol-based, a new class of benzoxazine dimer containing benzimidazoel moiety can be obtained through cyclization and oxazine-ring opening reaction (Chapter V). The benzoxazine dimer containing benzimidazoel moiety is performed as fluorophore with pH-sensitive multicolor emission behavior.

CHAPTER II

LITERATURE REVIEW

2.1 Benzoxazines

Benzoxazines are heterocyclic compounds, which consist of benzene ring and oxazine ring. There are 8 isomers, which are different at methylene position and substituted hydrogen atom position (Scheme 2.4).

Scheme 2.1 Isomers of benzoxazine.

1,2-Benzoxazine

2,1-Benzoxazine

1,3,2-Benzoxazine

3,1,4-Benzoxazine

1,3,4-Benzoxazine

1,4,2-Benzoxazine

2,3,1-Benzoxazine
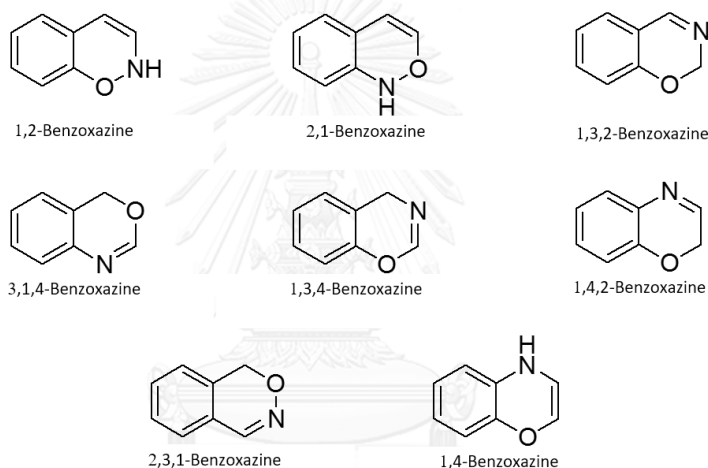
1,4-Benzoxazine

In 1964, Burke *et al.*[7] reported the preparation of benzoxazine derivative (3,4-dihydro-1,3-2H-benzoxazines) by using one step of Mannich reaction between phenol derivative, formaldehyde and amine derivative (Scheme 2.2).

Scheme 2.2 Preparation of benzoxazine derivative.
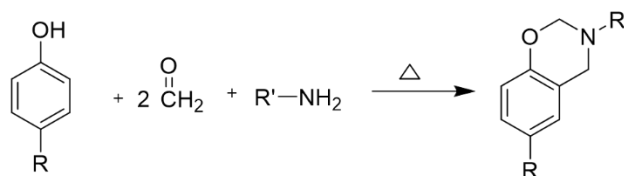
In 1965, Burke *et al.*[8] reported on the preparation of *N,N*-bis(2-hydroxyalkylbenzyl)alkylamine derivatives via a single ring opening of benzoxazine. For example, *N,N*-bis(2-hydroxy-1-naphthylmethyl)methylamine was carried out by the ring opening reaction of 2,3-dihydro-2-methyl-1H-naphth-(1,2-e)-1,3-oxazine with 2-naphthol (Scheme 2.3).

Scheme 2.3 Ring opening reaction of 2,3-dihydro-2-methyl-1H-naphth-(1,2-e))-1,3-oxazine with 2-naphthol.
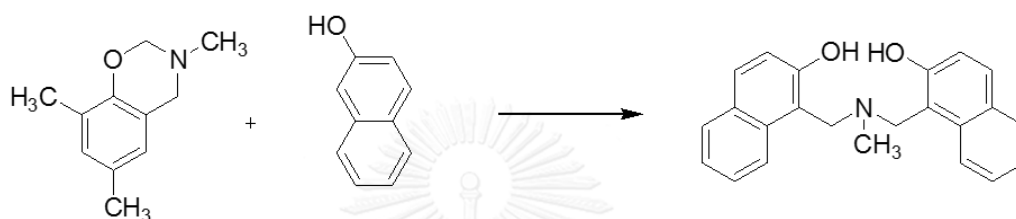

However, nowadays, benzoxazines are known as novel thermosetting materials with superb characteristic properties such as thermal resistant ans size stability during polymerization by thermal curing of bisphenol A-based benzoxazines as shown in Figure 2.4.[1]

Scheme 2.4 Polymerization of bisphenol A-based benzoxazine.
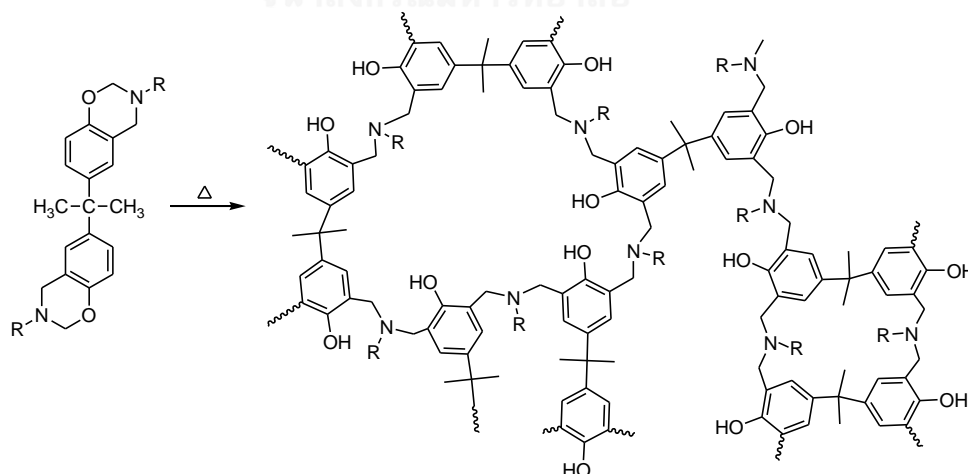
According to the para-substituted phenol-based benzoxazines, linear polybenzoxazine should be formed via oxazine ring opening reaction. However, Riess

et al.[9] found that only four to six benzoxazine units can be proceeded. The involved factors and limitations of linear benzoxazine polymerization still were not clarified.

In recently, Chirachanchai and coworkers demonstrated self-termination of benzoxazine ring-opening reaction leads to 80% - 90% yield of benzoxazine dimers, *N,N*-bis(2-hydroxyalkylbenzyl)alkylamine, as shown in scheme 2.5.[3, 5, 10] Considering the structure of these derivatives, the single crystallography analyses suggested that the molecules obtained show the unique structures under inter- and intramolecular hydrogen bonds leading to stable asymmetric structures (Figure 2.1).[10]

Scheme 2.5 Self-termination of benzoxazine ring-opening reaction.
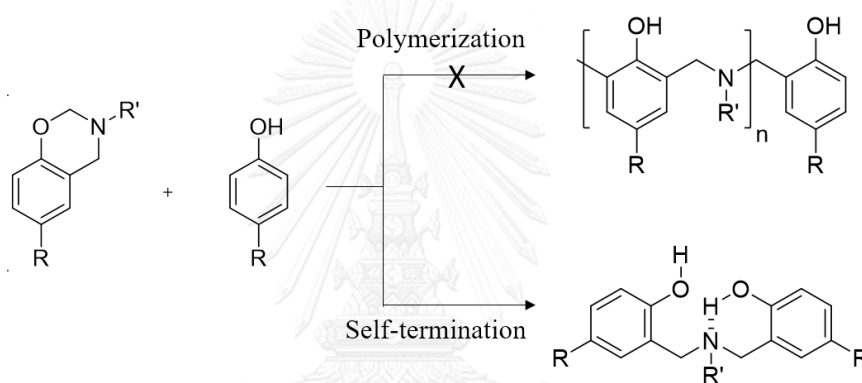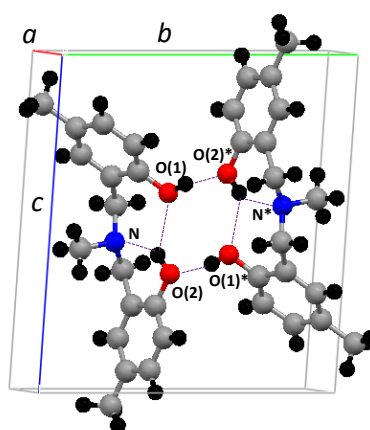
Figure 2.1. Crystal structure of *N,N*-bis(5-methyl-2-hydroxybenzyl) cyclohexylamine.

2.2 Supramolecular chemistry of Benzoxazines

Considering the molecular structures, chemical structures of N,N-bis(2-hydroxy alkylbenzyl)alkylamine are resemble to aza-calixarenes as illustrated in Scheme 2.6. Aza-calixarenes is a derivative of calixarenes with aza-ethylen linkage that has the molecular properties of ions capture. Focus on the ions capture, benzoxazine dimer structures are expected to observe the molecular perform as host compounds to accept various kinds of guest species via host-guest chemistry thought non covalent bond.

Scheme 2.6 Resemble structure of aza-calixarenes and ring-opened benzoxazines.
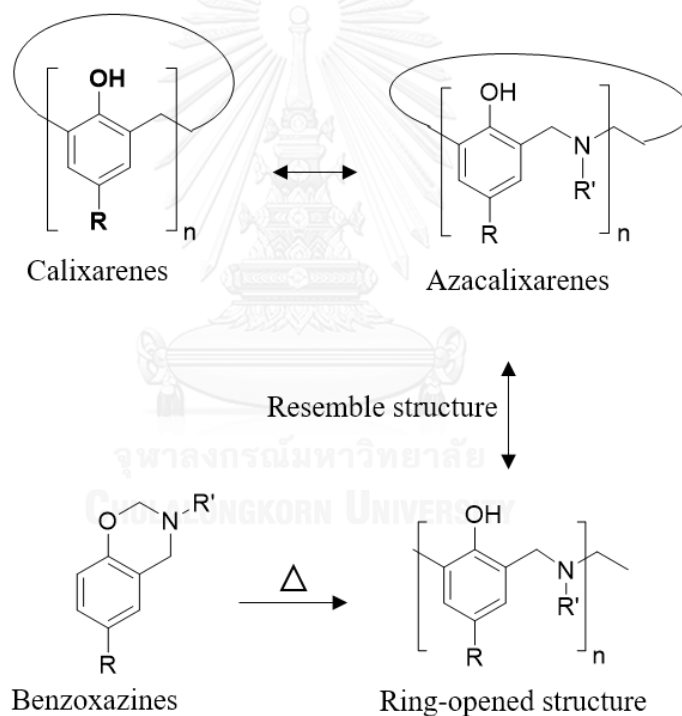
In the past, Laobuthee *et al.*[11] succeeded in showing inclusion phenomena of *N,N*-bis(2-hydroxyalkyl benzyl)alkylamine derivatives (host molecule) with alkali and alkaline earth metal picrate (guest molecule). They also demonstrated transition metal ions, i.e., Cu^{2+}, Zn^{2+}, and Cd^{2+}, binding properties of *N,N*-bis(2-hydroxyalkylbenzyl) alkylamine derivatives without destroying the host framework under double-oxygen-bridged dimeric molecular assembly system by using X-ray single crystal analysis.[5-6]

Figure 2.2 shows crystal structure of ions binding with *N,N*-bis(2-hydroxyalkylbenzyl) alkylamine derivatives.
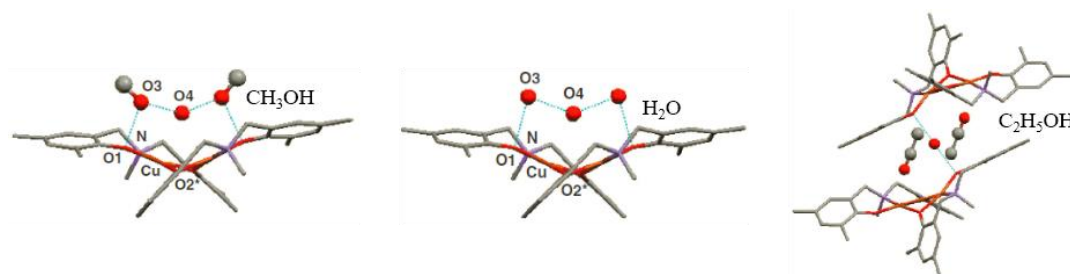
Figure 2.2. Crystal structure of ions binding with N,N-bis(2-hydroxyalkylbenzyl) alkylamine derivatives.

N,N-bis(2-hydroxyalkylbenzyl) alkylamine derivatives also performed selective macrocyclic compounds through a simple reactions of either esterification or etherification. Rungsimanon *et al.*[4] proposed [1+1] and [2+2] ether-likage macrocycles derived from the reaction between *N,N*-bis(2-hydroxyalkylbenzyl)alkylamine (benzoxazine dimers) and ditosyl compounds. The benzoxazine dimers with methyl group at ortho and para positions of benzene ring and at nitrogen atom provided [1+1] dibenzo-monoazacrowns. By contrast, benzoxazine dimers without methyl group at ortho position gave [2+2] macrocyclic benzoxazine. These macrocycles showed inclusion phenomena with metal ions. Moreover, Laobuthee and coworkers[2] have reported a simple, effective, and selective approach to prepare ester-linked macrocyclic benzoxazine via esterification of terephthaloyl and benzoxazine dimer to obtain a well-defined structure product with high yield and without using expensive catalysts and multistep reactions in specific conditions.

2.3 Polylactide (PLA)

Biodegradable polymers have received much attention due to their wide range of applications in environmentally friendly products. Among numerous kinds of biodegradable polymers, PLA is the most promising due to the reliable industrial scaled productions and the attractive properties especially the high-strength and high-modulus as compared to other biodegradable polymers. PLA is an aliphatic polyester derived

from renewable agricultural resources such as corn starch, tapioca roots, and sugarcane.[12-13] PLA has been considered as a replacement for some commodity polymers in the industrial packaging field or used in the biocompatible/biomedical devices field. PLA can be degraded by simple hydrolysis of ester bond without the presence of enzyme catalysts to produce lactic acid, lactide reformation, oxidative main chain scission, and inter- or intramolecular transesterification reactions.[14] Currently, PLA can be produced by the ring-opening polymerization (ROP) of lactide (Scheme 2.7), a process can be initiated by hydroxyl groups of initiators with co-catalysts or metal-ligand complexes.

Scheme 2.7 Ring-opening polmerization of lactide.
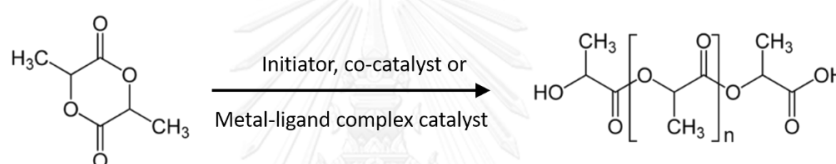
Polymerization of lactide (LA) can be devided into two route. The first route, Tin (II) 2-ethylhexanoate ($Sn(Oct)_2$) has been most widely used as a co-catalyst because of high reaction rates, the solubility in the monomer melt, and the ability to produce high molecular weights.[15] In the present of alcohol or water (ROH), the initiation and propagation involve reaction of three simultaneously interacting compounds for example a macromolecule fitted with a terminal -OH group, monomer, and $Sn(Oct)_2$ in propagation. In every propagation step, a macromolecule with an -OH is reformed as a longer one by one monomer unit and one intact $Sn(Oct)_2$, either "free" or complexed, emerges from this step. If it's enough to stress, according to this group of mechanisms, $Sn(Oct)_2$ survives during polymerization as such and is not converted into any other species chemically different from $Sn(Oct)_2$.[16-17] The coordination-insertion mechanism is shown in Scheme 2.8. Mechanism suggests that two equiv. of alcohols (these alcohols can be initiators or the propagating hydrolyzed lactide) exchange with the ligands followed by the coordination of lactide to the metal center (a). Insertion of the alcohol and ring-opening (b) generates a linear monomer (c) and starts propagation.

Scheme 2.8 Coordination-insertion mechanism.
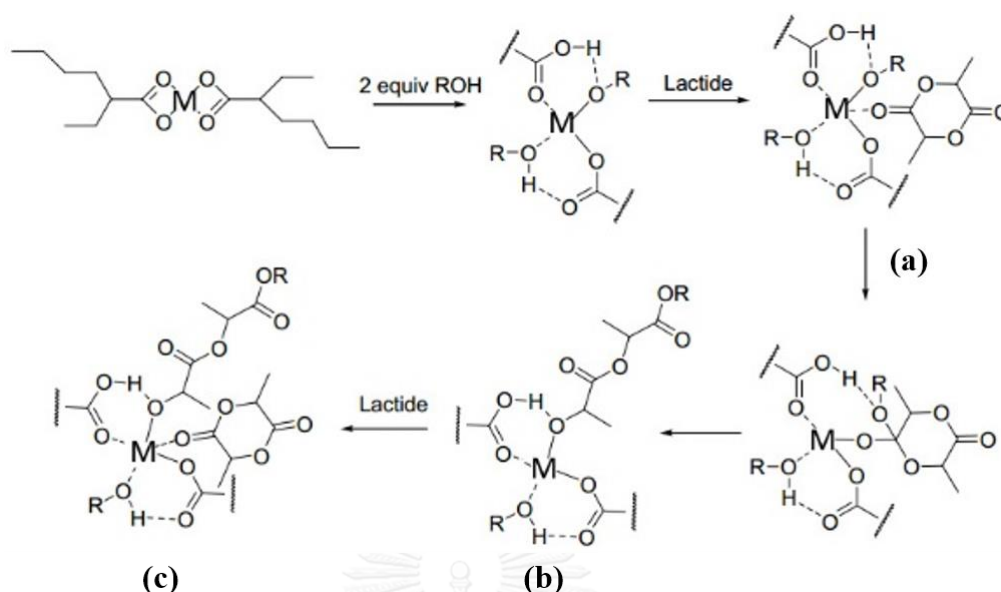
However, a major drawback of the Sn(Oct)$_2$ is the incorporation of the toxic metal on the polymer chain end and the resulting toxicity risk in biomedical and environmental applications.[18] The application of organocatalysts to controlled lactide polymerization is considered because these organic catalysts are relatively inexpensive, highly active and metal-free system. Hedrick et al. were the first to report the use of organic catalyst 4-(dimethylamino)pyridine (DMAP) in the ROP of lactide. Miao et al.[19] reported the used of cyclodextrins as co-initiators for coordinative with organocatalyzed ring-opening polymerization of cyclic esters. The molecular weight can be controlled by adjusting the lactide:cyclodextrin ratio, and the distribution is rather narrow (ĐM < 1.15). For the second route, metal-ligand complex systems are focused. Numerous ligand derivatives containing initiating groups such as amides, carboxylates, and alkoxides have been used with main-group elements[20] (s- and p-block) and d-block metals[21-22] as well as lanthanides[23] to form organometallic complexes as effective catalysts for ROP of LA. Systematic studies have demonstrated the influence both of the initiating group and of the ligand architecture on polymerization behaviors. Among the variety of initiators, aluminium alkoxide complexes seems to be attractive and suitable in preparing the well-defined polyesters due to their generally high Lewis acidity, low toxicity, low cost. Aluminum alkoxides

promote a coordination-insertion type of polymerization, and polylactides of predetermined molecular weight and low polydispersity have been synthesized.[13]

2.4 Diacetylenes (DA) and Polydiacetylenes (PDAs)

PDAs are known as a conductive polymers which can be polymerized by topochemical polymerization of DAs in solid state, such as in form of mono-layer film or crystal, via UV- or γ- irradiation.[24] The first polydiacetylene was discovered by Wegner et al. in 1969. This achievement was occurred when crystals of 1,6-bishydroxy hexa-2,4-diyne was exposed to UV light.[25] They assumed that it occur because of the spatial arrangement of diynes in the crystal, but this was not confirmed until Raymond H. Baughman coined the term "topochemical polymerization" in 1972 to describe polymerization of diynes due to spatial arrangement and put forth the spatial requirements needed for a polymerization of this sort.[26] It results in a highly ordered orientation of ene-yne conjugated back bone of obtained PDAs. However, a preorganization of DA monomer in closed-packing structure under a repeat distance ~5 Å and an orientation angle ~45° is required (Figure 2.2).[27] Thus, alternatively, polymerization by thermal treatment in solid[28] or melt[29] state has been reported. Due to the conjugated back bone of PDAs, they show unique electrical and optical properties which are promising in multiple applications such as development of organic films to immobilization of other molecules[30], light-emitting diodes (OLEDs)[31], sensors[32-34] and etc.
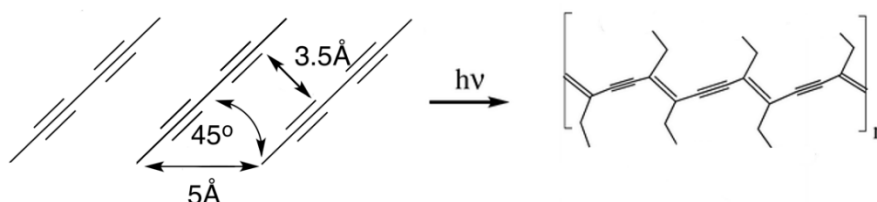

Figure 2.3. Typical preorganization of DA monomer for topochemical polymerization.

The topochemical polymerization requires the assembly of DA monomers in an appropriate arrangement to favour 1,4-addition polymerization which the minimum

requirement as mentioned above (translational period (*d*) must be in range of 4.7 to 5.2 Å, the tilt angle (γ) between the diacetylene rod and *d* must be close to 45°, and a 3.5Å distance between C1 of one monomer and C4 of the adjacent diyne monomer), then the initiation step can be created. Because the topochemical polymerization results in a change of the atomic coordinates inside the crystal, the nature of the substituent directly attached to the butadiyne unit has a significant impact on the polymerization process. After polymerization, PDAs are known for their unique thermochromic properties based on the unique linear π-electron conjugated or ene-yne conjugated polymer structures. The transitions from blue to red represent a disruption in the planar conformation and a reduction in the conjugation length of the PDAs backbone. It is important to note that although PDAs are variously applied, the thermochromic reversibility is not always the case. In fact, the substituents should be able to accommodate structure changing within the crystal lattice upon change in temperature. Several reports point out that the thermochromic reversibility occurs when PDAs are in a particular framework under molecular interaction. For example, Yuan *et al.*,[35-36] and Kim *et al.*[37] demonstrated PDAs with pH and thermochromic reversibility under the hydrogen bond network within terephthalic acid groups on the side chains. Moreover, Chanakul *et al.*[38] fabricated PDA/ZnO nanocomposite, which exhibited reversible thermochromic behaviors. The thermochromic reversibility of the PDA/ZnO nanocomposites was due to the strong interfacial interactions between carboxylate head of PDAs and hydroxyl groups on ZnO surface that limited the dynamics of PDAs backbone structure. Although there are many reports of PDAs with reversible thermochromic behaviors, to the best of our knowledge, there is no report about PDA-based reversible thermochromic free standing film. It should be noted that although several potential applications, especially, sensors, are reported, in most cases, the fabrications of PDAs materials are quite sophisticated such as vesicles in aqueous solution,[39] Langmuir monolayers,[40] dip-coating[41] and spin-coating[42] on solid-support. The use of PDAs as a bulk product obtaining from the blend or compounding has not yet been reported.

2.5 Point of Study

Taking the above mentioned about benzoxazine chemistry and advantages of benzoxazine molecules, herein, we propose the molecular design and development of benzoxazine dimer structures for their potential applications. In Chapter III, benzoxazine dimers are applied for ring opening polymerization of lactide. These compounds perform as initiators and ligands for metal-ligand complex catalysts. Polylactides obtained are polymerized with narrow polydispersity index and well controlled molecular weight. In Chapter V, we demonstrate tetra-branched benzoxazine dimers with a distinguished molecular design and synthesis. By simply polymerization of lactide on tetra-branched benzoxazine dimers as well as the conjugation with diacetylene, a precise eight-armed poly(ʟ-lactide) conjugated diacetylene can be obtained. The blend with PLA resin followed by solution casting leads to the reversible thermochromic film. This is the first time proposed reversible thermochromic free-standing poly(ʟ-lactic acid) film as a model case. In Chapter V, we propose a convenient, environmentally friendly, and simple procedure to obtain benzimidazoles through the cyclization between aldehyde and phenylenediamine derivatives under reduced pressure. The selection of benzaldehyde and phenylenediamine with reactive functional group leads to the precursor for synthesis a new class of benzoxazine dimer with pH-sensitive fluorescent intensity and multichromatic emissions.

CHAPTER III

SIMPLE AND SELECTIVE PREPARATION OF N,N-BIS(2-HYDROXYBENZYL)ALKYLAMINE: DUAL FUNCTIONS AS LIGANDS AND INITIATORS FOR RING-OPENING POLYMERIZATION OF LACTIDE

3.1 Abstract

Amine bis(phenolate) compounds are known as versatile ligands for metal-ligand catalysts in ring-opening polymerization of cyclic esters. The chemical structure of amine bis(phenolate) ligands consists of two phenols linked with azamethylene linkage and it is resemble to that of *N,N*-bis(2-hydroxybenzyl)alkylamine, so-called benzoxazine dimer (BzD), which can be obtained from a single ring opening of benzoxazine due to its inevitable self-termination. As the reaction of phenol, amine, and formaldehyde derivatives quantitatively leads to benzoxazine, whereas the consequent oxazine ring opening gives the BzD in high yield. When applying BzD aluminium alkoxide as the catalyst, the PLA obtained shows the PDI as less as 1.2 with 90% conversion. This BzD synthesis pathway also offers the branching structured BzD which can be applied as multi-branched initiator so that the star polylactide is easily obtained. The use as an initiator in combination with 4-dimethylaminopyridine (DMAP) organocatalyst in bulk leads to both conversion and yield for 90% with the narrow PDI as less as 1.10. Moreover, the eight-armed polylactide is obtained from the tetra-branched benzoxazine dimers. The present work shows how the two-step preparation via benzoxazine and BzD is a simple and selective pathway to obtain dual functioned molecules to be the metal catalyst ligand as well as the various structures of initiator for linear and/or branched polylactide.

Keywords: Lactide, benzoxazine dimer, metal-ligand complex, initiator, ring-opening polymerization, Catalyst

3.2 Introduction

In the past decade, amine bis(phenolate) compounds are known as versatile ligands for using in metal-ligand complexes formation. Numerous ligand derivatives have been used with main-group elements[1] (s- and p-block) and d-block metals[2-3] as well as lanthanides.[4] Many of these complexes have been reported to be excellent initiators for ring opening polymerization (ROP) of cyclic esters[5-8] and aluminium alkoxide based system seems to be attractive and suitable in preparing the well-defined polyesters because of their generally high Lewis acidity, low toxicity, and low cost.[8-11] For example, Gendler, et al.[12] produced dianionic amine bis(phenolate) ligand precursors by a single step Mannich reaction between formaldehyde, amines and phenols to obtain 57-68% yield of the colorless products after recrystallization from ether and methanol. The ROP initiated with metal-ligand catalysts yielded poly(L-lactide) with 6-75% conversion. Yang, et al.[13] reported [ONOO]-typed bis(phenolate)amine ytterbium complexes for polymerization of *rac*-lactide. It should be emphasized that the two species of amine bis(phenolate) ligand precursors (abbreviated I and II were synthesized via condensation as shown in Scheme 3.1(A) Route A. The preparations, in general, were done by one pot synthesis using primary amines, formaldehyde, and phenol derivatives after refluxing for 24 to 40 h. By using the multi-step purification which are separation, precipitation, trituration and recrystallization, the yields of I, and II were as low as 43%, 85%, respectively. The use of these ligands led to polylactides with 52% - 95% yield.

To our idea, the structure of amine bis(phenolate) compounds is similar to the BzD which consist of two phenols linked with azamethylene unit. For the past few year, our group have focused on the monophenol-based benzoxazine supramolecular chemistry. We reported two-step reaction to quantitatively form *N,N*-bis(2-hydroxybenzyl)alkylamines or BzD via a simple and selective ring-opening reaction of monophenol based benzoxazines.[14] As soon as a single ring opening of benzoxazine occurs, the dimeric benzoxazine forms inter- and intra- molecular hydrogen bonds and this obstructs the polymerization of benzoxazines. Therefore, the high yield and selective BzD is obtained (80-90%). In addition, the BzD also showed molecular assembly between two dimers to accept copper ions and neutral molecule guests.[15]

On this viewpoint, it is our challenge to clarify whether the BzD form complex with metal and function as catalyst for ROP of lactide as seen in the case of amine bis(phenolate) compounds.

In fact, alcohols or phenols are good initiators with Tin(II) 2-ethylhexanoate (Sn(Oct)$_2$) catalyst to initiate the ROP of lactide in molten stage to result in high reaction rate and high molecular weight. The catalyst remained in PLA might lead to the toxicity, therefore, the system is not practical if the medical grade PLA is needed.[16] The application of organocatalysts to control lactide polymerization is considered because these organocatalysts are relatively inexpensive, highly active without metal containing. Hedrick et al. reported the use of DMAP in the ROP of lactide. Miao et al.[17] applied cyclodextrins with 21 hydroxyl groups as co-initiators for coordination with organocatalyzed of lactide ROP to obtain PLA. It was reported that the molecular weight can be controlled by the lactide:cyclodextrin ratio whereas the polydispersity is below 1.15.

Based on the abovementioned point, it is also our challenge to clarify BzD as initiators for lactide ROP. The fact that BzD consist of two phenols, the OH groups play their role as initiator in combination with organocatalyst. To this end, the use of core molecules containing four primary amines allows us obtaining tetra-branched benzoxazine dimers (4BzD) with 8 phenol units at the terminal. This brings us the possibility to obtain the star and/or multi-branched PLLA.

Here, the present work presents a simple and selective synthesis of BZD as they are the essential molecules to be ligands and initiators. For ligand, the structures under the effect of alkyl and alkoxide coordinates of aluminium are studied. The work aims to show the optimal conditions through the analysis of catalytic activity in the specific condition. Furthermore, the detailed experiments with systematic variations on the factors related to the polymerization are focused.

Initially, *N,N*-Bis(2-hydroxy-5-methylbenzyl)cyclohexylamine (**1**), *N,N*-bis(2-hydroxy-3,5-dimethylbenzyl)cyclohexylamine (**2**), and *N,N*-bis(2-hydroxy-3,5-dimethylbenzyl)methylamine (**3**) (Scheme 3.1(A) Route B) were prepared via ring-opening reaction of the relevant benzoxazine and phenol derivatives as reported previously.[14] In brief, the mixture of 3-cyclohexyl-6,8-dimethyl-3,4-dihydro-*2H*-1,3-benoxazine and 2,4-dimethylphenol (1:1) was prepared and stirred at 60 °C until the

solution became viscous (Scheme 3.1(A) Route B). The viscous product was collected and recrystallized in isopropanol to obtain **2** with 85% yield. The total two-step reaction time was 14 h. In similar, the ring-opening reaction of 3-cyclohexyl-6-methyl-3,4-dihydro-*2H*-1,3-benoxazine and 3,6-dimethyl-3,4-dihydro-*2H*-1,3-benoxazine using *p*-cresol and 2,4 dimethylphenol, obtains **1** (83% yield) and **3** (90% yield), respectively, as confirmed by ^{1}H-NMR (Figures A1-A3).
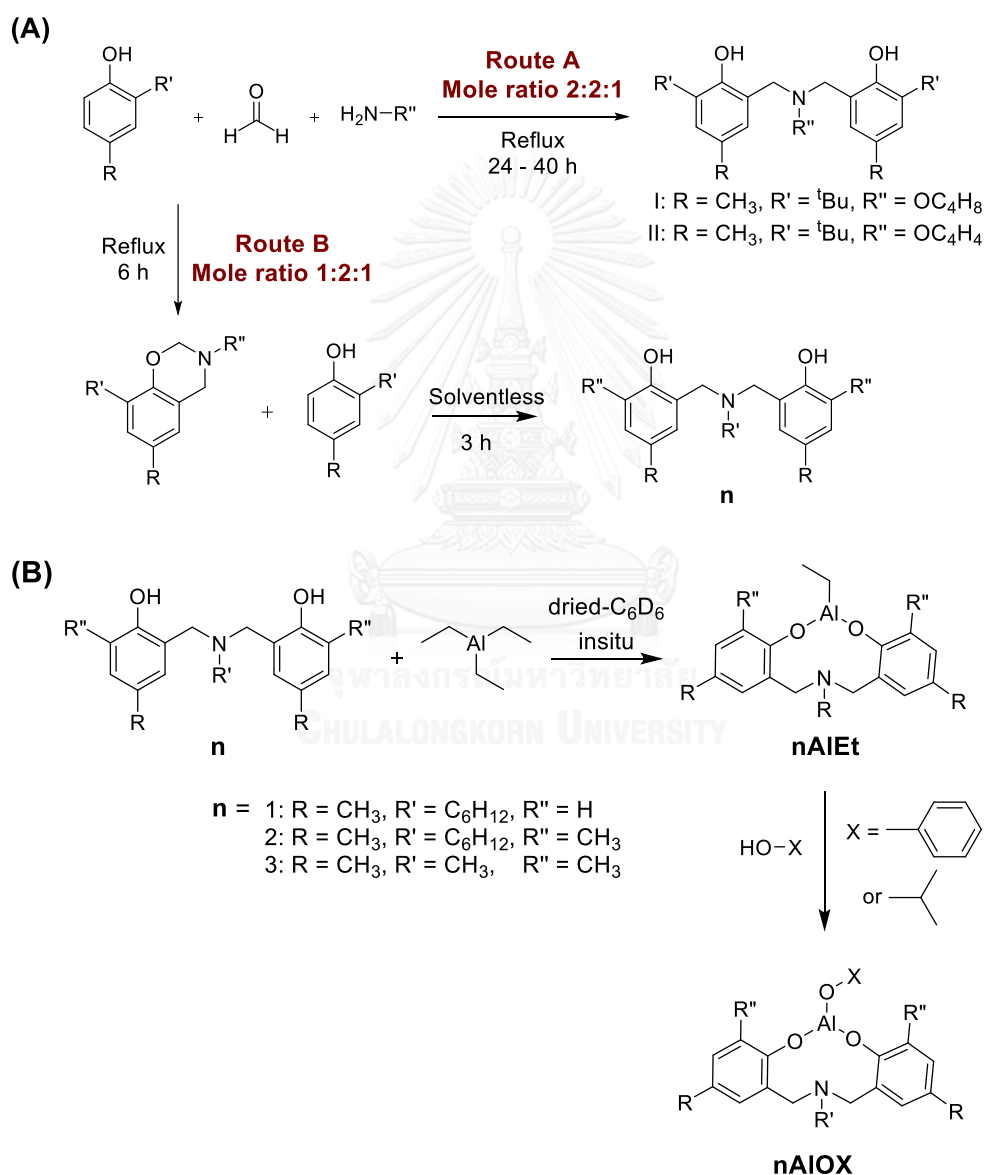
Scheme 1 (A) amine bis(phenolate) ligand formation (Route A), benzoxazine dimer formation (route B) and (B) Complexation of benzoxazine dimer ligand.

It should be noted that aluminium alkoxide based with amine bis(phenolate) system is known as the good metal-ligand catalyst for cyclic esters ROP to obtain the well-defined polyesters because of their generally high Lewis acidity, low toxicity, and low cost.[8-11] Here, **1**, **2**, and **3** were purified by sublimation and mixed with triethylaluminium in toluene at room temperature for 30 min to obtain the complexes **1AlEt**, **2AlEt** and **3AlEt** (Scheme 3.1(B)). From ^{1}H-NMR of **2AlEt** (Figure A4), two singlet peaks of aromatic protons at δ_H 6.82 ppm and 6.74 ppm were shifted to δ_H 6.97 ppm (lower field) and δ_H 6.49 ppm (higher field), respectively. This might be due to the change in electron shielding based on the disappearance of the intramolecular hydrogen bond in **2** and the formation of complex. The signals of aromatic protons of **3AlEt** (Figure A5) are shifted as seen in the case of **2AlEt**. For **1AlEt** (Figure A6), a multiplet peak of aromatic protons at δ_H 6.90 ppm is shifted and split to three peaks at δ_H 7.54 ppm, 7.03 ppm, and 6.65 ppm. This implies the free ortho position of phenol under the different environment after complexation. Moreover, for **2AlEt**, a singlet peak at δ_H 3.63 ppm of methylene protons of benzoxazine dimer shifted and split to doublet of doublet at δ_H 3.52 ppm and 3.42 ppm. The shifting and splitting of methylene protons indicated the environment of protons at methylene was changed due to the structural dynamic effect. This led to withdrawal of the electrons of methylene groups and as a result the electron density of the aforementioned protons was decreased as demonstrated by Philipsborn et al.[18] The complexes **1AlEt** and **3AlEt** were found in similar behaviors with **2AlEt**.
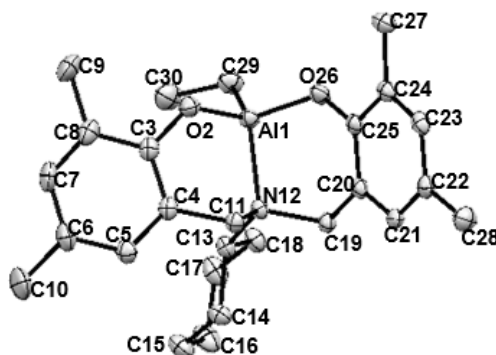

Figure 3.1. An ORTEP drawing of **2AlEt**.

Table 3.1 ROP of lactide using **3** as an initiator with different catalysts, solvents under various reaction temperature and time.

Entry	initiator	[L-LA] : 2 OH-group	Catalyst	Solvent	T (°C)	Time (min.)	Conversion (%)	Isolated yield (%)	$M_{n\ theo}$ (gmol^{-1})	$M_{n\ exp}$ (gmol^{-1})	PDI
1	**3**	20	-	-	120	120	47	67	1654	2938	1.45
2	**3**	20	DMAP	-	120	20	98	95	3124	3820	1.14
3	**3**	20	1% TBD	-	120	5	87	43	2951	5072	1.12
4	**3**	20	1% DBU	-	120	180	90	39	3009	5214	1.27
5	**3**	20	DMAP	CH$_2$Cl$_2$	40	10080	83	93	2692	4303	1.06
6	**3**	20	1% TBD	CH$_2$Cl$_2$	RT	40	97	44	3095	4480	1.07
7	**3**	20	1% DBU	CH$_2$Cl$_2$	RT	300	97	51	3095	5281	1.28
8	**3**	100	DMAP	-	120	60	90	90	12839	11770	1.10
9	4BzD	25	DMAP	-	120	100	95	93	28768	24652	1.19

In schlenk flask, a toluene solution of triethylaluminium was added to a yellowish toluene solution of **2**. The solution was stirred at room temperature overnight. After concentration, the solution was placed at −2 °C for crystallization. After several days, colorless microcrystals of **2AlEt** was obtained (Figure 3.1 and Table A1). The preliminary lactide polymerization suggested that poly(lactide) chains were formed as **1AlEt** and **2AlEt** were involved in the reaction. For further investigation, **1AlEt** and **2AlEt** were used to study their catalytic potential in lactide ROP in the presence and absence of alcohol co-initiators. Alcohol species are important in activation of many initiators via the formation of alkoxide metal allowing the ROP though a coordination-insertion mechanism.[1, 19-20] Complex **1AlEt** was applied for ROP of lactide (1:200 **1AlEt**:lactide) in toluene at 70 °C to give 41% yield (PDI = 1.15, M_n = 9.04 kg mol^{-1}) in 24 h. When 1 equiv. of propan-2-ol (HOiPr) was added into **1AlEt** solution, **1AlOiPr** (Scheme 3.1(B)) was obtained. The lactide ROP was as high as 82% conversion. In the presence of benzyl alcohol (HOBz), **1AlOBz** (Scheme 3.1(B)) was formed. The PLA was obtained with 96 % conversion and PDI = 1.22. The molecular weight was observed by GPC (M_n = 18.09 kg mol^{-1}). For **2AlOiPr** and **2AlOBz** (Scheme 3.1(B)), the polymerizations were as high as 100 % conversion with narrow molecular weight distribution (PDI = 1.26, M_n = 25.52 kg mol^{-1} and 100 PDI = 1.23, M_n = 27.28 kg mol^{-}

[1], respectively). Among six catalysts in the studies, it is clear that **2AlOiPr** and **2AlOBz** give the highest M_n of PLA when the reactions were carried out in toluene. It should be noted that the PLA obtained from all reactions show narrow polydispersity index (Table A2). For examining the polymerization activity, **2AlOBz** was used as a catalyst. ^{1}H-NMR of aliquot was collected in relevant to the reaction time. The %conversions were calculated and plotted between In $[M_o/M_t]$ versus time (h) (Figure A7). The linear relationship suggested the first order reaction. Therefore, the slope (0.03) refers to the rate constant of reaction.
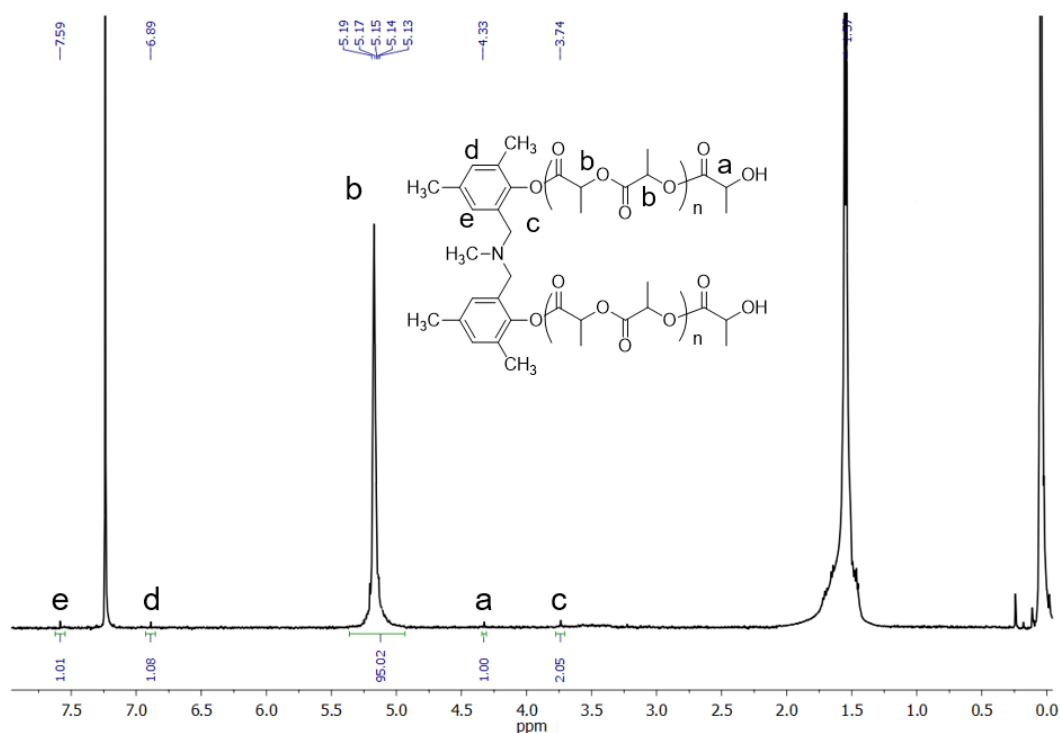

Figure 3.2. ^{1}H NMR of lactide ROP using **3** as an initiator (entry 8).

The ROP of lactide in the bulk is initiated by **3**. The polymerization was extensively characterized by ^{1}H NMR. The M_n, M_w and PDIobtained were adjusted by using the correction factor of 0.58 as reported by Kowalski et al.[21] The cold diethyl ether was used for precipitation to avoid the chain scission of PLA and resulted in 95% yield.

Table 3.1 shows a systematic variation based on **3** to clarify the optimal condition for lactide polymerization. Here, three types of organocatalyst, i.e. 4-

dimethylaminopyridine (DMAP), triazabicyclodecene (TBD), and 1,8-diazabicycloundec-7-ene (DBU), were used. The reactions were proceeded in the bulk with and without organocatalysts. In the case of without catalysts, ^{1}H NMR indicates 47% conversion with isolated yield around 55% (Table 3.1 entry 1). On the other hand, in the presence of DMAP catalyst, ^{1}H NMR indicated %conversion for as high as 98% with polydispersity index about one (Table 3.1 entry 2). For TBD and DBU, the yields are lower than 50%. This reflects the low catalytic activity of TBU and DBU on **3** (Table 3.1 entries 3 and 4). To study the effect of solvent, the reactions were carried out in dichloromethane in the presence of catalysts (Table 3.1 entries 5-7). The polymerization in solvent took the longer reaction time comparing to that in the bulk. This indicates the less reaction efficiency as the solvent may obstruct the polymerization activity.

Considering the molar ratio between lactide and **3**, the lactide ratios were increased from 20 to 100 times. In the case of the content of lactide for 20 times (Table 3.1 entries 1 – 7), it is clear that the condition using DMAP in molten stage of lactide is considerable as the reaction was carried out for only 20 minutes but giving 98% conversion and 95% yield. When the lactide content was extended to 100 times, the conversion as well as yield still maintains for 90% with the narrow PDI (Table 3.1 entry 8)

Figure 3.2 shows the ^{1}H NMR of the product obtained from Table 3.1 entry 8. The signal at 5.15 (assigned as b) ppm, 4.33 (assigned as a) ppm and 3.74 ppm (assigned as c) are referred to $-OC(O)CH(CH_3)-$ of L-lactide repeating unit along the polymer chains, $-OC(O)CH(CH_3)-OH$ of terminal PLLA chains and $Ar-CH_2-N$ of benzoxazine dimer, respectively. The integration ratio between c and a confirms the polymerization of lactide on both phenols of benzoxazine dimers. According to the ^{1}H NMR, the degree of polymerization (DPn) of PLA branches in average could be estimated by dividing the integration of b by that of a plus 1 for the terminal lactate unit as shown in eq. (3.1). The integration ratio suggests DPn of 47 lactide units per chain.

$$DPn = \frac{I_b}{I_a} + 1 \qquad\qquad (3.1)$$

By simply modifying the hydroxyl groups of pentaerithritol to amine groups, the tetra-branched benzoxazines was formed. A single ring-opening reaction allows us forming 4BzD as reported previously.[22] The ROP of lactide was carried out for 100 min in the presence of DMAP catalyst. ^{1}H NMR (Figure A8) indicated %conversion for as high as 95% with polydispersity index nearly to 1.1 (Table 3.1 entry 9). ^{1}H NMR spectrum of star and/or branched polylactide (Figure A8) showed the eight methine protons of –OC(O)CH(CH$_3$)-OH of terminal PLLA chains at δ_H 4.37 ppm and methine proton of –OC(O)CH(CH$_3$)– of L-lactide repeating unit along the polymer chains at δ_H 5.15 ppm with the sixteen protons of methylene bridge of 4BzD at δ_H 3.51 ppm. According to ^{1}H NMR result, DPn of star and/or branched polylactide suggested 19 lactide units per chain.

In conclusion, this work demonstrated simple route to prepare benzoxazine dimers with yield as high as 90%. The benzoxazine dimers performed as ligands and initiators for ROP of lactide. For ligands, the stable metal-ligand complex catalysts were formed and the PLA obtained showed narrow PDI with above 90% conversion. In the case of initiators, polymer chains of polylactide were formed on –OH group of phenols by using DMAP organocatalyst. The modification of benzoxazine dimers to be branching structure allowed us a successful multi-branched PLA chains. The two-step pathway synthesis via benzoxazine and BzD offers the quantitative amount of amine bis(phenolate) compounds which their metal complex not only gives us the high yield and high conversion of lactide but also their branching structure plays the role as initiator for special molecular structure, especially star-shaped PLA.

3.6 Acknowledgments

3.7 References

1.   Saunders, L. N.; Dawe, L. N.; Kozak, C. M., Alkali metal complexes of tridentate amine-bis(phenolate) ligands and their rac-lactide ROP activity. *Journal of Organometallic Chemistry* **2014,** *749* (0), 34-40.

2.   Yang, S.; Nie, K.; Zhang, Y.; Xue, M.; Yao, Y.; Shen, Q., New [ONOO]-Type Amine Bis(phenolate) Ytterbium(II) and -(III) Complexes: Synthesis, Structure, and Catalysis for Highly Heteroselective Polymerization of rac-Lactide. *Inorganic Chemistry* **2013**.

3.   Liang, Z.; Zhang, M.; Ni, X.; Li, X.; Shen, Z., Ring-opening polymerization of cyclic esters initiated by lithium aggregate containing bis(phenolate) and enolate mixed ligands. *Inorganic Chemistry Communications* **2013,** *29*, 145–147.

4.   Giesbrecht, G. R.; Whitener, G. D.; Arnold, J., Mono-guanidinate complexes of lanthanum: synthesis, structure and their use in lactide polymerization. *Journal of the Chemical Society, Dalton Transactions* **2001,** (6), 923-927.

5.   Chisholm, M. H.; Gallucci, J.; Phomphrai, K., Lactide polymerization by well-defined calcium coordination complexes: comparisons with related magnesium and zinc chemistry. *Chemical Communications* **2003,** (1), 48-49.

6.   Kramer, J. W.; Treitler, D. S.; Dunn, E. W.; Castro, P. M.; Roisnel, T.; Thomas, C. M.; Coates, G. W., Polymerization of Enantiopure Monomers Using Syndiospecific Catalysts: A New Approach To Sequence Control in Polymer Synthesis. *Journal of the American Chemical Society* **2009,** *131* (44), 16042-16044.

7.   Nie, K.; Fang, L.; Yao, Y.; Zhang, Y.; Shen, Q.; Wang, Y., Synthesis and Characterization of Amine-Bridged Bis(phenolate)lanthanide Alkoxides and Their Application in the Controlled Polymerization of rac-Lactide and rac-β-Butyrolactone. *Inorganic Chemistry* **2012,** *51* (20), 11133-11143.

8.   Chen, C.-T.; Huang, C.-A.; Huang, B.-H., Aluminium metal complexes supported by amine bis-phenolate ligands as catalysts for ring-opening

polymerization of [varepsilon]-caprolactone. *Dalton Transactions* **2003,** (19), 3799-3803.

9. Ko, B.-T.; Lin, C.-C., Efficient "Living" and "Immortal" Polymerization of Lactones and Diblock Copolymer of ε-CL and δ-VL Catalyzed by Aluminum Alkoxides. *Macromolecules* **1999,** *32* (25), 8296-8300.

10. Chen, H.-L.; Ko, B.-T.; Huang, B.-H.; Lin, C.-C., Reactions of 2,2'-Methylenebis(4-chloro-6-isopropyl-3-methylphenol) with Trimethylaluminum: Highly Efficient Catalysts for the Ring-Opening Polymerization of Lactones. *Organometallics* **2001,** *20* (24), 5076-5083.

11. Huang, C.-H.; Wang, F.-C.; Ko, B.-T.; Yu, T.-L.; Lin, C.-C., Ring-Opening Polymerization of ε-Caprolactone and l-Lactide Using Aluminum Thiolates as Initiator. *Macromolecules* **2001,** *34* (3), 356-361.

12. Gendler, S.; Segal, S.; Goldberg, I.; Goldschmidt, Z.; Kol, M., Titanium and Zirconium Complexes of Dianionic and Trianionic Amine−Phenolate-Type Ligands in Catalysis of Lactide Polymerization. *Inorganic Chemistry* **2006,** *45* (12), 4783-4790.

13. Yang, S.; Nie, K.; Zhang, Y.; Xue, M.; Yao, Y.; Shen, Q., New [ONOO]-Type Amine Bis(phenolate) Ytterbium(II) and -(III) Complexes: Synthesis, Structure, and Catalysis for Highly Heteroselective Polymerization of rac-Lactide. *Inorganic Chemistry* **2013,** *53* (1), 105-115.

14. Phongtamrug, S.; Chirachanchai, S.; Tashiro, K., Supramolecular Structure of N,N-Bis(2-hydroxy-benzyl)alkylamine: From Hydrogen Bond Assembly to Coordination Network in Guest Acceptance. *Macromolecular Symposia* **2006,** *242* (1), 40-48.

15. Phongtamrug, S.; Miyata, M.; Chirachanchai, S., Concerted Contribution of Cu–O Coordination and Hydrogen Bonds in N,N-Bis(2-hydroxybenzyl)alkylamine–Copper–Solvent System. *Chemistry Letters* **2005,** *34* (5), 634-635.

16. Swift, G., Directions for environmentally biodegradable polymer research. *Accounts of Chemical Research* **1993,** *26* (3), 105-110.

17. Miao, Y.; Zinck, P., Ring-opening polymerization of cyclic esters initiated by cyclodextrins. *Polymer Chemistry* **2012,** *3* (5), 1119-1122.

18. von Philipsborn, W., Probing organometallic structure and reactivity by transition metal NMR spectroscopy[dagger]. *Chemical Society Reviews* **1999,** *28* (2), 95-105.

19. Ikpo, N.; Hoffmann, C.; Dawe, L. N.; Kerton, F. M., Ring-opening polymerization of [varepsilon]-caprolactone by lithium piperazinyl-aminephenolate complexes: synthesis, characterization and kinetic studies. *Dalton Transactions* **2012,** *41* (22), 6651-6660.

20. Lu, M.; Yao, Y.; Zhang, Y.; Shen, Q., Synthesis and characterization of anionic rare-earth metal amides stabilized by phenoxy-amido ligands and their catalytic behavior for the polymerization of lactide. *Dalton Transactions* **2010,** *39* (40), 9530-9537.

21. Kowalski, A.; Duda, A.; Penczek, S., Polymerization of l,l-Lactide Initiated by Aluminum Isopropoxide Trimer or Tetramer. *Macromolecules* **1998,** *31* (7), 2114-2122.

22. Sutapin, C.; Mantaranon, N.; Chirachanchai, S., Eight-armed Polydiacetylene under Benzoxazine Dimer Branched Polylactide: A Structural Combination for Reversible Thermochromic Effect and Its Model Case for Free-Standing Poly(lactic acid) Film. *Journal of Materials Chemistry C* **2017**.

CHAPTER IV
EIGHT-ARMED POLYDIACETYLENE UNDER BENZOXAZINE DIMER BRANCHED POLYLACTIDE: A STRUCTURAL COMBINATION FOR REVERSIBLE THERMOCHROMIC EFFECT AND ITS MODEL CASE FOR FREE-STANDING POLY(LACTIC ACID) FILM

4.1 Abstract

Thermochromic polydiacetylenes (PDAs) are known for its conjugated bonds with reversibility when the molecules are maintained with the bond distance of the polymer backbone along with the stacking angle. With this structural requirement, the fabrication of PDAs has to rely on the thin films or coatings on the substrates which the alignment and packing of the molecules can be controlled at the molecular level. The present work demonstrates for the first time, a free standing thermochromic film based on the poly(lactic acid) (PLA) film as a model case. Here, the PDA under the star structure is considered as the approach to provide the symmetrical chains for PDA so that the PDA molecules are aligned under the chain distance is controlled by the steric branches. By simply constructing an eight-armed benzoxazine dimer from the tetra-branched benzoxazine core followed by lactide ring opening polymerization as well as the conjugation with diacetylenes at each terminal, a precise eight-branched diacetylenes, i.e. 4BzD-8PPLA-8DA, can be easily obtained. The blend of this compound with PLA resin followed by solution casting leads to the free standing film with reversible thermochromic properties. The comparative studies on PLA films containing other types of branching PLLA terminated with PDA clarifies to us that those films do not show reversible thermochromism at all. The microstructure analyses indicate the symmetrically eight-armed 4BzD-8PPLA core play an important role to provide the framework for maintaining the ene-yne conjugated bond under a certain mobility 4BzD-8PPLA-8PDA/PLA upon heating and cooling to result in the reversible thermochromic behavior.

Keywords: Benzoxazine dimer, Polydiacetylene, Poly(latic acid) film, Reversible thermochromic film, Lactide

4.2 Introduction

Polydiacetylene (PDA) is known for its unique thermochromism based on the ene-yne conjugated structure. PDA can be prepared by photo-irradiation of molecularly assembled diacetylene (DA) monomer without the need of initiators or catalysts. In general, a topochemical polymerization occurs within DA crystal when a translation distance is around 5 Å and a stacking angle of 45°.[1-2] PDA can be either planar or non-planar form to show an absorbance maximum at 650 nm (blue) or at 540 nm (red),[3] respectively. The colorimetric transitions of PDAs take place in response to various external stimuli such as solvent,[4-5] temperature,[6] mechanical strain,[7] and ligand-receptor interactions.[8]

The transition from blue to red represents a disruption in the planar conformation and a reduction in the conjugation length of the PDA backbone. With the thermochromic property, PDA is applied for sensors, indicators, etc., through the several fabrications such as vesicles in aqueous solution,[9] Langmuir monolayers,[10] dip-coating,[11] and spin-coating[12] on solid-support or blend with host polymers. It is important to note that although PDAs are variously applied, the reversibility of thermochromic is not always the case. Several reports point out that the thermochromics reversibility occurs when PDAs are in a particular framework under molecular interaction. For example, Yuan *et al.*[13-14] and Kim *et al.*[15] demonstrated PDAs with pH and thermochromic reversibility under the hydrogen bond network within terephthalic acid groups on the side chains. Lee *et al.*[16] successfully developed a new PDA derivative (Bis-PDA-Ph) that consists of two PDAs linked via a *p*-phenylene group. The Bis-PDA-Ph exhibited excellent thermochromic reversibility because the hydrophobic interactions between alkyl chains and π−π interactions between aryl groups. Moreover, Chanakul *et al.*[17] fabricated PDA/ZnO nanocomposite, which exhibited reversible thermochromic behaviors. The thermochromic reversibility of the PDA/ZnO nanocomposites was due to the strong interfacial interactions between carboxylate head of PDAs and hydroxyl groups on ZnO surface that limited the dynamics of PDAs backbone structure.

It should be noted that although several potential applications are reported, in most cases, the material fabrications has to rely on the neat and sophisticated steps such

as coating and etc. so that the molecular packing can be maintained. In fact, those preparations obstruct the practical uses. To the best of our knowledge, the reversible thermochromic PDAs as a bulk product in the blend or compounding has not yet been reported. It comes to our viewpoint to aim for the free standing thermochromic film with reversibility.

In order to achieve the goal, the PDA chains have to be satisfied with the framework to maintain the conformation under a stacking angle and the ene-yne conjugation length. In fact, the star molecule with highly symmetrical chains is considerable since each chain to chain distance is controlled by the steric branches.

On this viewpoint, various types of core molecules, e.g. linear, tetra-, eight- and multi-branches, have to be taken into the consideration. In addition, as the present work aims to show the free-standing film with thermochromic properties, it is necessary to focus on the polymer with an ease of film fabrication property as well as the functionalization. To this end, the use of core molecules containing hydroxyl group allows us a simple conjugation with poly(L-lactide) via the ring opening polymerization to obtain poly(L-lactide) (PLLA) star molecules. Scheme 4.1 shows an example in the case of eight-armed branched core molecule. This leads to star and/or multi-branched PLLA which the terminal ends contain reactive groups, i.e. hydroxyl and/or carboxyl groups, for further modification with DA derivatives. In this way, the star and/or multi-branched PLLA terminated with DA can be obtained accordingly which can be considered as functional additives for PLA resin. The blend with PLA resin followed by film casting allows us to obtain a free-standing film with DA chains.

Based on the abovementioned steps, the present work demonstrates molecular designs and syntheses of star/multi-branched PLLA with PDA terminals and focuses on the PLA film performances. The challenge of this work is, therefore, to declare the favourable conditions as well as the factors that bring PDA chains expressing the thermochromic reversibility in the free-standing film.

4.3 Experimental

4.3.1 Materials

Pentaerythritol**,** 2-bromoethylamine hydrobromide, paraformaldehyde, 2,4-dimethyl phenol, methylamine, 1-ethyl-3-(3-dimethylaminopropyl)carbodiimide, *N*-hydroxysuccinimide, 10,12-pentacosadiynoic acid, tin(II) 2-ethylhexanoate, L-lactide, phenol, branched polyethylenimine with Mn ~10,000 by GPC, *N'N*-dimethylformamide, , and deuterated chloroform (CDCl$_3$) were purchased from Sigma-Aldrich Co. LLC, Germany. L-Lactide was purified by recrystallization three times in toluene under argon atmosphere followed by sublimation under vacuum at 85 °C. Sodium hydroxide**,** potassium hydroxide**,** 4-dimethylaminopyridine, and sodium sulfate anhydrous were obtained from Fluka, Germany. Acetonitrile, chloroform, methanol, dichloromethane, HPLC-grade chloroform, and diethyl ether were received from RCI Labscan, Thailand. Commercial PLLA (trade name 2002D), hereinafter abbreviated as PLLA, (M$_n$ = 163,500, M$_w$ = 287,900, a polydispersity index of M$_w$/M$_n$ = 1.76, T$_g$ = 57.6 °C, T$_c$ = 127 °C, and T$_m$ = 153 °C) was bought from NatureWorks LLC, USA.

4.3.2 General methods and instrumentation

^{1}H NMR spectra were recorded at 25 °C in deuterated chloroform (CDCl$_3$) on a Bruker Biospin Avance 500 nuclear magnetic resonance (NMR) spectrometer. All chemical shifts were reported in parts per million (ppm) and measured relative to the solvent in which the sample was analyzed (CDCl$_3$ δH = 7.26 ppm). Molecular weight and polydispersity were determined by a Shimadzu Class-VP size-exclusion chromatograph (SEC) equipped with a PLgel 5 μm MIXED-D column 300 x 7.5 mm (Polymer Laboratories, Varian Inc.) and a refractive index detector. Chloroform was used as an eluent at a flow rate of 1.0 mL min-1. Polystyrene standards were used and the measurements were performed at 40 °C. The injection volume was 20 μL. Mass spectroscopy was analyzed by a Bruker micrOTOF II electrospray ionization mass spectrometer (ESI-TOF MS). Polymerization of diacetylene unit was performed by irradiating the solid in a UV chamber (400 W) for 20 min. Absorption spectra were recorded using an Agilent cary 300 UV-Vis spectrophotometer. The X-ray wavelength (λ) was tuned at 0.1549 nm, and the scattering vector (q) defined by q = (4π/λ)sin(θ/2) (θ: the scattering angle), was calibrated by silverbehenate (AgBH). The packing structure was characterized by a Rigaku RINT 2000 wide angle X-ray diffraction (WAXD) using Cu Kα line as the incident X-ray beam. The diffraction profiles were

measured in a reflection mode at 5° 2θ - 60° 2θ at a scanning rate of 2°/min. Raman scattering measurements were performed with a Thermo Scientific DXR Raman microscope at a laser excitation wavelength of 780 nm. Optical and fluorescence microscopy images were obtained by using an Olympus BX51 W/DP70 microscope.

4.3.3 Preparation of eight-armed diacetylene (4BzD-8PLLA-8DA)

2,2'-((2,2-bis((2-aminoethoxy)methyl)propane-1,3 diyl)bis(oxy))bis(ethan-1-amine) (core molecule) was prepared by stirring pentaerythritol (136.15 mg, 1 mmol) with 2-bromoethylamine hydrobromide (819.5 mg, 4 mmol) in N'N-dimethylformamide (DMF) at 90 ˚C for 12 h. Sodium hydroxide solution (0.5 N) was added dropwise into the reaction. The mixture was stirred for 3 h before filtration. The product was precipitated in DI water and dried under vacuum to yield core molecule as a white precipitate (73% yield).

The formation of 3,3'-(((2,2-bis((2-(6,8-dimethyl-2H-benzo[e][1,3]oxazin-3(4H)-yl)ethoxy)methyl)propane-1,3-diyl)bis(oxy))bis(ethane-2,1-diyl))bis(6,8-dimethyl-3,4-dihydro-2H-benzo[e][1,3]oxazine), 4BzM, was achieved according to Mannich reaction of 2,4-dimethyl phenol (343.3 mg, 2.8 mmol), core molecule (215.9 mg, 0.7 mmol), and p-formaldehyde (180.2 mg, 6.0 mmol) in 20 ml dioxane. The reaction was accomplished under reflux condition for 17 h. The yellowish crude product obtained was dissolved in chloroform and purified by column chromatography eluting with chloroform to obtain 4BzM (380.5 mg, 60% yield).

The ring opening reaction of 4BzM to obtain 4BzD was carried out by mixing 2,4-dimethyl phenol (196.2 mg, 1.6 mmol) and 4BzM (380.5 mg, 0.4 mmol) in molten stage. The crude product was purified by column chromatography eluting with chloroform to yield 4BzD for 41 %. ^{1}H NMR (500 MHz, CDCl$_3$, ppm): δH 6.87 (d, J = 8.09 Hz, 8H, Ar-H), 6.69 (d, J = 8.10 Hz, 8H, Ar-H), 3.88 (s, 8H, -CH$_2$- of pentaerytritol), 3.69 (s, 16H, N-CH$_2$-), 3.40 (d, J = 7.76 Hz, 8H, -CH$_2$-), 2.27 (d, J = 7.36 Hz, -CH$_3$); ESI-TOF m/z: calculated for [M+Na$^+$] = 1403.82, found 1403.88.

In a glove box under Argon gas, 4BzD (69.0 mg, 0.1 mmol) was used as initiator for ring opening polymerization of L-lactide (1441.4 mg, 20 mmol) at molar ratio 1:200 of 4BZD: L-lactide in bulk at 120 °C with 4-dimethylaminopyridine (97.8 mg, 0.8 mmol). At the end of the reaction, the medium was viscous (95% conversion as judged by ^{1}H NMR). The crude product was precipitated in cold diethyl ether and

washed three times with this solvent before being dried under vacuum to obtain eight-armed polylactide (4BzD-8PLLA). ^{1}H NMR (500 MHz, CDCl$_3$, ppm): δH 8.12 (m, 4H, Ar-H), 7.62 (s, 4H, Ar-H), 6.93 (s, 4H, Ar-H), 6.77 (m, 4H, Ar-H), 5.15 (m, 298H, -OCH(CH$_3$)C(O)- of PLLA), 4.37 (m, 8H, terminal -OC(O)CH(CH$_3$)-OH), 3.72 (s, 8H, -CH$_2$- of pentaerythritol), 3.51 (d, J = 13.04 Hz, 8H, N-CH$_2$- of BzD), 3.42 (s, 16H, O-CH$_2$-), 2.59 (s, 8H, -CH$_2$-), 1.58 (OCH(CH$_3$)C(O)- of PLLA and -CH$_3$ of 4BzD). GPC analysis indicated M_n = 24562 g mol^{-1} and M_w/ M_n = 1.19. The average degree of polymerization (DP$_n$) of PLLA branches in average could be calculated based on integration of the proton of –CH– of PLLA and the proton of –CH– terminal group, which are at δH 5.15 ppm and 4.37 ppm, respectively. ^{1}H NMR analysis indicated a DP$_n$ of 19 lactide units per chain.

The mixture of 1-ethyl-3-(3-dimethylaminopropyl)carbodiimide (76.7 mg, 0.4 mmol), *N*-hydroxysuccinimide (46.1 mg, 0.4 mmol), and 10,12-pentacosadiynoic acid (DA) was stirred at 0 °C in 10 ml chloroform. The solution was stirred at room temperature for 12 h. to obtain pink clear solution. 4BzD-8PLLA (246.5 mg, 0.01 mmol) was dissolved in chloroform (5 ml) and added dropwise into pink clear solution. The conjugation reaction was allowed stirring at room temperature for 20 h. The solution was purified by precipitating in cold diethyl ether. The product was filtrated and dried under vacuum to obtain 85% yield of 4BzD-8PLLA-8DA. ^{1}H NMR (500 MHz, CDCl$_3$, ppm): δH 7.38 (m, 8H, Ar-H), 7.12 (m, 8H, Ar-H), 6, 5.15 (m, 180H, -OCH(CH$_3$)C(O)- of PLLA), 4.37 (m, 8H, terminal -OC(O)CH(CH$_3$)-OH), 3.72 (s, 8H, -CH$_2$-), 3.54 (m, 16H, N-CH$_2$-), 3.42 (s, 8H, O-CH$_2$-), 2.65 (s, 16H, -CH$_2$-) 2.51 (m, 8H, PLLA-OC(O)CH$_2$- of DA), 2.23 (m, 32H, -CH$_2$-C≡C-), 1.58 (OCH(CH$_3$)C(O)- of PLLA and -CH$_3$ of 4BzD), 1.27 (m, 240H, -CH$_2$-), 0.88 (t, 16H, -CH$_2$-CH$_3$).GPC analysis indicated M_n = 11153 g mol^{-1} and M_w/ M_n = 1.13.

Furthermore, other diacetylene compounds, i.e. linear diacetylene (PLLA-DA), 4-armed diacetylene (4PLLA-4DA), and multi-armed diacetylene (mPEI-PLLA-DA) were prepared as shown in Supporting Information. Chemical structures of DA, PLLA-DA, 4PLLA-4DA, and mPEI-PLLA-DA are shown in Scheme 4.2.

Scheme 4.1 Overall reactions for preparing 4BzD-8PLLA-8DA.
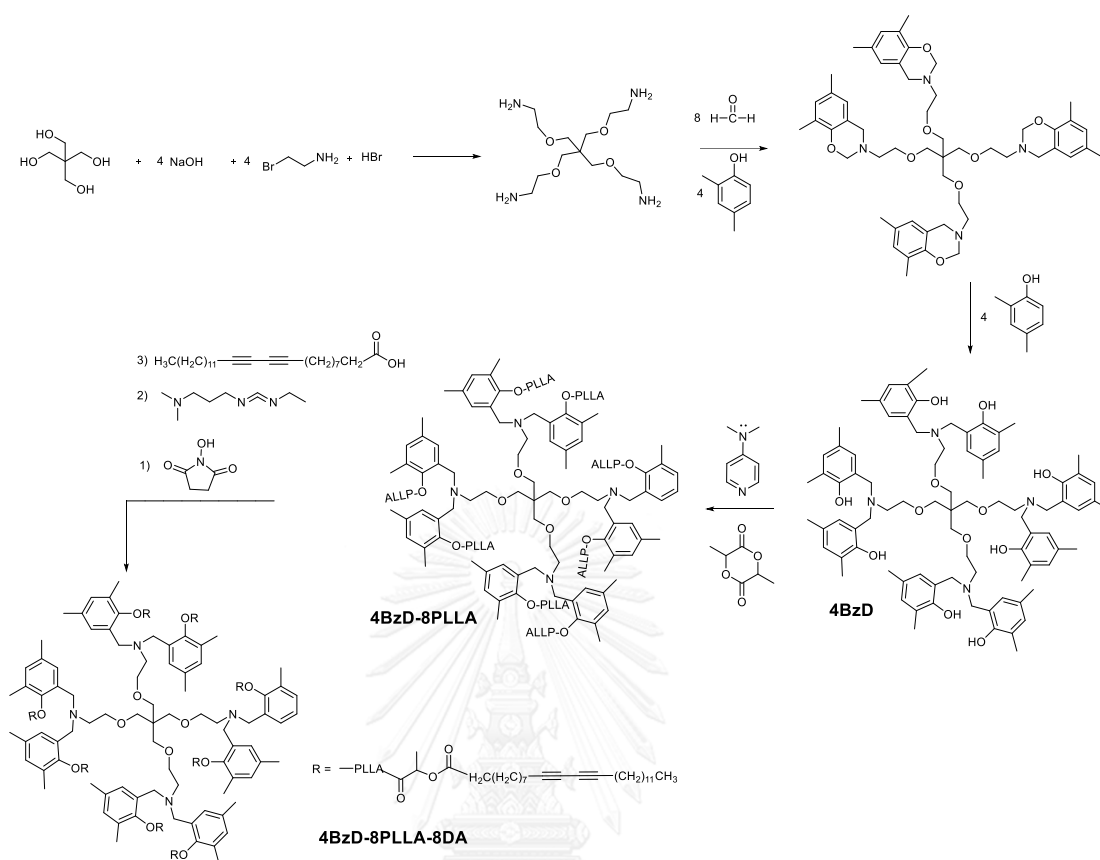
Scheme 4.2 Chemical structures of DA, PLLA-DA, 4PLLA-4DA, and mPEI-PLLA-DA.
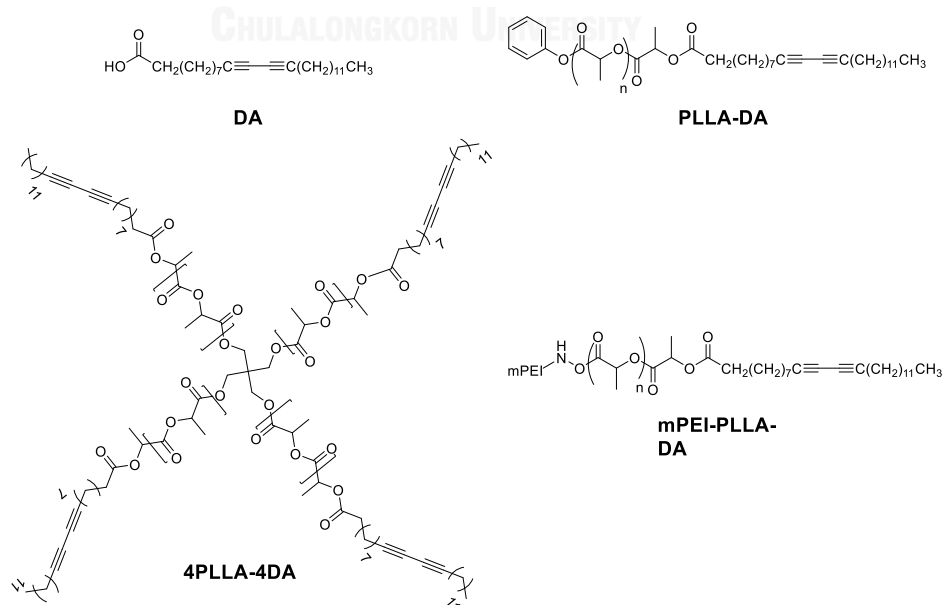
4.3.4 Film preparation and diacetylene polymerization

PLA resin was mixed with 5 phr of 4BzD-8PLLA-8DA in chloroform at room temperature under stirring. The solution was casted on a Teflon plate. The solvent was evaporated naturally to obtain 4BzD-8PLLA-8DA/PLA casted film. The films obtained were exposed to UV light at 254 nm for 30 min. Polydiacetylene was formed in PLA matrix of the casted film, so-called 4BzD-8PLLA-8PDA/PLA film.

Similarly, the blend and polymerization were carried out by using DA, PLLA-DA, 4PLLA-4DA, and mPEI-PLLA-DA instead of 4BzD-8PLLA-8DA to obtain PDA/PLA, PLLA-PDA/PLA, 4PLLA-4PDA/PLA, and mPEI-PLLA-PDA/PLA film, respectively.

In fact, the increase of PLLA-DA, 4PLLA-4DA, and mPEI-DA content to 50%, 15% and 25% induced the topochemical polymerization of DA in PLA matrices, thermochromic properties of prepared films can be observed but they cannot completely reversible. 5 phr is the optimal content for further investigation.

4.4 Results and Discussion

4.4.1 Preparation of branched diacetylene

In order to develop the free-standing film with thermochromic based on PDA, the PLA films were focused as model cases. As shown in Schemes 4.1 and 4.2, for comparative studies, PDA molecules in the forms of linear-, tetra-, eight-, including multi-armed star on PLLA chain terminals were prepared via lactide ring opening polymerization. For 4BzD, the compound was easily prepared by the use of pentaerithritol as the core molecules and as the initiator for ʟ-lactide ROP at the same time. The compound obtained was confirmed to be a tetra-armed PLLA branched. The reaction with DA led to the DA molecules at the four terminals which are ready for topochemical polymerization to obtain 4PLLA-4DA. The ^{1}H NMR in Figure B1 showed four peaks of five aromatic protons at δH 7.36 ppm, 7.07 ppm, 6.90 ppm, and 6.80 ppm, respectively, which is an initiator with one proton of terminal PLLA chains and two methylene protons of PLLA–OC(O)CH$_2$– of DA at δH 4.34 ppm and 2.51 ppm, respectively. The signals at δH 4.35 ppm, 3.45 ppm, and 2.58 ppm (Figure B2) are referred to terminal PLLA chains, –CCH$_2$O– of initiator and PLLA–OC(O)CH$_2$– of

DA, respectively. For mPEI-PLLA-DA, the preparation is rather simple. The mPEI was directly initiated the ROP of L-lactide. The terminals were similarly modified with DA. Figure B3 confirmed the signal at δH 3.59 ppm for mPEI core molecule apart from the signals at δH 4.34 ppm and 2.58 ppm referring to terminal PLLA chains and PLLA–OC(O)CH$_2$– of DA, respectively.

In the case of eight-armed PLLA, the molecular design was considered as follows. In the past, our group demonstrated how monophenol-based benzoxazine develops a single ring opening under self-termination to result in the benzoxazine dimer containing two phenols.[23-24] In other words, as shown in Scheme 4.1, this molecule is useful for developing the eight-armed core. Here, the modification of hydroxyl groups of pentaerythritol to amine groups allows us forming benzoxazines and benzoxazine dimers, respectively. This brings us not only obtaining eight-armed core molecules but
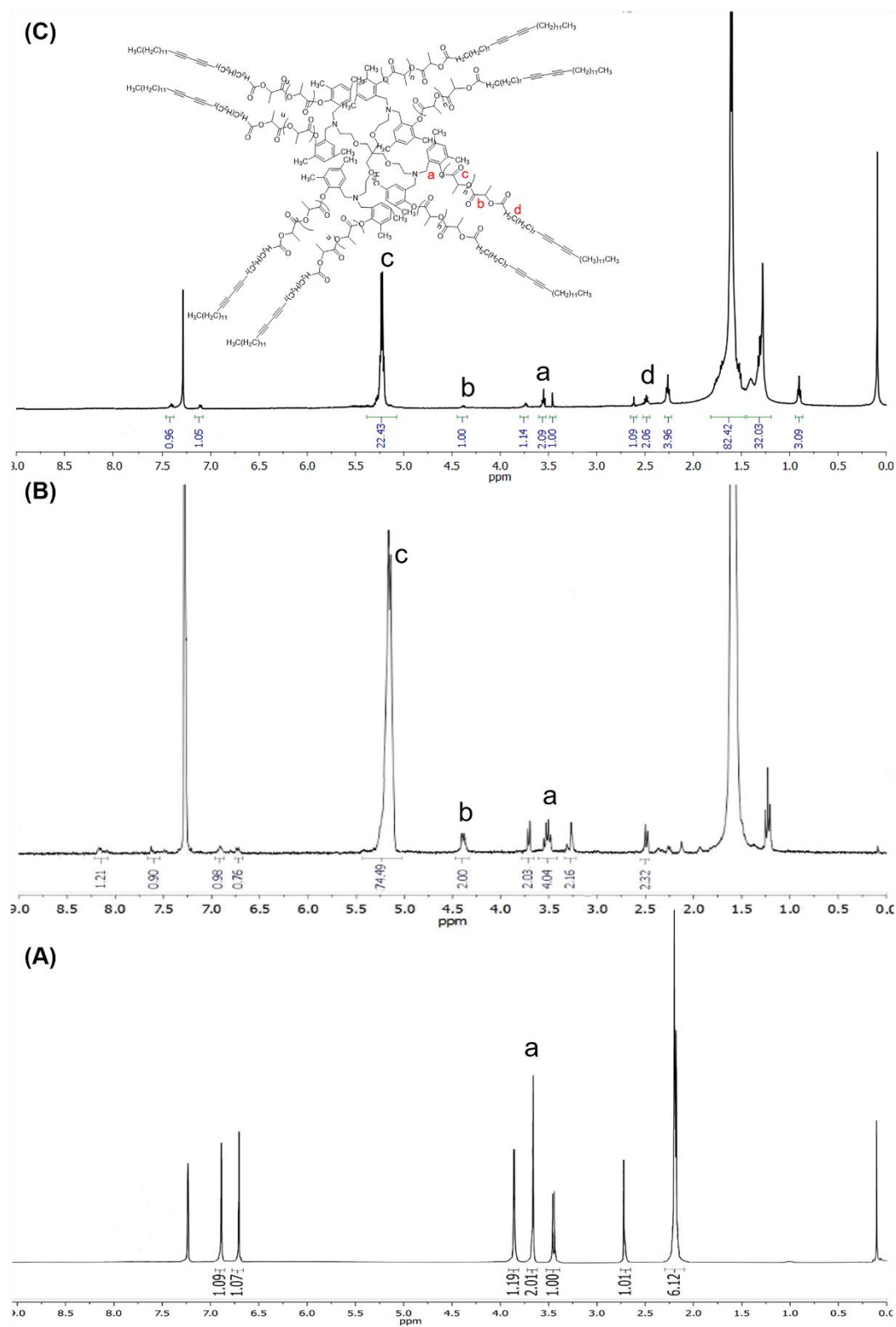
Figure 4.1. ^{1}H NMR of (A) 4BzD, (B) 4BzD-8PLLA, and (C) 4BzD-8PLLA-8DA.

also the possibility to extend the PLLA chains by ring opening polymerization of L-lactide based on phenol initiators. To these PLLA terminals, the conjugation with diacetylene derivatives followed by photo-polymerization leads us to the PDA under eight-armed branching structure. Figure 4.1(A) shows the ^{1}H NMR spectrum of 4BzD. After L-lactide ROP (Figure 4.1(B)), the eight methine protons of $-OC(O)CH(CH_3)$-OH of terminal PLLA chains at δH 4.37 ppm (assigned as b) and methine proton of $-OC(O)CH(CH_3)-$ of L-lactide repeating unit along the polymer chains at δH 5.15 ppm (assigned as c) are observed with the sixteen protons of methylene bridge of 4BzD at δH 3.51 ppm (assigned as a). For 4BzD-8PLLA-8DA (Figure 4.1(C)), sixteen methylene protons of PLLA$-OC(O)CH_2-$ of DA at δH 2.51 ppm (assigned as d) is appeared with eight protons of terminal PLLA chains and sixteen methylene protons of 4BzD. Further analysis by total correlated spectroscopy (TOCSY) indicated the linkage of proton at δH 4.37 ppm with δH 2.51 ppm through 5 chemical bonds (Figure B4) suggesting the connection of hydroxyl groups of PLLA and carboxylic groups of DA via conjugation.
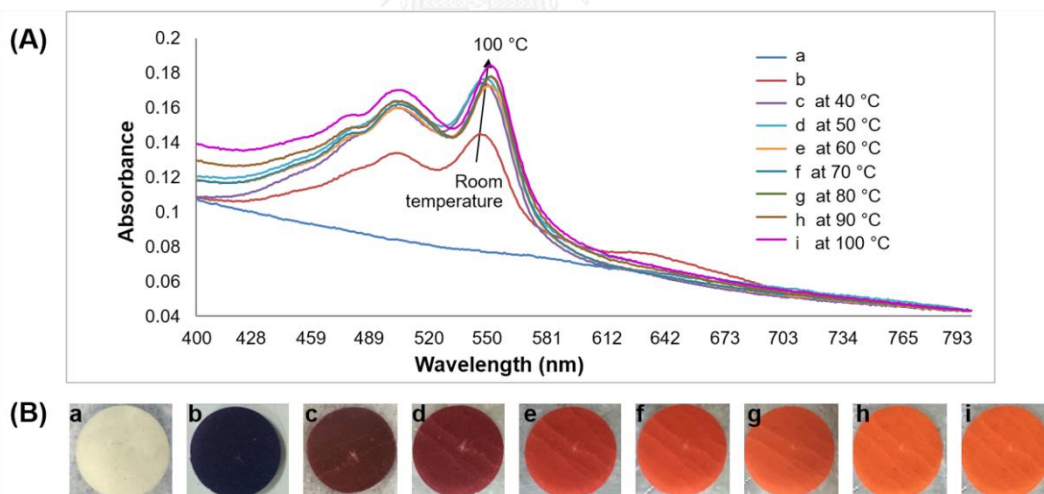
Figure 4.2. (A) UV-Vis spectra and (B) color appearances of 4BzD-8PLLA-8DA.

4.4.2 Thermochromic behaviors

In the case of 4BzD-8PLLA-8DA, topochemical polymerization of diacetylene was primarily traced by UV-Vis spectra and the color appearances. Figure 4.2(A) shows that before UV light exposure, 4BzD-8PLLA-8DA (curve a) does not show any peak in UV spectrum. After UV light exposure for 30 min, two absorption

peaks of π-π* transition (excitonic absorption) at 630 nm and 547 nm and one absorption peak of the phonon side band of the PDA at 500 nm are observed (Figure 4.1(A) curve b) and at that time the color is changed from white to dark blue (Figure 4.2(B) b). This confirms the topochemical polymerization of DA to obtain BzD-8PLLA-8PDA. After PDA was formed, the further thermal treatment was carried out. Figure 4.2(A), the spectra c-i, show that when the film was treated at 100 ˚C, the peak at 630 nm is disappeared whereas the peak at 547 nm is shifted to 550 nm. At that time, the film color develops from the dark blue to red, and orange gradually. This implies the change of crystal formation on a shorter delocalization length of the π-electron by distortion of PDA as reported by Kuriyama et al.[20] The UV spectra of DA, PLLA-DA, 4PLLA-4DA, and mPEI-PLLA-DA after UV exposure were similar to that of 4BzD-8PLLA-8DA (Figures B5).
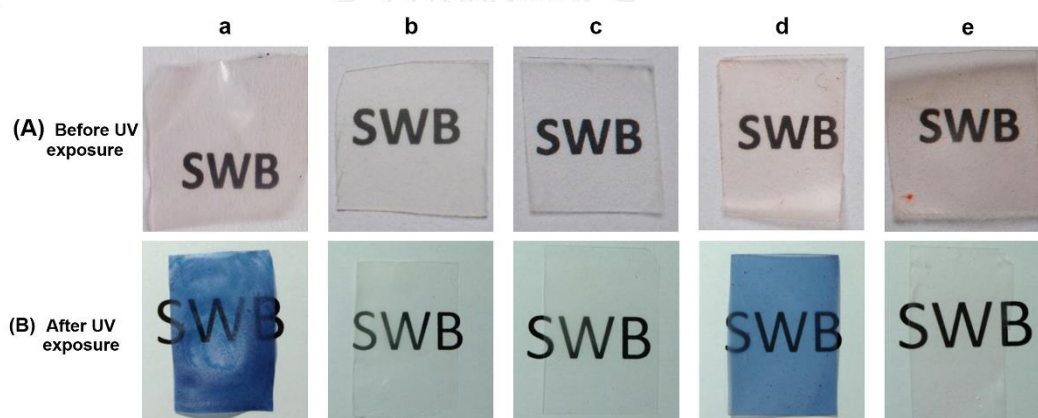
Figure 4.3. Various PLA films containing DA derivatives, (a) DA/PLA, (b) PLLA-DA/PLA, (c) 4PLLA-DA/PLA, (d) 4BzD-8PLLA-8DA/PLA, and (e) mPEI-DA/PLA, for (A) as-prepared films, and (B) after UV exposure.

4.4.3 Thermochromic properties of PLA films containing DA derivatives

All types of derivatives, i.e. DA, PLLA-DA, 4PLLA-4DA, 4BzD-8PLLA-8DA and mPEI-PLLA-DA were blended with PLA resin followed by solution casting to obtain five different types of PLA films (Figure 4.3(A)). Before the blended films were exposed to UV light, the polymerization kinetics of 4BzD-8PLLA-8DA/PLA film exposed to 254 nm UV light were studied (Figure B6(A)). The maximum absorbance at 640 nm was plotted as a function of exposure time as showed

in Figure B6(B). The polymerization finished at exposure time 30 min. It might be due to the DA polymerization occurred in PLA matrix which disturb the polymerization process so this process takes longer time than that of pure DA. After UV exposure, only PLA films containing DA (Figure 4.3(B) a) and 4BzD-8PLLA-8DA (Figure 4.3(B) d) change from the colorless transparent film to the dark blue transparent films. This indicates the topochemical polymerization occurs only in the cases of a and d. In other words, DA/PLA and 4BzD-8PLLA-8DA/PLA are changed to PDA/PLA and 4BzD-8PLLA-8PDA/PLA, respectively. By heating from 35°C to 100°C, the chromatic transformations of PDA/PLA and 4BzD-8PLLA-8DA/PLA were clearly identified as seen from the color changing from blue to purple, red and orange (movie S1), respectively. However, only the 4BzD-8PLLA-8DA/PLA film shows a complete reversibility between blue and orange when the temperature was in range 35°C to 100°C.

4.4.4 Reversible thermochromic behaviors

The ene-yne conjugated backbone in PLA matrices was confirmed by Raman spectroscopy. The characteristic vibration band of $–C≡C–C≡C–$ is known to appear at 2260 cm^{-1}.[21] After irradiation, PDA/PLA, 4BzD-8PLLA-8PDA/PLA, and mPEI-PDA/PLA films clearly show a significant peak at 2100 cm^{-1}, implying topochemical polymerization of ene-yne backbone (Figure B7). It is important to note that as PLLA-PDA/PLA and 4PLLA-PDA/PLA films did not show the peak at 2100 cm^{-1} but at 1760 cm^{-1}, this reflects the intermediate step of polymerization to form $(–C=C=C=C–)_n$ backbone.[21] In other words, the topochemical polymerizations were uncompleted. It might be due to the loose packing structure of DA unit in PLA matrix obstructing the polymerization. The colorimetric transformation of the films allows us evaluating the thermochromic behaviour. Here, the temperature dependence Raman spectroscopy technique (Figures 4.4 and B7) was applied. It is important to note that in the case of mPEI core molecule, the PDA is in the randomly and highly multi-branched structure. In other words, the color transformation of mPEI-PDA/PLA film reflects how the highly branching structure favours the thermochromic behaviour. As shown in Figures 4.4(C), the mPEI-PDA/PLA film did not show any Raman shift upon heating and cooling. In fact, the film did not show any color changes. This implies that the

highly branched PEI might give the steric hindrance under the disordered structure to obstruct the distortion of ene-yne conjugated backbone. For PDA/PLA, the shift is suddenly increased from 2090 cm^{-1} to 2118 cm^{-1} during the increase of temperature from 30 ˚C to 70 ˚C (Figure 4.4(A)). The color was also changed from dark blue to orange. This indicated the distorted side chain imposed on a shorter conjugation length.[20] However, in the cooling step, the Raman shift is not observed and the color was remained orange. This reflects the remaining of distorted side chain in between the PLA matrices where the more free volume might be offered due to the loose packing structure of DA in PLA matrices.
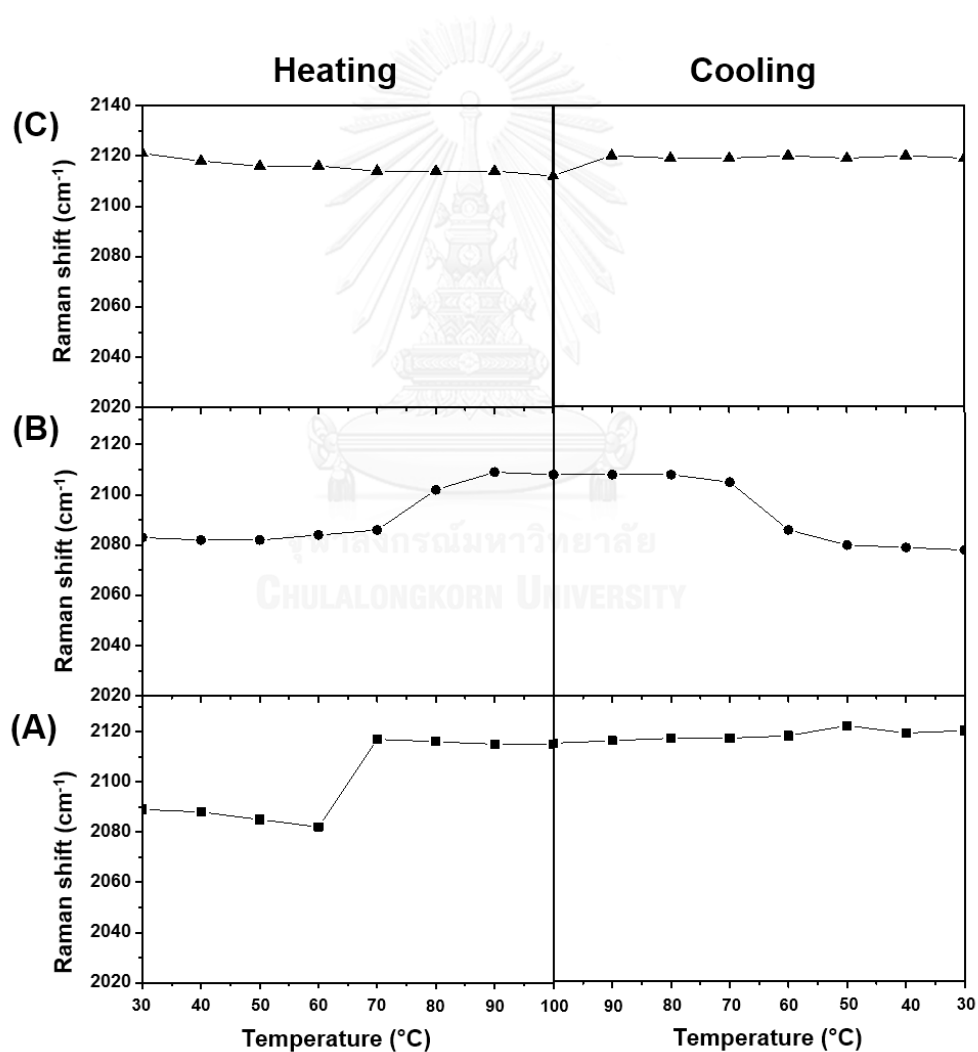
Figure 4.4. Temperature dependence Raman Spectroscopy of (A) PDA/PLA, (B) 4BzD-8PLLA-8DA/PLA, and (C) mPEI-PDA/PLA upon heating and cooling.

The reversible thermochromic effect was observed only in the case of 4BzD-8PLLA-8PDA/PLA (Figure 4.4(B)). Here, the Raman shift slightly increases from 2085 cm^{-1} to 2114 cm^{-1} with an increase in temperature from 30 ˚C to 100 ˚C. On the other hand, the Raman shift during cooling indicates the re-emergence of the peak around 2075 cm^{-1} corresponds to the blue phase of 4BzD-8PLLA-8PDA/PLA. Importantly, the blue-orange transition was reversible even many heating-cooling cycles were carried out. It should be noted that while several reports showed the temperature-cycled color reversible transformations of PDA systems,[22-23] those are the thin films where the ene-yne structure was controlled in nanometer level. In other words, the color reversible transition in the free-standing film as seen in the present case has not yet been previously reported.

4.4.5 Observation of 4BzD-8PPLA-8DA/PLLA chain packing

It comes to the question why the thermochromic behavior occurred only in the case of 4BzD-8PPLA-8PDA/PLA. In other words, how the molecular alignment of PDA in the case of 4BzD-8PPLA-8PDA in PLA matrix is differed from other cases, for example the case of PDA/PLA. Figure 4.5 shows the temperature dependence WAXD patterns which help us declaring the packing structure of PDA/PLA and 4BzD-8PPLA-8PDA/PLA while the thermal treatment. For PDA/PLA (Figure 4.6(A)), the crystalline phase of PLA was found to decrease upon heating whereas the PDA packing was also found to be distinctly decreased.
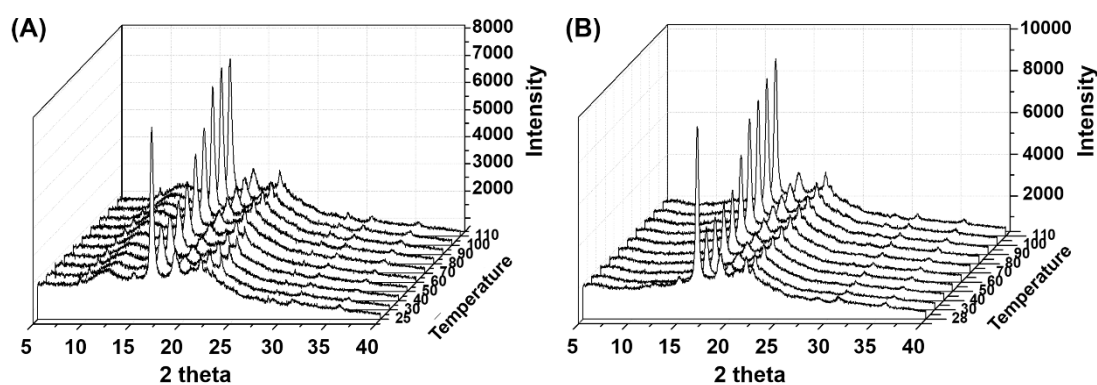

Figure 4.5. Temperature dependent of (a) PDA/PLLA film and (b) 4BzD-8PPLA-8DA/PLLA film.

This suggested the chain mobility at high temperature induces the amorphous phase. When it comes to the cooling step, the WAXD patterns indicate clearly that the crystalline phase is remained unchanged. This implies the distortion of PDA chains in PLA matrices resulting in the loose-packing structure of PDA.
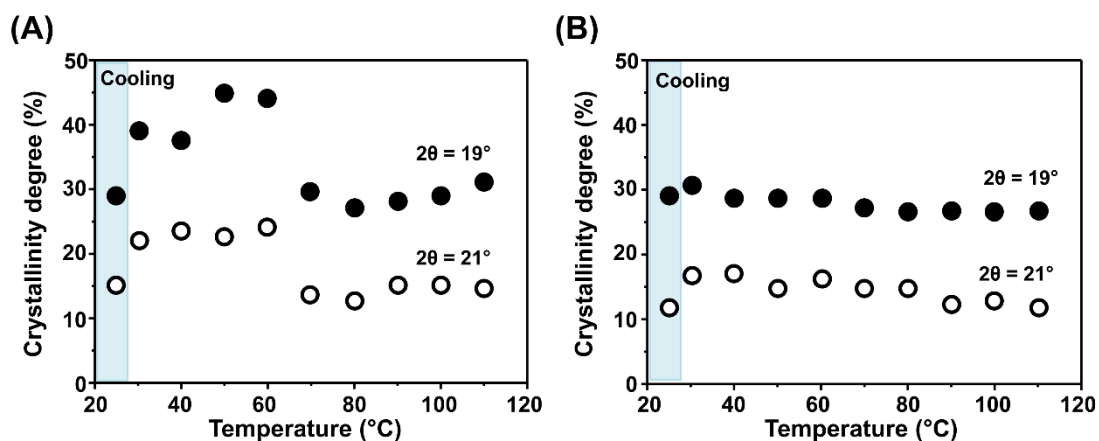

Figure 4.6. Crystallinity degree of (•) PLA and (○) PDA in (A) PDA/PLA and (B) 4BzD-8PPLA-8PDA/PLA calculated from curve fitting of temperature dependence WAXD patterns.

In the case of 4BzD-8PPLA-8PDA/PLA (Figure 4.6(B)), the crystallinity degree is remained constant either upon heating or cooling. This implies that the eight-armed branched PLLA controlled the chain mobility of PDA in the framework under the highly symmetrical branches. The highly ordered structure of the eight armed PLLA might lead to the dense packing of 4BzD-8PPLA-8PDA and allow a certain distortion but it is still recoverable between the planar and non-planar of ene-yne conjugated backbone in PLA matrices. Moreover, DSC thermogram in Figure B8(A) d, Only 4BzD-8PPLA-8PDA/PLA showed Tc around 77°C at cooling scan that refer the well packing structure of 4BzD-8PPLA-8PDA initiated crystalline phase of PLA.

4.5 Conclusions

PDA is known for its thermochromic which is responsive to the temperature

when the planar structure as well as the ene-yne conjugated bonds was in a certain level of chain mobility to recover the structure. The present work proposed the use of star structure to maintain the framework for PDA so that the reversible thermochromic is possible. A comparative studies on linear and branching structure declared that the eight-armed star control the packing structure of PDA leading to a successful thermochromic effect. The benzoxazine dimers extended from pentaerythritol core enable us to obtain an eight-armed star, 4BzD-8PPLA-8DA. The conjugation with PLLA on the core molecules followed by conjugating with DA led to a functional additive for the blend with PLA resin. The free standing 4BzD-8PPLA-8DA/PLA film was easily obtained by solution casting. The film developed the color changing from blue to red upon UV exposure and the color was responsive and reversible to the temperature. The comparative studies based on linear DA, four-armed star DA, and multi-branched DA, clarified that only eight-armed star controls the packing structure of PDA even the chain mobility was significant during thermal treatment to result in the reversible thermochromic behaviour. The present work showed for the first time a PLA film with eight-armed branches PDA showing the thermochromic properties which is a model case to develop other PDA free-standing films.

4.6 Acknowledgements

4.7 References

1. Baughman, R. H.; Yee, K. C., Solid-state polymerization of linear and cyclic acetylenes. *Journal of Polymer Science: Macromolecular Reviews* **1978,** *13* (1), 219-239.

2. Curtis, S. M.; Le, N.; Nguyen, T.; Ouyang, X.; Tran, T.; Fowler, F. W.; Lauher, J. W., What have We Learned about Topochemical Diacetylene Polymerizations? *Supramol. Chem.* **2005,** *17* (1-2), 31-36.

3. Schott, M., The Colors of Polydiacetylenes: a Commentary. *The Journal of Physical Chemistry B* **2006,** *110* (32), 15864-15868.

4. Yoon, J.; Chae, S. K.; Kim, J.-M., Colorimetric Sensors for Volatile Organic Compounds (VOCs) Based on Conjugated Polymer-Embedded Electrospun Fibers. *J. Amer. Chem. Soc.* **2007,** *129* (11), 3038-3039.

5. Pumtang, S.; Siripornnoppakhun, W.; Sukwattanasinitt, M.; Ajavakom, A., Solvent colorimetric paper-based polydiacetylene sensors from diacetylene lipids. *J. Colloid Interface Sci.* **2011,** *364* (2), 366-372.

6. Wacharasindhu, S.; Montha, S.; Boonyiseng, J.; Potisatityuenyong, A.; Phollookin, C.; Tumcharern, G.; Sukwattanasinitt, M., Tuning of Thermochromic Properties of Polydiacetylene toward Universal Temperature Sensing Materials through Amido Hydrogen Bonding. *Macromolecules* **2010,** *43* (2), 716-724.

7. Robert, W. C.; Darryl, Y. S.; Matthew, S. M.; Eriksson, M. A.; Alan, R. B., Polydiacetylene films: a review of recent investigations into chromogenic transitions and nanomechanical properties. *J. Phys.: Condens. Matter.* **2004,** *16* (23), R679.

8. Dogra, N.; Li, X.; Kohli, P., Investigating ligand-receptor interactions at bilayer surface using electronic absorption spectroscopy and Fluorescence Resonance Energy Transfer. *Langmuir* **2012,** *28* (36), 12989-12998.

9. Kolusheva, S.; Kafri, R.; Katz, M.; Jelinek, R., Rapid Colorimetric Detection of Antibody−Epitope Recognition at a Biomimetic Membrane Interface. *J. Am. Chem. Soc.* **2001,** *123* (3), 417-422.

10.   Ritenberg, M.; Kolusheva, S.; Ganin, H.; Meijler, M. M.; Jelinek, R., Biofilm Formation on Chromatic Sol–Gel/Polydiacetylene Films. *ChemPlusChem* **2012,** *77* (9), 752-757.

11.   You, X.; Zou, G.; Ye, Q.; Zhang, Q.; He, P., Ruthenium(ii) complex-sensitized solid-state polymerization of diacetylene in the visible light region. *J. Mater. Chem.* **2008,** *18* (39), 4704-4711.

12.   Jiang, H.; Pan, X.-J.; Lei, Z.-Y.; Zou, G.; Zhang, Q.-J.; Wang, K.-Y., Photocontrol of chiroptical properties of polydiacetylene carrying azobenzene in the side chain. *Chem. Phys. Lett.* **2010,** *500* (1–3), 100-103.

13.   Yuan, Z.; Lee, C.-W.; Lee, S.-H., Reversible Thermochromism in Hydrogen-Bonded Polymers Containing Polydiacetylenes. *Angew. Chem. Int. Ed.* **2004,** *43* (32), 4197-4200.

14.   Yuan, Z.; Lee, C.-W.; Lee, S.-H., Reversible thermochromism in self-layered hydrogen-bondedpolydiacetylene assembly. *Polymer* **2006,** *47* (9), 2970-2975.

15.   Kim, J.-M.; Lee, J.-S.; Choi, H.; Sohn, D.; Ahn, D. J., Rational Design and in-Situ FTIR Analyses of Colorimetrically Reversibe Polydiacetylene Supramolecules. *Macromolecules* **2005,** *38* (22), 9366-9376.

16.   Lee, S.; Lee, J.; Lee, M.; Cho, Y. K.; Baek, J.; Kim, J.; Park, S.; Kim, M. H.; Chang, R.; Yoon, J., Construction and Molecular Understanding of an Unprecedented, Reversibly Thermochromic Bis-Polydiacetylene. *Adv. Funct. Mater.* **2014,** *24* (24), 3699-3705.

17.   Chanakul, A.; Traiphol, N.; Traiphol, R., Controlling the reversible thermochromism of polydiacetylene/zinc oxide nanocomposites by varying alkyl chain length. *J. Colloid Interface Sci.* **2013,** *389* (1), 106-114.

18.   Laobuthee, A.; Chirachanchai, S.; Ishida, H.; Tashiro, K., Asymmetric Mono-oxazine: An Inevitable Product from Mannich Reaction of Benzoxazine Dimers. *J. Am. Chem. Soc.* **2001,** *123* (41), 9947-9955.

19. Phongtamrug, S.; Chirachanchai, S.; Tashiro, K., Supramolecular Structure of N,N-Bis(2-hydroxy-benzyl)alkylamine: From Hydrogen Bond Assembly to Coordination Network in Guest Acceptance. *Macromolecular Symposia* **2006,** *242* (1), 40-48.

20. Kuriyama, K.; Kikuchi, H.; Oishi, Y.; Kajiyama, T., Molecular aggregation state-photopolymerization behavior relationship of lithium 10,12-heptacosadiynoate monolayer. *Langmuir* **1995,** *11* (9), 3536-3541.

21. Melveger, A. J.; Baughman, R. H., Raman spectral changes during the solid-state polymerization of diacetylenes. *J. Polym. Sci., Part B: Polym. Phys.* **1973,** *11* (4), 603-619.

22. Cui, C.; Choi, H.; Lee, G. S.; Ahn, D. J., Fluorescence Switch in Red-Phase Polydiacetylene Films and Vesicles Upon Thermal Cycles. *J. Nanosci. Nanotechnol.* **2011,** *11* (7), 5754-5760.

23. Seo, S.; Lee, J.; Choi, E.-J.; Kim, E.-J.; Song, J.-Y.; Kim, J., Polydiacetylene Liposome Microarray Toward Influenza A Virus Detection: Effect of Target Size on Turn-On Signaling. *Macromol. Rapid Commun.* **2013,** *34* (9), 743-748

CHAPTER V

CONVENIENT AND SIMPLE PROCEDURES FOR BENZIMIDAZOLE CYCLIZATION UNDER REDUCED PRESSURE AND MODIFICATION OF BENZIMIDAZOLE TO pH-SENSITIVE WITH MULTICOLOR EMISSIONS COMPOUND VIA BENZOXAZINE CHEMISTRY

5.1 Abstract

The condensation of phenylenediamines with benzaldehydes in the presence of catalysts to obtain benzimidazoles under harsh condition is achieved by various reported conditions. The present work demonstrates a convenient, environmentally friendly, and simple procedure to obtain benzimidazoles through the cyclization between benzaldehydes and phenylenediamines under reduced pressure. By simply adding benzaldehydes to diaminobenzene derivatives and allowing the stoichiometric reaction at room temperature under reduced pressure at 66.6 Pa, the dehydrogenation leads to benzimidazoles with the yield as high as 80-90%. In addition, the purging of H_2 gas to benzimidazoles results in the hydrogenation of imidazole to obtain the intermediate benzimidazolidine form. This confirms how the cyclization relies on the reduced pressure. This synthesis pathway not only gives the benzimidazoles with high yield from the mild condition but also the selection of benzaldehydes and phenylenediamines with reactive functional groups leads to the precursors for synthesis a new class of benzimidazole compound with pH-sensitive site. Herein, pH-sensitive fluorescent compound is prepared via a Mannich reaction of benzoxazine under mild condition. The spectral behavior of molecule is evaluated in dimethylsulfoxide. It shows pH-sensitive fluorescent intensity and multichromatic emissions with sodium hydroxide. This is corresponding to the specific molecular state of molecule resulting in different self-assembly morphologies at nanoscale.

Keywords: Benzimidazoles, Benzoxazine, Reduced pressure, pH-sensitive fluorescence, Multicolor emissions

5.2 Introduction

Benzimidazole and its derivatives are important and valuable as they are expected for various potential applications, for example trypsin-like serine protease (FXa) inhibitor,[1] antiviral drugs[2-6] including the benzimidazole-based polymers for the fuel cell membranes. [7] Up to present, several preparation methods have been proposed. For example, Yue *et al.* reported a symmetrical diamine containing *bis*-benzimidazole by condensing 3,3'-diaminobenzidine with *p*-aminobenzoic acid in the presence of phosphorus pentoxide (P_2O_5) and polyphosphoric acid under nitrogen (N_2) at 150 °C for 12 h.[8] The reaction resulted in 65% yield after crystallization in aqueous methanol. Not only the acid catalyst but also nitrobenzene at 150 °C was used as both solvent and oxidant for the condensation between aryl aldehyde and 3,3',4,4'-tetraaminobiphenyl.[9] The yields of these conditions were about 30%. Solid-phase synthesis of benzimidazoles from readily available amines and aldehydes was also proposed. The route involves an *o*-nitroaniline intermediate. The reaction of polymer-bound *o*-nitroaniline with aldehydes in dimethylsulfoxide (DMF) in the presence of tin(II) chloride dihydrate at 60 °C overnight gave benzimidazole (42%) along with by-products (53%) after trifluoroacetic acid (TFA) cleavage.[10] Currently, as the syntheses using rare earth metal triflate catalyst via solvent-free,[11] rapid microwave-assisted liquid-phase,[12-13] aryl derivatives modification using copper- and palladium-catalyst,[14-15] montmorillonite clays as catalyst in water,[12, 16] and etc. are also reported.

It should be noted that the above mentioned methods have their own limits related to acidic conditions, low yield, long reaction time and tedious workup procedures, co-occurrence of side reactions, poor selectivity, high temperature condition and the use of hazard reagents, including catalysts and/or solvents. In other words, the preparation method with easy-handling, highly efficient and selective, and in addition, environmentally friendly condition is still on the expectation. Actually, the key mechanism for benzimidazoles is the intermediate step (Scheme 5.1) where the removal of two hydrogen atoms or dehydrogenation resulting in five-membered ring of imidazoles.[17] Normally dehydrogenation of organic compounds can be done by several routes such as oxidation by inorganic oxidants, dehydrogenation by peroxides and hydride, and proton absorption by catalytic transfer dehydrogenation.[18-20]

Scheme 5.1. Mechanisms for benzimidazole formation: (route A) general mechanism and (route B) dehydrogenation under reduced pressure.
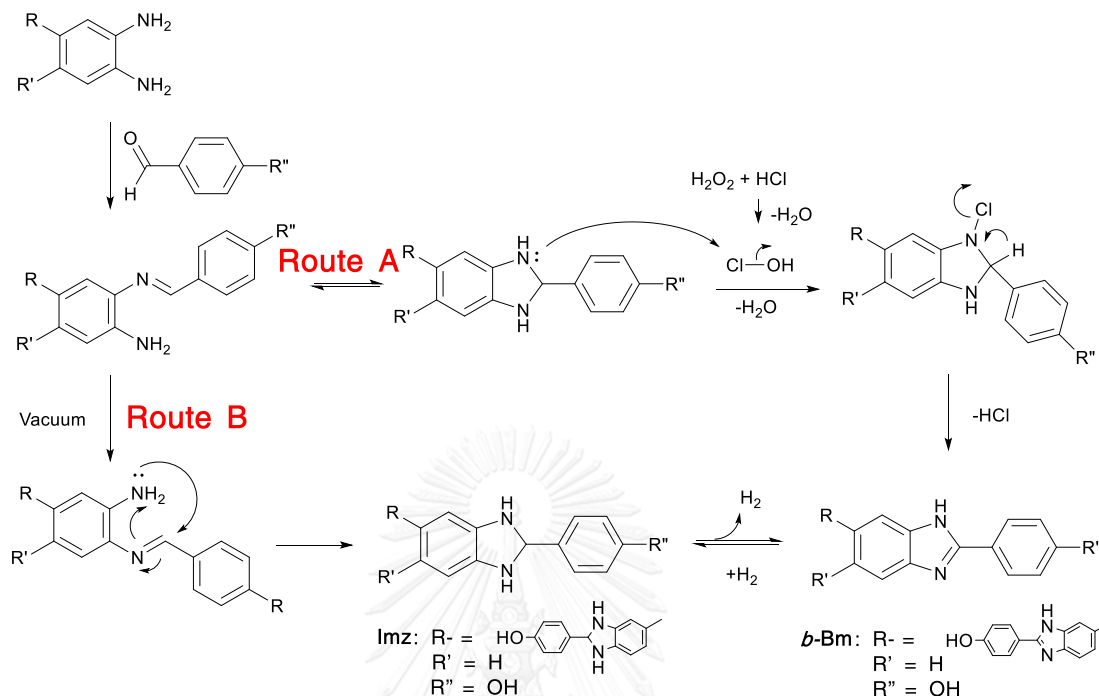
Moreover, the heterocyclic rings can function as selective and effective ion receptor systems leading to design of synthetic receptors that can selectively recognize ions and act as sensors. Immense synthetic potential and applications of such a class of compounds have inspired researchers to develop new strategies for their synthesis and potential properties. For example, Jang *et al*. demonstrated benzimidazole-based tripodal receptor by applying the condensation of tripodal aldehyde with 2-aminobenzimidazole and reduction of imine linkages in the presence of catalytic amount of toluenesulfonic acid.[21] Three benzimidazole groups performed as iodide selective sites in aqueous solution. Fluorescent intensity was quenched upon addition of I^-. Ray *et al*. developed synthetic methodology of polycyclic benzimidazole derivative through coupling reaction.[22] A fluorescent probe for Zn^{2+} was prepared based on modified benzimidazole amide backbone connected by dipicolylamine group.[23] A bis(2-pyridylmethyl)amine subunit can coordinated with Zn^{2+} while a triphenylamine benzimidazole group act as fluorophore. The derivative which has aryl group containing –OMe group showed the decreasing of fluorescent intensity after protonation due to the low basicity of benzimidazolium *N* is attributed to the extended

conjugation with side group. The heating under microwave of *o*-phenylenediamine with nitrophenylfuran led to the formation of nitrophenylfuran-benzimidazole-based fluorescence pH chemosensors bearing benzimidazole moiety as pH sensing site and nitrophenylfuran moiety as chromophore and fluorophore.[24] Though there are several reports dealing with the synthesis of benzimidazole derivatives and their potential properties, the efficient synthetic routes toward functionalized benzimidazole with structural diversity are limited.

In the past decade, our group demonstrated simple, selective, and effective preparation of monophenol-based benzoxazines via Mannich reaction of phenols, formaldehyde, and amines. A single ring opening of oxazine ring always ends up with the self-terminated species, *N,N'*-bis(2-hydroxybenzyl) alkylamines, namely benzoxazine dimers.[25-26]

In view of this, herein, the present work shows a convenient, environmentally friendly, and simple procedure for benzimidazole cyclizations of phenylenediamines with benzaldehyde. The formation of benzimidazole is favored by effective elimination of hydrogen in gas state (H_2) under reduced pressure system. As a result, the product can be obtained in high yield without the use of catalyst and harsh conditions. Moreover, we propose a facile method to introduce *bis*-benzimidazole into the design of fluorimetric response for pH stimuli. The Mannich reaction is used to obtain benzimidazole-based benzoxazine dimers by simply changing mono-phenol to bis-benzimidazole. The product obtained containing four –OH groups of phenol shows pH-sensitive fluorescence with multicolor emissions.

5.3 Experimental

5.3.1 Materials

Methylamine, *p*-cresol, and deuterated dimethylsulfoxide (DMSO-d_6) were purchased from Sigma-Aldrich. Formaldehyde solution (37%), 1,4-dioxane, dimethylformamide, and dimethylsulfoxide were obtained from Wako Pure Chemical Industries. Sodium hydroxide and sodium sulfate anhydrous were received from Fluka. All chemicals were used without further purification. Distilled water was purified through Milli-Q Advantage A10 Ultrapure Water System.

5.3.2 General methods and instrumentation

Thin-layer chromatography (TLC) was carried out using TLC Silicagel 60 F254 (Merck) and compounds visualized using UV irradiation at 365 nm. NMR spectra were recorded at 25 °C in dimethyl sulfoxide-d_6 (DMSO-d_6) on a Bruker Biospin Avance 500 nuclear magnetic resonance (NMR) spectrometer. All chemical shifts were reported in parts per million (ppm) and measured relative to the solvent in which the sample was analyzed (DMSO-d_6 δH = 2.50 δC = 39.52 ppm). The product analysis by mass spectrometry were performed on a Bruker micrOTOF II. Elemental analysis Elementary analysis (EA) was done by a Yanako CHN CORDER to determine number of nitrogen and carbon contents of products. The pH values were recorded on a SevenMulti type pH meter with InLab Semi-Micro electrodes (Mettler Toledo, Switzerland). The UV-vis absorbance measurements were carried out on a UV-1800 SHIMADZU spectrophotometer in the range of 250–700 nm. A Hitachi F-7000 fluorescence spectrometer was used to measure the fluorescence emission. Emission spectra were recorded in the range of 340–700 nm. The Fourier transform infrared spectra were recorded on a Nicolet iN10 MX infrared spectrometer (Thermo Scientific Co., America). The samples were dissolved in DMSO at a defined concentration and dried before measuring. The compounds were dissolved in DMSO at a defined concentration, and a drop of the resulting solution was dispersed on an amorphous carbon film supported by a Cu grid. Excess solution was removed by filter paper. The samples were placed in desiccator at room temperature for drying before observation. A Tecnai G2 F20 TEM (120 kV) was employed to observe the morphology of assemblies.

5.3.3 Preparation of 2'-(4-hydroxyphenyl)-3H,3'H-[5,5'-bibenzo[d]imi dazol]-2-ol (*b*-Bm)

A mixture of 3,3'-diaminobenzidine (0.2141 g, 1 mmol), 4-hydroxybenzaldehyde (0.2442 g, 2 mmol), and DMF (5 mL) was stirred at room temperature under N2 atmosphere for 14 hours, when TLC analyses revealed the consumption of all starting material. Then vacuum system was applied for 4 hours. The reaction was precipitated by an addition of DI water (20 mL). The crude product obtained was washed with acetone (3 x 10 mL) and dried under vacuum to obtain *b-*

Bm. 85-90 % yield; Rf = 0.13 (in CHCl3); 1H NMR (500 MHz, DMSO-d_6, ppm): δ 12.72 (s, 2H, N-H), 9.96 (s, 2H, O-H), 8.01 (d, J = 8.26 Hz, 4H, Ar-H), 7.75 (s, 2H, Ar-H), 7.60 (d, J = 7.24 Hz, 2H, Ar-H), 7.49 (d, J = 8.37 Hz, 2H, Ar-H), 6.91 (d, J = 8.431 Hz, 4H, Ar-H); ^{13}C NMR (500 MHz, DMSO-d_6, ppm): δ159.17 (4C), 152.31 (2C), 135.49 (2C), 128.16 (6C), 121.42 (2C), 121.08 (2C), 115.70 (8C); ESI-TOF m/z: calculated for [M+H]+ = 419.14, found 419.15; Elemental analysis, Calcd for C26H18N4O2: C 74.62, H 4.34, N 13.46, found C 74.17, H 4.49, N 13.68.

5.3.4 Preparation of 2-phenyl-1H-benzo[d]imidazole (**Bm1**)

o-Phenylenediamine (0.1081 g, 1mmol) and benzaldehyde (0.1060 g, 1 mmol) were mixed in DMF at room temperature under N_2 atmosphere for 8 h., when TLC analyses showed new spot of product obtained. Then vacuum system was applied for 4 h. The solvent was removed under vacuum at 70 °C. The solid was dissolved in dichloromethan (DCM) and wash with DI water for 3 times. The organic phase was dried over sodium sulfate anhydrous. The crystal of compound **Bm1** was formed in DCM. 93 % yield; R_f = 0.81 (in CHCl$_3$); ^{1}H NMR (500 MHz, DMSO-d_6, ppm): δ 12.95 (s, 1H, N-H), 8.20 (d, J = 8.63 Hz, 2H, Ar-H), 7.75 (d, J = 8.55 Hz, 2H, Ar-H), 7.60 (d, J = 8.75 Hz, 3H, Ar-H), 7.31 (t, 2H, Ar-H); ESI-TOF m/z: calculated for [M+H]$^+$ = 195.09, found 195.04.

5.3.5 Preparation of 4-(1H-benzo[d]imidazol-2-yl)phenol (**Bm2**)

The synthesis of **Bm2** was carried out in the same conditions as **Bm1** but using 4-hydroxybenzaldehyde (0.1081 g, 1mmol) to obtain **Bm2**. 87 % yield; R_f = 0.64 (in CHCl$_3$); ^{1}H NMR (500 MHz, DMSO-d_6, ppm): δ 12.79 (s, 1H, N-H), 10.03 (s, 1H, O-H), 8.49 (s, 1H, Ar-H), 7.81 (d, J = 8.68 Hz, 2H, Ar-H), 7.03 (d, J = 8.26 Hz, 1H, Ar-H), 6.88 (m, 2H, Ar-H), 6.67 (d, J = 7.95 Hz, 1H, Ar-H), 6.53 (t, 1H, Ar-H); ESI-TOF m/z: calculated for [M+Na]$^+$ = 233.07, found 233.06.

5.3.6 Preparation of 2,2'-diphenyl-3H,3'H-5,5'-bibenzo[d]imidazole (**Bm3**)

The synthesis of **Bm3** was carried out in the same conditions as *b*-**Bm** but using benzaldehyde (0.2122 g, 2 mmol) to obtain **Bm3**. 78.2 % yield; R_f = 0.67 (in

CHCl$_3$); ^{1}H NMR (500 MHz, DMSO-d_6, ppm): δ 12.93 (s, 2H, N-H), 8.18 (m, 4H, Ar-H), 7.55 (m, 8H, Ar-H), 7.21 (s, 4H, Ar-H); ESI-TOF m/z: calculated for [M+H]$^+$ = 387.16, found 387.17.
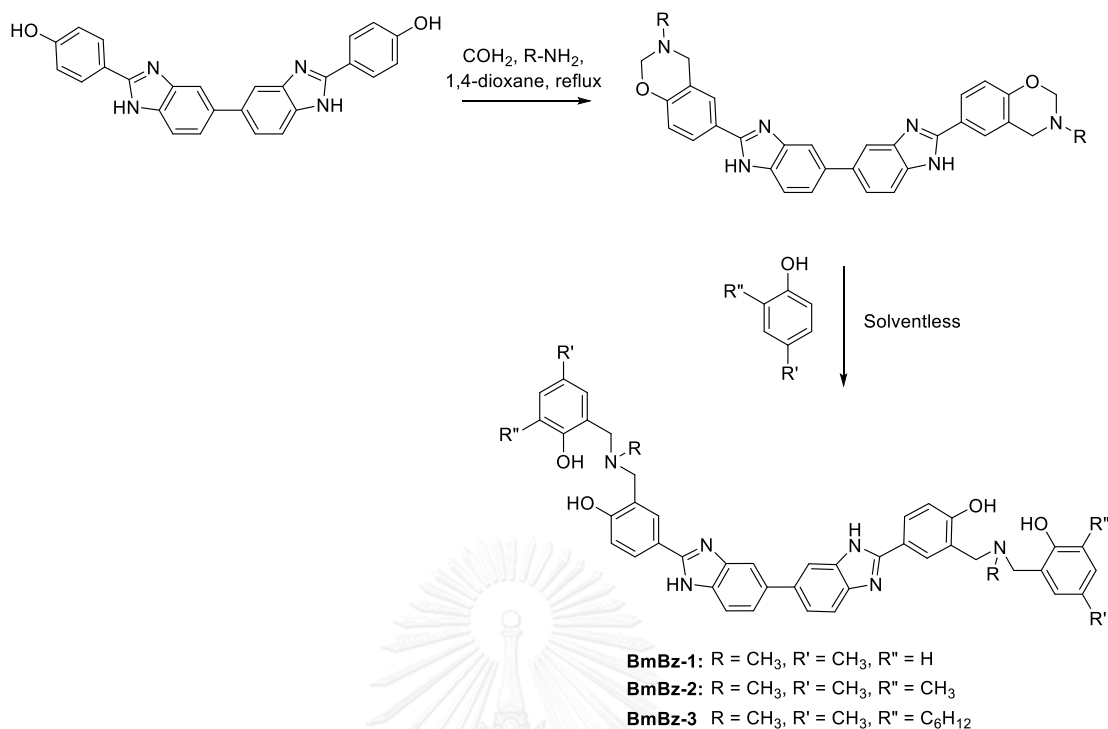
5.3.7 Preparation of 4,4'-(2,2',3,3'-tetrahydro-1H,1'H-[5,5'-bibenzo[d]imidazole]-2,2'-diyl)diphenol (Imz)

Hydrogenation of *b*-**Bm** was carried out in NMR tube by using DMSO-d_6 solvent. H$_2$ gas was purged into purified *b*-**Bm** solution for 21 days to obtain **Imz**. ^{1}H NMR (500 MHz, DMSO-d_6, ppm): δ 10.30 (s, 2H, O-H), 8.50 (s, 4H, N-H), 7.97 (d, J = 8.40 Hz, 4H, Ar-H), 7.81 (s, 2H, Ar-H), 7.62 (d, *J* = 2.55 Hz, 4H, Ar-H), 7.53 (d, *J* = 8.99 Hz, 4H, Ar-H), 6.94-6.92 (d, 4H, Ar-H), 6.02 ppm (s, 2H, C-H); ^{13}C NMR (500 MHz, DMSO-d_6, ppm): δ159.58 (4C), 152.86 (2C), 136.02 (2C), 128.70 (6C), 122.20 (2C), 121.10 (4C), 116.36 (8C).

5.3.8 Preparation of 4,4'-(1H,3'H-[5,5'-bibenzo[d]imidazole]-2,2'-diyl)bis(2-(((2-hydroxy-5-methylbenzyl)(methyl)amino)methyl)phenol) (BmBz-1)

BmBz-1 (Scheme 5.2) was prepared via ring-opening reaction of the relevant benzoxazine and phenol derivatives as reported in previous literature.[25] In brief, methylamine (62.1 mg, 2mmol) was reacted with *p*-formaldehyde (178.1 mg, 4mmol) and *b*-**Bm** (418.5 mg, 1mmol) in 1,4-dioxane at reflux. The completion of oxazine ring formation was followed by thin layer chromatography (TLC) which indicated the reaction time of 10 h. Then, the ring-opening reaction was carried out by adding *p*-cresol (216.3 mg, 2mmol) and stirring at 120 °C until a yellow viscous product was obtained. The crude product was further purified by precipitate in chloroform. The brown precipitate was dried under vacuum to yield **BmBz-1** at 74%; ^{1}H NMR (500 MHz, DMSO-d_6, ppm): δ 12.69 (s, 2H, -NH-), 9.95 (s, 4H, -OH), 9.06 (s, 2H, Ar-H), 8.02 (d, *J* = Hz, 1H, Ar-H), 7.94 (s, 1H, Ar-H), 7.67 (m, 1H, Ar-H), 7.49 (m, 1H, Ar-H), 6.93 (t, 2H, Ar-H), 6.63 (t, 1H, Ar-H), 3.32 (s, 4H, -CH$_2$- of mannich bridge), 2.72 (s, 3H, N-CH$_3$), 2.16 (s, 3H, Ar-CH$_3$).

Scheme 5.2 Synthesis of **BmBz**

BmBz-1: R = CH₃, R' = CH₃, R" = H
BmBz-2: R = CH₃, R' = CH₃, R" = CH₃
BmBz-3 R = CH₃, R' = CH₃, R" = C₆H₁₂

5.3.9 Preparation of 6,6'-(((((1H,3'H-[5,5'-bibenzo[d]imidazole]-2,2'-diylbis(6-hydroxy-3,1-phenylene))bis(methylene))bis(methylazanediylv)bis(methylene))bis(2,4-dimethylphenol) (BmBz-2)

The synthesis of **BmBz-2** (Scheme 5.2) was followed the preparation for **BmBz-1** except that 1 equiv. 2,4 dimethyl phenol (244 mg, 2 mmol) was used instead of *p*-Cresol giving **BmBz-2**. 83% yield; ^{1}H-NMR (500 MHz, DMSO-d_6, ppm): δ 12.67 (s, 2H, -NH-), 9.96 (s, 4H, -OH), 9.09 (s, 2H,), 8.04 (d, $J =$ Hz, 1H, Ar-H), 7.96 (s, 1H, Ar-H), 7.67 (m, 1H, Ar-H), 7.48 (m, 1H, Ar-H), 6.89 (s, 2H, *m*-H-Ar), 6.75 (s, 2H, *m*-H-Ar), 3.48 (d, $J =$ 7.72 Hz, 4H, -CH₂- of mannich bridge), 2.28 (q, 6H, *o*-CH₃-Ar), 2.00 (t, 6H, *p*-CH₃-Ar).

5.3.10 Preparation of 4,4'-(1H,3'H-[5,5'-bibenzo[d]imidazole]-2,2'-diyl)bis(2-((cyclohexyl(2-hydroxy-5-methylbenzyl)a mino)methyl)phenol) (BmBz-3)

Cyclohexylamine (199 mg, 2 mmol) was mixed with *p*-formaldehyde (178.1 mg, 4mmol) and *b*-**Bm** (418.5 mg, 1mmol) in 1,4-dioxane at reflux. Then, benzoxazine ring-opening reaction was carried out by adding *p*-cresol (216.3 mg,

2mmol) and stirring at 120 °C until a yellow viscous product was obtained. The crude product was purified by column chromatography to give **BmBz-3** (Scheme 5.2). 46% yield; ^{1}H-NMR (500 MHz, DMSO-d_6, ppm): δ 12.70 (s, 2H, -NH-), 9.96 (s, 4H, -OH), 9.02 (s, 4H, Ar-H), 7.82 (m, 8H, Ar-H), 6.90 (dd, 4H, *m*-H-Ar), 6.81 (s, 2H, *m*-H-Ar), 3.70 (s, 4H, -CH$_2$- of mannich bridge), 2.85 (m, 1H, N-CH-CH$_2$), 2.35 (s, 6H, *o*-CH$_3$-Ar), 2.29 (s, 6H, *p*-CH$_3$-Ar), 1.86 (d, 2H, *o*-CH$_2$), 1.61 (d, 2H, *o*-CH$_2$), 1.46 (s, 2H, *m*-CH$_2$), 1.21 (m, 2H, *m*-CH$_2$), 0.94 (m, 2H, *p* -CH$_2$)

5.3.9 Sample preparation

0.1 mM **BmBz-1**, **BmBz-2**, and **BmBz-3** solutions were obtained by dissolving **BmBz** compounds in DMSO. NaOH powder was dissolved in ultrapure water (Milli-Q, 18.2MU cm) to obtain NaOH solution at various mole. The mixtures of **BmBz-1**, **BmBz-2**, and **BmBz-3** solutions and NaOH were performed via mixing at desired molar ratios by controlling total volume at 2 mL. These solutions were mixed and kept for at least 3 hours before further analysis.

5. 4 Results and Discussion

^{1}H NMR, ^{13}C NMR, DEPT 90, DEPT 135, and Quantitative ^{13}C NMR were used to identify *b*-**Bm** product (Figure 5.1(B) and Figure C1-C5). These suggest the benzimidazole ring-closure with the yield as high as 85-90%. In order to confirm the effectiveness of this condition, a series of phenylenediamines in combination with aldehydes were used to find that the reactions lead to benzimidazole formation. For example, *o*-phenylenediamine and benzaldehyde were mixed and the reaction condition was similar to that of *b*-**Bm**. **Bm1** was obtained with the yield 93% similar to the product from the condition in Scheme 1 (route A) that requires catalysts. When 4-hydroxybenzaldehyde was used, **Bm2** was obtained at 87% yield. Moreover, the reaction between 3,3'-diaminobenzidine and benzaldehyde gave **Bm3**. All products obtained were identified by ^{1}H NMR (Figure C6-C8). It is important to note that the reduced pressure in the system is considered as the key factor for benzimidazole ring formation from azomethine group.
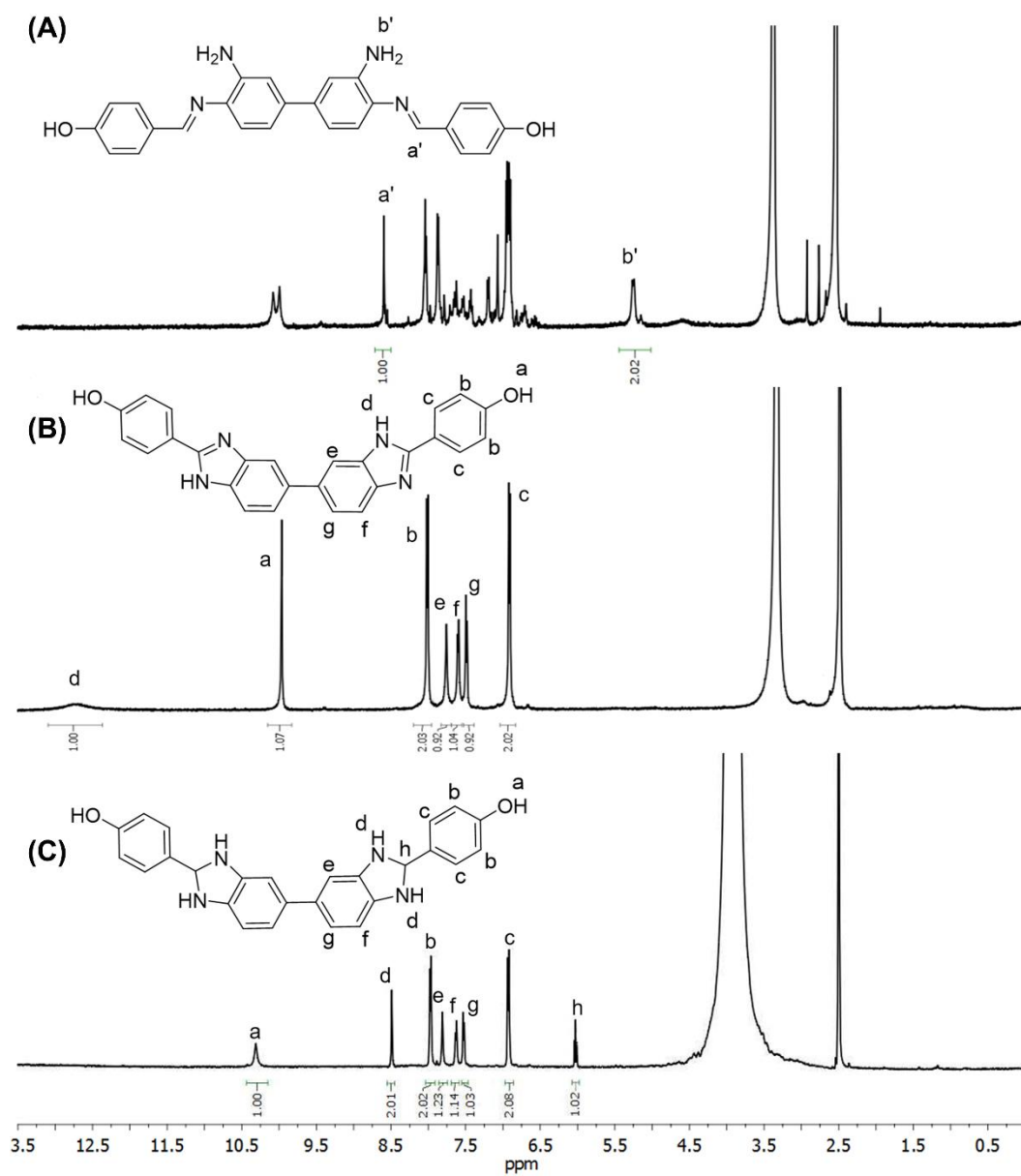
Figure 5.1. ^{1}H NMR of (A) intermediate product, (B) **b-Bm** after purification, and (C) product obtained after treating **b-Bm** after purification with H_2 for 21 days.
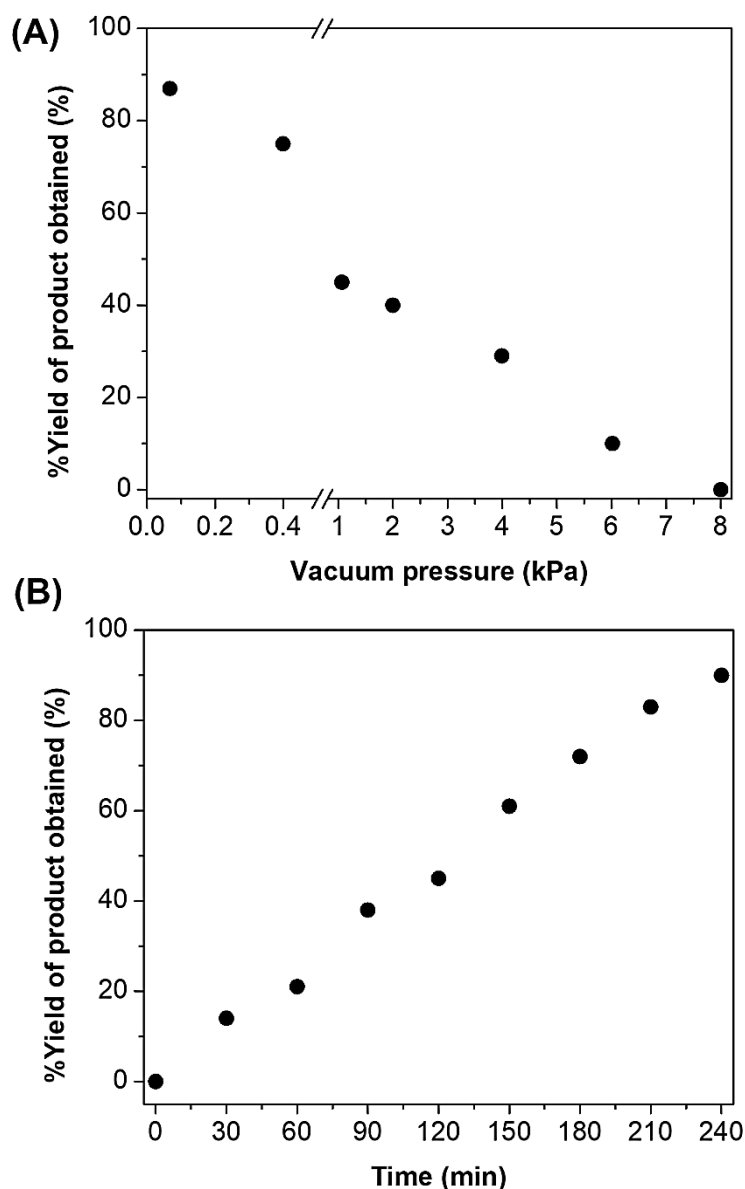
Figure 5.2. (A) Yield of the product obtained as a function of reduced pressure, and (B) yield of the product obtained as a function of time at the reduced pressure of 66.6 Pa.

It comes to the question how the reduced pressure controls the cyclization. Here, the reduced pressure was varied and the reaction was carried out until the -NH- belonging to amine group at δ_H 5.22 ppm (Figure 5.1(A)) was disappeared. Figure 5.2(A) shows the reduced pressure in the system related to the benzimidazole yield. When the reduced pressure is still low as seen in the cases that the pressure in the system are high, e.g. 8 kPa, there is no benzimidazole formation. When the reduced pressure is

significant until the pressure in the system becomes as low as 399 Pa, and 66.6 Pa, the yields of benzimidazole are as high as 75% and 87%, respectively. This implies the reduced pressure at appropriate level is needed for benzimidazole ring formation. Then the reduced pressure in the system was fixed at 66.6 Pa so that the optimal reaction time can be determined. Figure 5.2(B) shows that when the time increased, the percent yield of *b*-**Bm** is slightly increased until the maximum yield is found for 90% at 240 min.

In order to understand the formation of benzimidazole according to our reaction condition, the mechanism including intermediate is proposed in Scheme 5.1 (route B). In fact, the azomethine group and benzimidazolidine i.e. 4,4'-(2,2',3,3'-tetrahydro-1H,1'H-[5,5'-bibenzo[d]imidazole]-2,2'-diyl)diphenol, **Imz**, are proposed as the intermediate. At that time the reduced pressure is the key factor for benzimidazolidine formation and dehydrogenation of **Imz** to obtain five membered ring of benzimidazole.

It comes to the question that if the dehydrogenation of **Imz** is occurred under reduced pressure, we should be able to confirm **Imz**. Here, H_2 gas was purged into the *b*-**Bm** in DMSO-d_6. The changes of *b*-**Bm** were traced by ^{1}H NMR. It was found that after treating *b*-**Bm** with H_2 for 21 days, the proton of imidazole at δ_H 12.73 ppm was disappeared whereas the two protons of benzimidazolidine and one proton of methanetriyl group at 8.50 ppm and 6.02 ppm, respectively, were observed (Figure 5.1(C) and C9). In fact, the type and the number of carbon species are important since they allow us to confirm the structure of **Imz**. Therefore, ^{13}C, DEPT 90, DEPT 135, and quantitative ^{13}C NMR (Figures C10-C13) analyses were carried out. DEPT 90 spectrum showed three peaks of CH at 128.67 ppm, 122.17 ppm, and 116.32 ppm respectively. Here, DEPT 135 was applied and confirmed that there are no CH_2 and CH_3 in the structure. The quantitative ^{13}C NMR suggested two types of carbon species. First type is the C at 153.08 ppm, 136.26 ppm, and 121.28 ppm, for two carbon atoms and 159.83 ppm for four carbon atoms. The other is CH at 128.95 ppm for six carbon atoms, 122.46 ppm for two carbon atoms, and 116.60 ppm for eight carbon atoms. The informations obtained were a guideline to us that the treating of *b*-**Bm** with H_2 seemed to result in **Imz**. Further analysis by heteronuclear single quantum coherence (HSQC) indicated the attachment of proton at 6.02 ppm on the carbon atom at 122.22 ppm (Figure S14) suggesting the development of CH to result in benzimidazolidine. In this

way, the detailed analyses by NMR indicated the disappearance of double bond in benzimidazole ring by hydrogenation to give **Imz**. The proposed mechanism which contains the dehydrogenation of **Imz** is shown in Scheme 5.1 (route B).
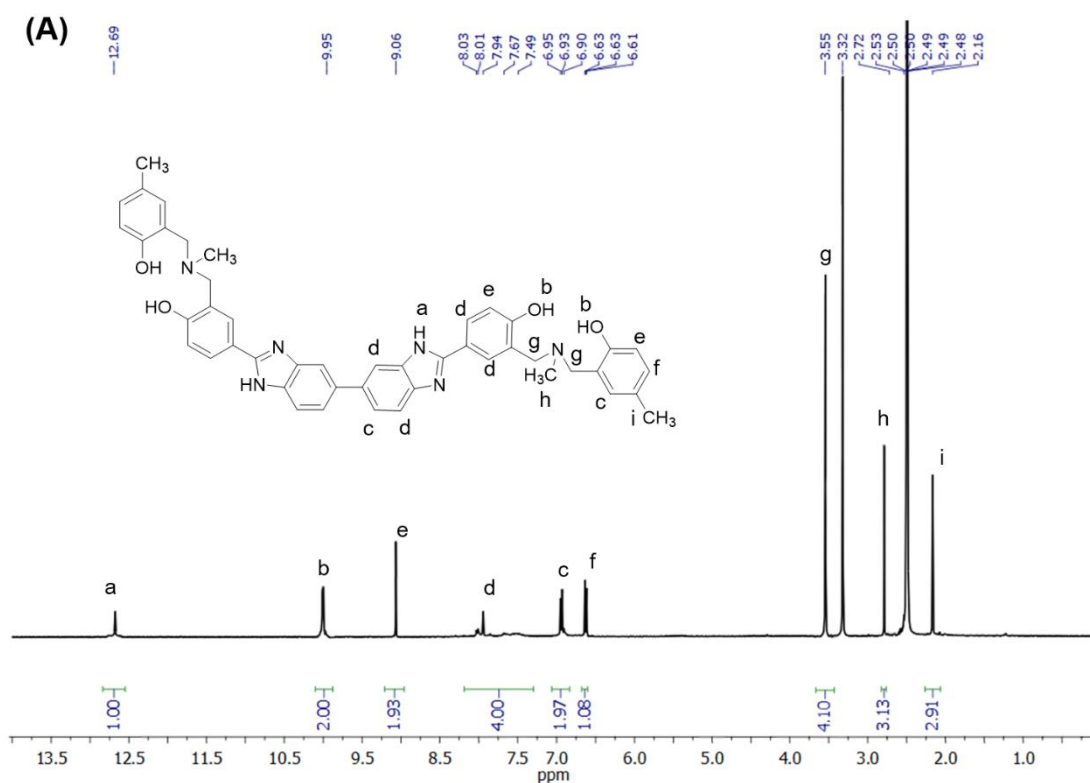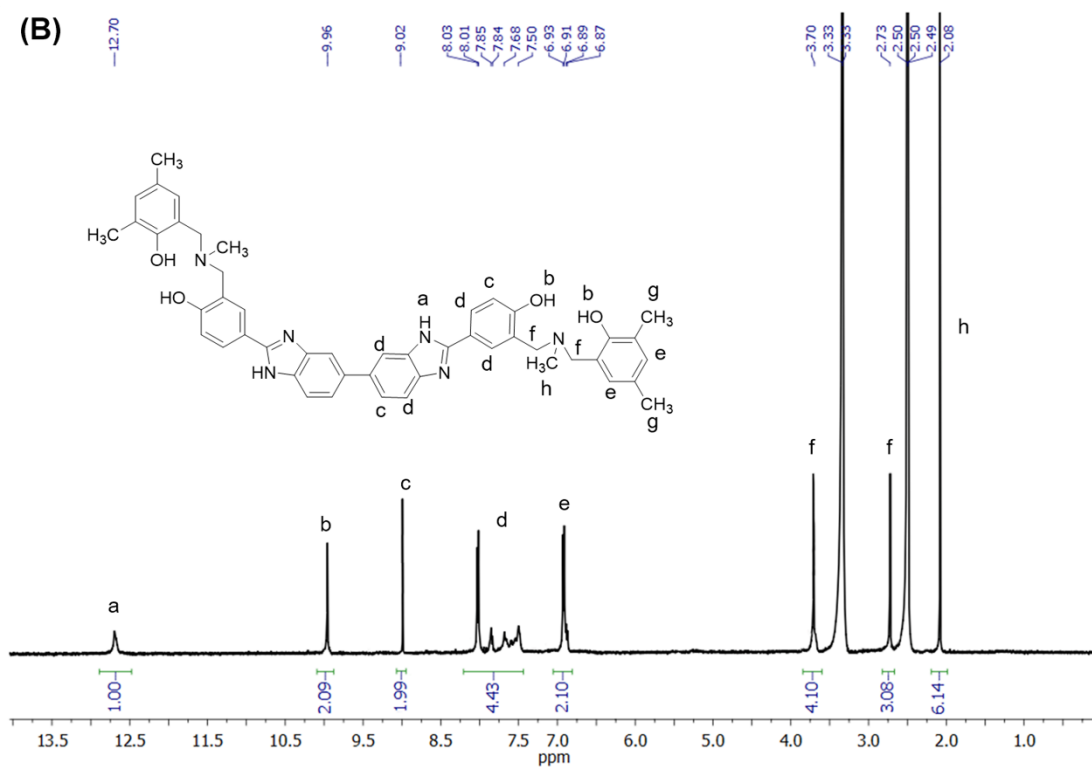

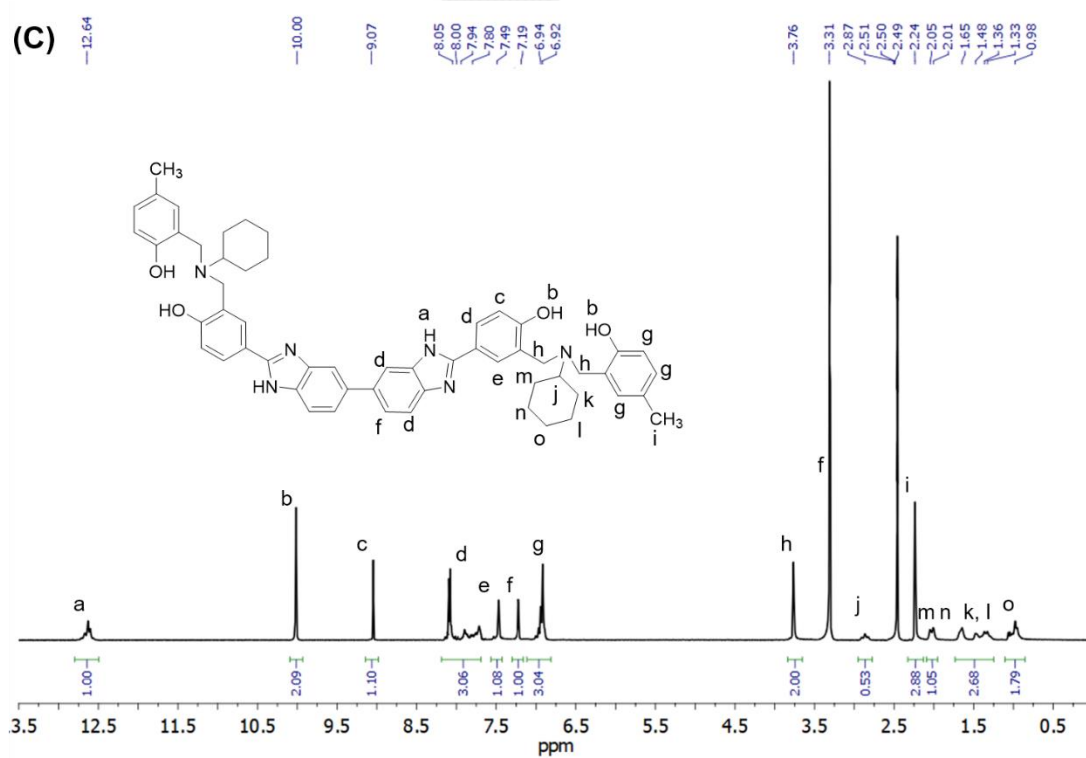**Figure 5.3.** ^{1}H NMR of **BmBz-1**.

(B)

Figure 5.4. ¹H NMR of **BmBz-2**.

(C)

Figure 5.5. ¹H NMR of **BmBz-3**.
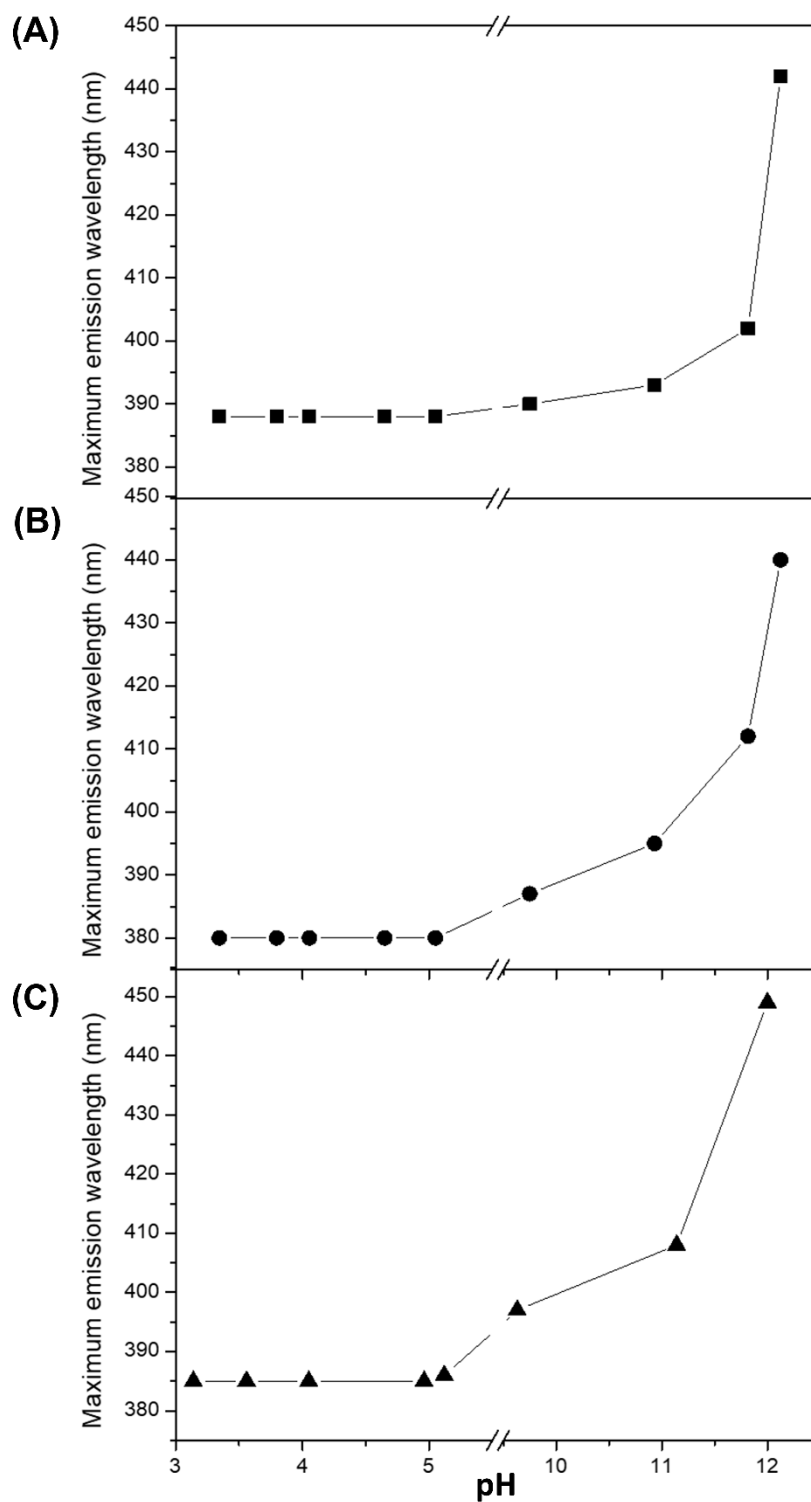
Figure 5.6. Fluorescent intensity of (A) **BmBz-1,** (B)**BmBz-2**, and (C) **BmBz-3** solution versus pH at various mole ratio of NaOH.
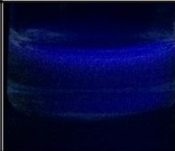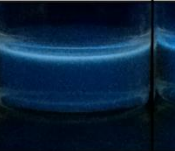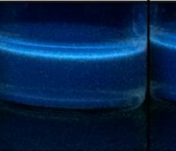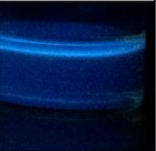
Mole of NaOH (mM)	0	0.1	0.2	0.3	0.4
pH	5.0	9.7	10.9	11.8	12.2
Appearance					

Figure 5.7. Color emission of **BmBz-1** at various mole ratio of NaOH.

b-**Bm** which has phonol on the both side was further used as precursor in Mannich reaction for benzoxazine formation. After a single oxazine ring opening, **BmBz-1**, **BmBz-2**, and **BmBz-3** were obtained. The chemical structure of **BmBz-1**, **BmBz-2**, and **BmBz-3** were characterized by ^{1}H NMR as shown in Figure 5.3-5.5. For **BmBz-1**, the compound solution (0.1 mM) displayed a maximum emission wavelength (λ_{em}) at 388 nm in DMSO at its pH (pH = 5.0) where the maximum absorption wavelength (λ_{abs}) at 335 nm as shown in Figure 5.6(A). Violet fluorescence was observed under fluorescent lamp (Figure 5.7). Upon addition of NaOH solution, pH value was measured (Figure C15) and plotted with mole equivalent of NaOH to **BmBz-1**. pH of the addition of 0, 0.1, 0.2, 0.3 and 0.4 mM NaOH were further used. Initially, when the pH changed, the color of the solution suddenly changed from pale yellow to yellowish. The changes in $\lambda_{em,}$ fluorescence intensity and emitted color of **BmBz-1** at different pH are shown in Figure 5.6(A). The increases in pH from 5.0 to 9.7, 10.9, 11.8, and 12.2 caused the decreases in intensity with concomitant red-shift of emission band 388 nm to 389 nm, 391 nm, 402 nm, and 442 nm, respectively (Figure 5.6(A)). In addition, the fluorescence color has been finely tuned from violet to green as shown photographs in Figure 5.7. It might be due to lower activation energy with deceasing of quantum yield for the emission process. For comparison, 0.1 mM *b*-**Bm** solution was prepared in DMSO. The absorption and emission spectra of *b*-**Bm** upon addition of NaOH were examined (Figure C16). *b*-**Bm** (0.1 mM) which has pH around 6.5 displayed λ_{em} at 385 nm when λ_{abs} at 332 nm with visible color in violet under fluorescent lamp. The pH of solution increased as the concentration of NaOH increased. The λ_{em} of solution still remained at 385 nm with similar fluorescent color. It should be noted that the similar fluorescence emission was observed in case of **BmBz-2** and

BmBz-3 as shown in Figure 5.6(B) and 5.6(C), respectively. It might be due to the ion equilibrium of sodium hydroxide solution that fit with ion equilibrium of OH group of BmBz compounds. Conjugated acid-base was formed even the bulkiness of BmBz structure were changed. **BmBz-1** was used for further studies.
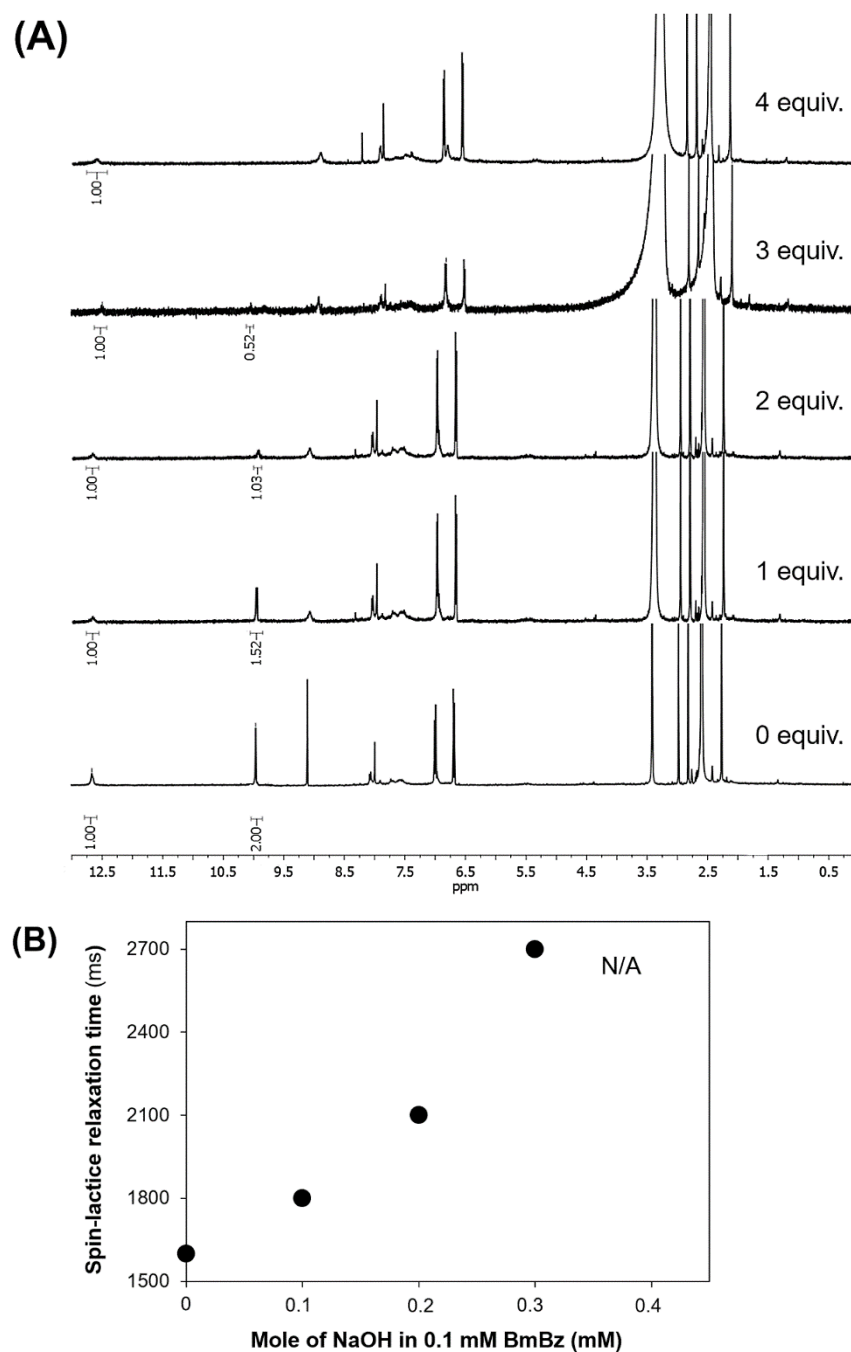

Figure 5.8. (A) ^{1}H NMR spectra and (B) Spin–lattice relaxation time (T1) of **BmBz-1** on addition of sodium hydroxide.

In order to find the attachment of NaOH ion on **BmBz-1** molecules, NMR technique was used. As can be seen from Figures 5.8(A), the integration of hydroxyl proton at 9.9 ppm decreases one by one upon the addition of NaOH from 0 to 4 equivalent mole. This suggests that the deprotonation on **BmBz-1** molecule occurred only at –OH group. Moreover, the molecular assemblies via hydrogen bonding in the solution state of **BmBz-1** were examined by evaluating spin–lattice relaxation ($T1$ relaxation) using ^{1}H NMR in DMSO-d_6 under different NaOH concentrations. Basically, when molecules form an interaction with each other, the interaction obstructs the degree of freedom of the molecules, resulting in a short $T1$ relaxation time.
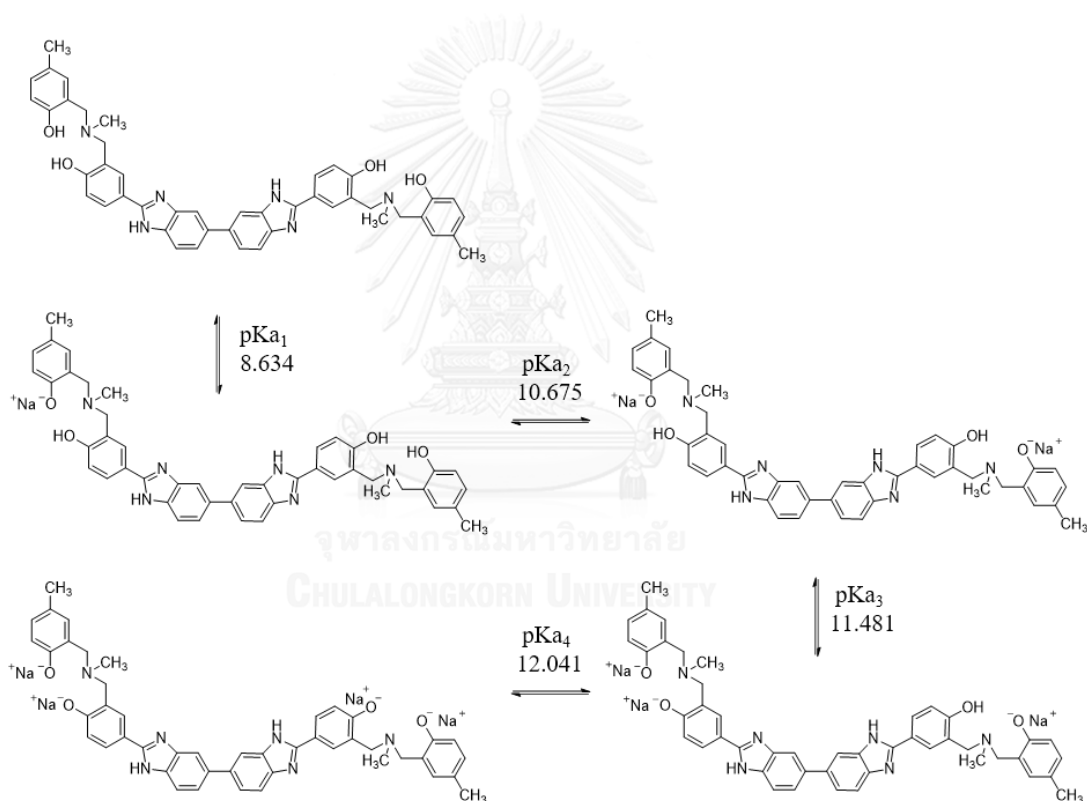
Figure 5.9. Illustration of **BmBz-1** formation at different pKa.

Therefore, the differences in $T1$ values reflect the molecular self-assembly under hydrogen bond interaction. To investigate this, a chemical shift at 9.9 ppm of hydroxyl was focused on. It was found that the $T1$ value at this position significantly changes with NaOH concentration increased as shown in Figure 5.8(B). This suggests that hydroxyl group of **BmBz-1** plays an important role in forming the molecular

hydrogen bonding. The deprotonation at hydroxyl group caused the longer *T1* due to the loss of hydrogen bond network. The change of fluorescence intensity is also a result of the fracture of hydrogen bond because of the deprotonation of hydroxyl. In this case, the oxygen anion is a strong electron donor which also alters the intramolecular charge transfer (ICT) effect and causes red-shift in fluorescence spectra.

The pKa values of **BmBz-1** after deprotonation are calculated as 8.634, 10.675, 11.481, and 12.041 from the titration curve (Figure C17). The deprotonation and **BmBz-1** formation at different pKa were illustrated as shown in Figure 5.9. Moreover, the morphologies are found to be fine-tuned by NaOH concentrations (Figure C18). For example, 50 nm spheres of **BmBz-1** at pH 5.0 changes to hollow spheres at pH 9.7 and to irregular shape at pH 10.9, 11.8, and 12.2 respectively. However, it should be noted that, the distinct photophysical behavior of **BmBz-1** in different environment, including the fluorescence intensity and the λ_{em}, endow the molecule with the ability to discriminate pH values in a wide range.

5.5 Conclusions

In conclusion, the cyclization of benzimidazoles could be qualitatively and quantitatively obtained by simply applying phenylenediamines and benzaldehydes at room temperature under mild condition. The key to control the cyclization, in other words, dehydrogenation, is reduced pressure. As shown in Scheme 5.1 (route B), this synthesis pathway offers the benzimidazoles with functional groups of which further modification and polymerization are possible. Moreover, a novel fluorophore with pH-resposive site has been designed and synthesis in a good yield by simply applying *b-***Bm** via Mannich reaction. The fluorescent property of this molecule was also carefully investigated. It showed an extremely responsible for NaOH and obvious fluorescent color changes due to the loss of hydrogen bond after deprotonation.

5.6 Acknowledgements

5.7 References

1. Zhao, Z.; Arnaiz, D. O.; Griedel, B.; Sakata, S.; Dallas, J. L.; Whitlow, M.; Trinh, L.; Post, J.; Liang, A.; Morrissey, M. M.; Shaw, K. J., Design, synthesis, and in vitro biological activity of benzimidazole based factor Xa inhibitors. *Bioorg. Med. Chem. Lett.* **2000,** *10* (9), 963-966.

2. Hamdouchi, C.; de Blas, J.; del Prado, M.; Gruber, J.; Heinz, B. A.; Vance, L., 2-Amino-3-substituted-6-[(E)-1-phenyl-2-(N-methylcarbamoyl)vinyl]imidazo[1,2-a]pyridines as a Novel Class of Inhibitors of Human Rhinovirus: Stereospecific Synthesis and Antiviral Activity. *J. Med. Chem.* **1999,** *42* (1), 50-59.

3. Herrmann Jr, E. C.; Herrmann, J. A.; Delong, D. C., Comparison of the antiviral effects of substituted benzimidazoles and guanidine in vitro and in vivo. *Antiviral Res.* **1981,** *1* (5), 301-314.

4. Porcari, A. R.; Devivar, R. V.; Kucera, L. S.; Drach, J. C.; Townsend, L. B., Design, Synthesis, and Antiviral Evaluations of 1-(Substituted benzyl)-2-substituted-5,6-dichlorobenzimidazoles as Nonnucleoside Analogues of 2,5,6-Trichloro-1-(β-d-ribofuranosyl)benzimidazole. *J. Med. Chem.* **1998,** *41* (8), 1252-1262.

5. Tebbe, M. J.; Spitzer, W. A.; Victor, F.; Miller, S. C.; Lee, C. C.; Sattelberg, T. R.; McKinney, E.; Tang, J. C., Antirhino/Enteroviral Vinylacetylene Benzimidazoles: A Study of Their Activity and Oral Plasma Levels in Mice. *J. Med. Chem.* **1997,** *40* (24), 3937-3946.

6. Zarrinmayeh, H.; Nunes, A. M.; Ornstein, P. L.; Zimmerman, D. M.; Arnold, M. B.; Schober, D. A.; Gackenheimer, S. L.; Bruns, R. F.; Hipskind, P. A.; Britton, T. C.; Cantrell, B. E.; Gehlert, D. R., Synthesis and Evaluation of a Series of Novel 2-[(4-Chlorophenoxy)methyl]-

benzimidazoles as Selective Neuropeptide Y Y1 Receptor Antagonists. *J. Med. Chem.* **1998,** *41* (15), 2709-2719.

7. Pangon, A.; Totsatitpaisan, P.; Eiamlamai, P.; Hasegawa, K.; Yamasaki, M.; Tashiro, K.; Chirachanchai, S., Systematic studies on benzimidazole derivatives: Molecular structures and their hydrogen bond networks formation toward proton transfer efficiency. *J. Power Sources* **2011,** *196* (15), 6144-6152.

8. Yue, Z.; Cai, Y.-B.; Xu, S., Facile synthesis of a symmetrical diamine containing bis-benzimidazole ring and its thermally stable polyimides. *J. Polym. Res.* **2014,** *21* (6), 1-8.

9. Sun, X.-W.; Neidle, S.; Mann, J., Synthesis of a novel dimeric bis-benzimidazole with site-selective DNA-binding properties. *Tetrahedron Lett.* **2002,** *43* (40), 7239-7241.

10. Wu, Z.; Rea, P.; Wickham, G., 'One-pot' nitro reduction–cyclisation solid phase route to benzimidazoles. *Tetrahedron Lett.* **2000,** *41* (50), 9871-9874.

11. Wang, L.; Sheng, J.; Tian, H.; Qian, C., An Efficient Procedure for the Synthesis of Benzimidazole Derivatives Using Yb(OTf)3 as Catalyst Under Solvent-Free Conditions. *Synth. Commun.* **2004,** *34* (23), 4265-4272.

12. Loupy, A.; Petit, A.; Hamelin, J.; Texier-Boullet, F.; Jacquault, P.; Mathé, D., New Solvent-Free Organic Synthesis Using Focused Microwaves. *Synthesis* **1998,** *1998* (09), 1213-1234.

13. Bendale, P. M.; Sun, C.-M., Rapid Microwave-Assisted Liquid-Phase Combinatorial Synthesis of 2-(Arylamino)benzimidazoles. *J. Comb. Chem.* **2002,** *4* (4), 359-361.

14. Evindar, G.; Batey, R. A., Copper- and Palladium-Catalyzed Intramolecular Aryl Guanidinylation: An Efficient Method for the Synthesis of 2-Aminobenzimidazoles. *Org. Lett.* **2003,** *5* (2), 133-136.

15. Reddy, G. V.; Rama Rao, V. V. V. N. S.; Narsaiah, B.; Shanthan Rao, P., A SIMPLE AND EFFICIENT METHOD FOR THE SYNTHESIS OF NOVEL TRIFLUOROMETHYL BENZIMIDAZOLES UNDER

MICROWAVE IRRADIATION CONDITIONS*. *Synth. Commun.* **2002,** *32* (16), 2467-2476.

16.   Dhakshinamoorthy, A.; Kanagaraj, K.; Pitchumani, K., Zn2+-K10-clay (clayzic) as an efficient water-tolerant, solid acid catalyst for the synthesis of benzimidazoles and quinoxalines at room temperature. *Tetrahedron Lett.* **2011,** *52* (1), 69-73.

17.   Bahrami, K.; Khodaei, M. M.; Kavianinia, I., A Simple and Efficient One-Pot Synthesis of 2-Substituted Benzimidazoles. *Synthesis* **2007,** *2007* (04), 547-550.

18.   Collins, J. P.; Schwartz, R. W.; Sehgal, R.; Ward, T. L.; Brinker, C. J.; Hagen, G. P.; Udovich, C. A., Catalytic Dehydrogenation of Propane in Hydrogen Permselective Membrane Reactors. *Industrial & Engineering Chemistry Research* **1996,** *35* (12), 4398-4405.

19.   Wolfson, A.; Dlugy, C.; Shotland, Y.; Tavor, D., Glycerol as solvent and hydrogen donor in transfer hydrogenation–dehydrogenation reactions. *Tetrahedron Lett.* **2009,** *50* (43), 5951-5953.

20.   Kim, K.-B.; Shim, J.-H.; Cho, Y. W.; Oh, K. H., Pressure-enhanced dehydrogenation reaction of the LiBH4-YH3 composite. *Chem. Commun.* **2011,** *47* (35), 9831-9833.

21.   Singh, N.; Jang, D. O., Benzimidazole-Based Tripodal Receptor: Highly Selective Fluorescent Chemosensor for Iodide in Aqueous Solution. *Org. Lett.* **2007,** *9* (10), 1991-1994.

22.   Manna, S. K.; Mondal, S. K.; Ahmed, A.; Mandal, A.; Jana, A.; Ikbal, M.; Samanta, S.; Ray, J. K., One-pot synthesis of highly fluorescent polycyclic benzimidazole derivatives. *RSC Advances* **2014,** *4* (5), 2474-2481.

23.   Zhang, N.; Tian, X.; Zheng, J.; Zhang, X.; Zhu, W.; Tian, Y.; Zhu, Q.; Zhou, H., A novel fluorescent probe based on the flexible dipicolylamine: Recognizing zinc(II) in aqueous solution and imaging in living cell. *Dyes and Pigments* **2016,** *124*, 174-179.

24. Zhu, X.; Lin, Q.; Zhang, Y.-M.; Wei, T.-B., Nitrophenylfuran-benzimidazole-based reversible alkaline fluorescence switch accurately controlled by pH. *Sensors Actuators B: Chem.* **2015,** *219*, 38-42.

25. Laobuthee, A.; Chirachanchai, S.; Ishida, H.; Tashiro, K., Asymmetric Mono-oxazine: An Inevitable Product from Mannich Reaction of Benzoxazine Dimers. *J. Am. Chem. Soc.* **2001,** *123* (41), 9947-9955.

26. Chirachanchai, S.; Laobuthee, A.; Phongtamrug, S., Self termination of ring opening reaction of p-substituted phenol-based benzoxazines: An obstructive effect via intramolecular hydrogen bond. *J. Heterocycl. Chem.* **2009,** *46* (4), 714-721.

CHAPTER VI
CONCLUSIONS

The present work demonstrated the simple molecular design and development of benzoxazine dimers for their potential applications. The depth analysis based on advanced instruments, especially X-ray single crystal analysis, GPC, ^{1}H NMR lead us to an original work of showing dual function of benzoxazine dimers as initiator and ligand for ring-opening polymerization of lactide. Lactide successfully polymerized on two hydroxyl groups of benzoxazine dimers. Moreover, we suggested that the substituted of phenol and types of methylene bridge unit effect to complexation with aluminium (Chapter III). The work also proved that not only benzoxazine dimers but also branched benzoxazine dimers can be performed as initiator for ring-opening polymerization of lactide. The conjugation of eight-armed polylactide with diacetylene led to a functional additive for the blend with PLLA resin. The free standing film was easily obtained by solution casting. The film developed the blue-red color transformation upon heating and and cooling. The comparative studies based on bulk DA, linea-, four-, and multi-armed DA, clarified that only eight-armed star controls the packing structure of PDA result in the reversible thermochromic propertiess. The present work showed for the first time a PLLA free standing film with reversible thermochromic properties which is a model case to develop PDA free standing film (Chapter IV). Moreover, by simply changing monophenol- to diphenol-based, the present work demonstrated a new class of benzoxazine dimer containing benzimidazole moiety. Benzimidazole was formed through the cyclization between aldehyde and phenylenediamine derivatives under reduced pressure. pH-sensitive fluorescent compound was prepared via a Mannich reaction of benzoxazine under mild condition. The spectral behavior of molecules were evaluated in dimethylsulfoxide. These compound showed pH-sensitive fluorescent intensity and multichromatic emissions with sodium hydroxide solution. This is corresponding to the specific molecular state of molecule resulting in different self-assembly morphologies at nanoscale (Chapter V).

REFERENCES

1.   Ning, X.; Ishida, H., Phenolic materials via ring-opening polymerization: Synthesis and characterization of bisphenol-A based benzoxazines and their polymers. *Journal of Polymer Science Part A: Polymer Chemistry* **1994,** *32* (6), 1121-1129.

2.   Apirat, L.; Suwabun, C., A simple, effective, and selective synthesis route for difunctional 30-membered macrocyclic ester and linear oligoester derived from benzoxazine dimers. *Chemistry Letters* **2002,** (6), 614-615.

3.   Phongtamrug, S.; Chirachanchai, S.; Tashiro, K., Supramolecular Structure of N,N-Bis(2-hydroxy-benzyl)alkylamine: From Hydrogen Bond Assembly to Coordination Network in Guest Acceptance. *Macromolecular Symposia* **2006,** *242* (1), 40-48.

4.   Rungsimanon, T.; Laobuthee, A.; Miyata, M.; Chirachanchai, S., [1+1] and [2+2] crown ethers derived from N,N-bis(2-hydroxyalkylbenzyl)alkylamine and their inclusion phenomena with metal ions. *Journal of Inclusion Phenomena* **2008,** *62* (3-4), 333-338.

5.   Phongtamrug, S.; Miyata, M.; Chirachanchai, S., Concerted Contribution of Cu–O Coordination and Hydrogen Bonds in N,N-Bis(2-hydroxybenzyl)alkylamine–Copper–Solvent System. *Chemistry Letters* **2005,** *34* (5), 634-635.

6.   Phongtamrug, S.; Pulpoka, B.; Chirachanchai, S., Inclusion Compounds Formed from N,N-bis(2-hydroxybenzyl)alkylamine Derivatives and Transition Metal Ions via Molecular Assembly. *Supramolecular Chemistry* **2004,** *16* (4), 269-278.

7.   Burke, W. J., 3,4-Dihydro-1,3,2H-Benzoxazines. Reaction of p-Substituted Phenols with N,N-Dimethylolamines. *Journal of the American Chemical Society* **1949,** *71* (2), 609-612.

8.   Burke, W. J.; Bishop, J. L.; Glennie, E. L. M.; Bauer, W. N., A New Aminoalkylation Reaction. Condensation of Phenols with Dihydro-1,3-aroxazines1. *The Journal of Organic Chemistry* **1965,** *30* (10), 3423-3427.

9.   Giesen, K.; Hage, F.; Himpsel, F. J.; Riess, H. J.; Steinmann, W., Two-photon photoemission via image-potential states. *Physical Review Letters* **1985,** *55* (3), 300-303.

10.   Laobuthee, A.; Chirachanchai, S.; Ishida, H.; Tashiro, K., Asymmetric Mono-oxazine: An Inevitable Product from Mannich Reaction of Benzoxazine Dimers. *Journal of the American Chemical Society* **2001,** *123* (41), 9947-9955.

11.   Laobuthee, A.; Ishida, H.; Chirachanchai, S., Metal Ion Guest Responsive Benzoxazine Dimers and Inclusion Phenomena of Cyclic Derivatives. *Journal of Inclusion Phenomena* **2003,** *47* (3-4), 179-185.

12.   Corneillie, S.; Smet, M., PLA architectures: the role of branching. *Polymer Chemistry* **2015,** *6* (6), 850-867.

13.   Auras, R.; Harte, B.; Selke, S., An Overview of Polylactides as Packaging Materials. *Macromolecular Bioscience* **2004,** *4* (9), 835-864.

14.   Drumright, R. E.; Gruber, P. R.; Henton, D. E., Polylactic Acid Technology. *Advanced Materials* **2000,** *12* (23), 1841-1846.

15.   In't Veld, P. J. A.; Velner, E. M.; Van De Witte, P.; Hamhuis, J.; Dijkstra, P. J.; Feijen, J., Melt block copolymerization of ϵ-caprolactone and L-lactide. *Journal of Polymer Science Part A: Polymer Chemistry* **1997,** *35* (2), 219-226.

16.   Doi, Y.; Kitamura, S.; Abe, H., Microbial Synthesis and Characterization of Poly(3-hydroxybutyrate-co-3-hydroxyhexanoate). *Macromolecules* **1995,** *28* (14), 4822-4828.

17.   Nijenhuis, A. J.; Grijpma, D. W.; Pennings, A. J., Lewis acid catalyzed polymerization of L-lactide. Kinetics and mechanism of the bulk polymerization. *Macromolecules* **1992,** *25* (24), 6419-6424.

18.   Swift, G., Directions for environmentally biodegradable polymer research. *Accounts of Chemical Research* **1993,** *26* (3), 105-110.

19.   Miao, Y.; Zinck, P., Ring-opening polymerization of cyclic esters initiated by cyclodextrins. *Polymer Chemistry* **2012,** *3* (5), 1119-1122.

20.   Saunders, L. N.; Dawe, L. N.; Kozak, C. M., Alkali metal complexes of tridentate amine-bis(phenolate) ligands and their rac-lactide ROP activity. *Journal of Organometallic Chemistry* **2014,** *749* (0), 34-40.

21.   Yang, S.; Nie, K.; Zhang, Y.; Xue, M.; Yao, Y.; Shen, Q., New [ONOO]-Type Amine Bis(phenolate) Ytterbium(II) and -(III) Complexes: Synthesis, Structure, and Catalysis for Highly Heteroselective Polymerization of rac-Lactide. *Inorganic Chemistry* **2013**.

22.   Liang, Z.; Zhang, M.; Ni, X.; Li, X.; Shen, Z., Ring-opening polymerization of cyclic esters initiated by lithium aggregate containing bis(phenolate) and enolate mixed ligands. *Inorganic Chemistry Communications* **2013,** *29*, 145–147.

23.   Giesbrecht, G. R.; Whitener, G. D.; Arnold, J., Mono-guanidinate complexes of lanthanum: synthesis, structure and their use in lactide polymerization. *Journal of the Chemical Society, Dalton Transactions* **2001,** (6), 923-927.

24.   Wegner, G., Solid-state polymerization mechanisms. In *Pure and Applied Chemistry*, 1977; Vol. 49, p 443.

25.   Wegner, G., Topochemische Reaktionen von Monomeren mit konjugierten Dreifachbindungen / Tochemical Reactions of Monomers with conjugated triple Bonds. In *Zeitschrift für Naturforschung B*, 1969; Vol. 24, p 824.

26.   Baughman, R. H., Solid-state polymerization of diacetylenes. *Journal of Applied Physics* **1972,** *43* (11), 4362-4370.

27.   Luo, L.; Wilhelm, C.; Sun, A.; Grey, C. P.; Lauher, J. W.; Goroff, N. S., Poly(diiododiacetylene): Preparation, Isolation, and Full Characterization of a Very Simple Poly(diacetylene). *Journal of the American Chemical Society* **2008,** *130* (24), 7702-7709.

28.   Chance, R. R.; Patel, G. N., Solid-state polymerization of a diacetylene crystal: Thermal, ultraviolet, and γ-ray polymerization of 2,4-hexadiyne-1,6-diol bis-(p-toluene sulfonate). *Journal of Polymer Science: Polymer Physics Edition* **1978,** *16* (5), 859-881.

29.   Fomina, L.; Allier, H.; Fomine, S.; Salcedo, R.; Ogawa, T., Synthesis and Molten-State Polymerization of Some Novel Conjugated Diacetylenes. *Polym J* **1995,** *27* (6), 591-600.

30.   Reppy, M. A.; Pindzola, B. A., Biosensing with polydiacetylene materials: structures, optical properties and applications. *Chemical Communications* **2007,** (42), 4317-4338.

31.   Takuya, H.; Naoyuki, Y.; Hideyuki, U.; Hiroyuki, Y.; Akihiko, F.; Masanori, O., Anisotropic Properties of Aligned π-Conjugated Polymer Films Fabricated by Capillary Action and Their Post-Annealing Effects. *Applied Physics Express* **2011,** *4* (9), 091602.

32.   Ahn, D. J.; Kim, J.-M., Fluorogenic Polydiacetylene Supramolecules: Immobilization, Micropatterning, and Application to Label-Free Chemosensors. *Accounts of Chemical Research* **2008,** *41* (7), 805-816.

33.   Kauffman, J. S.; Ellerbrock, B. M.; Stevens, K. A.; Brown, P. J.; Pennington, W. T.; Hanks, T. W., Preparation, Characterization, and Sensing Behavior of Polydiacetylene Liposomes Embedded in Alginate Fibers. *ACS Applied Materials & Interfaces* **2009,** *1* (6), 1287-1291.

34.   Kim, T. H.; Lee, B. Y.; Jaworski, J.; Yokoyama, K.; Chung, W.-J.; Wang, E.; Hong, S.; Majumdar, A.; Lee, S.-W., Selective and Sensitive TNT Sensors Using Biomimetic Polydiacetylene-Coated CNT-FETs. *ACS Nano* **2011,** *5* (4), 2824-2830.

35.   Yuan, Z.; Lee, C.-W.; Lee, S.-H., Reversible Thermochromism in Hydrogen-Bonded Polymers Containing Polydiacetylenes. *Angewandte Chemie International Edition* **2004,** *43* (32), 4197-4200.

36.   Yuan, Z.; Lee, C.-W.; Lee, S.-H., Reversible thermochromism in self-layered hydrogen-bondedpolydiacetylene assembly. *Polymer* **2006,** *47* (9), 2970-2975.

37.   Kim, J.-M.; Lee, J.-S.; Choi, H.; Sohn, D.; Ahn, D. J., Rational Design and in-Situ FTIR Analyses of Colorimetrically Reversibe Polydiacetylene Supramolecules. *Macromolecules* **2005,** *38* (22), 9366-9376.

38.   Chanakul, A.; Traiphol, N.; Traiphol, R., Controlling the reversible thermochromism of polydiacetylene/zinc oxide nanocomposites by varying alkyl chain length. *Journal of Colloid and Interface Science* **2013,** *389* (1), 106-114.

39.   Kolusheva, S.; Kafri, R.; Katz, M.; Jelinek, R., Rapid Colorimetric Detection of Antibody−Epitope Recognition at a Biomimetic Membrane Interface. *Journal of the American Chemical Society* **2001,** *123* (3), 417-422.

40.   Ritenberg, M.; Kolusheva, S.; Ganin, H.; Meijler, M. M.; Jelinek, R., Biofilm Formation on Chromatic Sol–Gel/Polydiacetylene Films. *ChemPlusChem* **2012,** *77* (9), 752-757.

41.   You, X.; Zou, G.; Ye, Q.; Zhang, Q.; He, P., Ruthenium(ii) complex-sensitized solid-state polymerization of diacetylene in the visible light region. *Journal of Materials Chemistry* **2008,** *18* (39), 4704-4711.

42.   Jiang, H.; Pan, X.-J.; Lei, Z.-Y.; Zou, G.; Zhang, Q.-J.; Wang, K.-Y., Photocontrol of chiroptical properties of polydiacetylene carrying azobenzene in the side chain. *Chemical Physics Letters* **2010,** *500* (1–3), 100-103.

APPENDIX

CHAPTER III

Materials and General Techniques

p-Formaldehyde, 2,4-dimethylphenol, chloroform, dioxane, dimethylformamide (DMF) and isopropanol were purchased from RCI Labscan, Thailand. Triethylaluminium, pentaerythritol, tetrahydrofuran, toluene p-cresol, cyclohexylamine, paraformaldehyde, methylamine, 4-dimethylaminopyridine (DMAP), triazabicyclodecene (TBD), 1,8-diazabicycloundec-7-ene (DBU), methanol, diethyl ether, hexane and deuterated benzene (C_6D_6) were purchased from Sigma-Aldrich Co. LLC, Germany. All experiments were carried out on a Schlenk line under argon or in a glove box under nitrogen. The solvents were deoxygenated, dried over sodium/benzophenone ketyl and distilled just before use. C_6D_6 was dried over sodium benzophenone.

NMR spectra of the complexes were recorded in Teflon-valved NMR tubes. NMR spectra were recorded by Bruker Avance 300 instrument at 293 K in benzene-d_6 (C_6D_6) and Chloroform ($CDCl_3$). All chemical shifts were reported in parts per million (ppm) and measured relative to the solvent in which the sample was analyzed (C_6D_6 δH = 7.16 ppm and $CDCl_3$ δH = 7.24 ppm). Molecular weight and polydispersity were determined by a Shimadzu Class-VP size-exclusion chromatograph (SEC) equipped with a PLgel 5 μm MIXED-D column 300 x 7.5 mm (Polymer Laboratories, Varian Inc.) and a refractive index detector. Chloroform was used as an eluent at a flow rate of 1.0 mL min^{-1}. Molecular weight and molecular weight distributions were calculated using polystyrene as standard, the Mn values of trans-polyisoprenes were corrected with coefficient 0.58. Single crystal X-ray analysis performed at 100(1) K) on a Bruker Smart Apex CCD 4K system. The structure was solved by charge flipping methods using superflip software and least-squares refined with JANA2006 software.

Synthesis of N,N-Bis(2-hydroxy-5-methylbenzyl)cyclohexylamine, 1

Cyclohexylamine (0.35 mL, 10.0 mmol) was mixed with paraformaldehyde (0.60, 20.0 mmol) in dioxane. Then, p-cresol (1.08 g, 10.0 mmol) was added and refluxed at 110 °C for 6 h. The solvent was removed under vacuum to obtain the crude product. p-C resol (1.08 g, 10.0 mmol) was added into crude product and stirred at 60

°C for 3 h. The mixture was recrystallized in isopropanol to obtain colorless crystal of **1**. 85% yield; R_f = 0.27 (5% MeOH in CHCl$_3$); FT-IR (KBr, cm^{-1}): 3338 cm^{-1} (s, O-H stretching), 3008–2853 cm^{-1} (m, C-H stretching), 1502 cm^{-1} (s, trisubstituted benzene), 1221 cm^{-1} (vs. C–N stretching), 950 cm^{-1} (w, trisubstituted benzene); ^{1}H-NMR (300 MHz, C$_6$D$_6$, ppm): δ$_H$ 1.02 (m, 2H, *p* -CH$_2$) 1.36 (m, 4H, *m*-CH$_2$)1.65 (s, 2H, *o*-CH$_2$), 2.13(d, 2H, *o*-CH$_2$), 2.24 (s, 6H, para-**CH$_3$**), 2.87 (t, 1H, N-**CH**-CH$_2$), 3.76 (s, 4H, Ar-**CH$_2$**-N), 6.96 (m, 6H, Ar-**H**).

Synthesis of *N,N*-bis(2-hydroxy-3,5-dimethylbenzyl)hexylamine, 2

The synthesis of **2** was followed the preparation for **1** except that 1 equiv. 2,4 dimethyl phenol (1.22 g, 10.0 mmol) was used instead of *p*-Cresol giving **2**. 83% yield; R_f = 0.29 (5% MeOH in CHCl$_3$); FT-IR (KBr, cm^{-1}): 3361 cm^{-1} (s, O-H stretching), 3017–2865 cm^{-1} (m, C-H stretching), 1223 cm^{-1} (vs. C–N stretching); ^{1}H-NMR (300 MHz, C$_6$D$_6$, ppm): δ$_H$ 0.94 (m, 2H, *p* -CH$_2$), 1.21 (m, 2H, *m*-CH$_2$), 1.46 (s, 2H, *m*-CH$_2$), 1.61 (d, 2H, *o*-CH$_2$), 1.86 (d, 2H, *o*-CH$_2$), 2.29 (s, 6H, *p*-CH$_3$-Ar), 2.35 (s, 6H, *o*-CH$_3$-Ar), 2.85 (m, 1H, N-**CH**-CH$_2$), 3.70 (s, 4H, Ar-**CH$_2$**-N), 6.81 (s, 2H, *m*-**H**-Ar), 6.89 (s, 2H, *m*-**H**-Ar).

Synthesis of *N,N*-bis(2-hydroxy-3,5-dimethylbenzyl)methylamine, 3

1 equiv. methylamine (0.31 g, 10.0 mmol) was used instead of cyclohexylamine with the same procedure as compound **2** giving **3**. 90% yield; R_f = 0.32 (5% MeOH in CHCl$_3$); FT-IR (KBr, cm^{-1}): 3352 cm^{-1} (s, O-H stretching), 3012–2863 cm^{-1} (m, C-H stretching), 1502 cm^{-1} (s, trisubstituted benzene), 1246 cm^{-1}(m-s, C-OH in plane bending), 950 (w, trisubstituted benzene), 860 cm^{-1}(s, out-of-plane C-H deformations); ^{1}H-NMR (300 MHz, C$_6$D$_6$, ppm): δ$_H$ 2.00 (t, 6H, *p*-**CH$_3$**-Ar), 2.28 (q, 6H, *o*-**CH$_3$**-Ar), 3.48 (d, 4H, Ar-**CH$_2$**-N), 6.75 (s, 2H, *m*-**H**-Ar), 6.89 (s, 2H, *m*-**H**-Ar).

1AlEt complex formation

In a glove box, Compound **1** (10.18 mg, 3 μmol) and triethylaluminium (4.10 μl, 3 μmol) were mixed in toluene at room temperature. The mixture was left for 30 minutes to obtain complex **1AlEt**. Lactide (86.5 mg, 600 μmol) was added into a

complex solution. The polymerization was performed at 70 ˚C for 24 hours to investigate catalytic potential for lactide ROP.

2AlEt and 3AlEt complex formation

The same procedure as **1AlEt** except that compound **2** (11.02 mg, 3 μmol) and compound **3** (8.98 mg, 3 μmol) were used giving **2AlEt** and **3AlEt**, respectively. Catalytic potential in lactide ROP was also investigated.

1AlEt: ^{1}H-NMR (300 MHz, C_6D_6, ppm): δ_H 7.54 (s, 2H, Ar-H), 7.03 (d, J = 7.86 Hz, 2H, Ar-H), 6.65 (s, 2H, Ar-H), 3.72 (s, 2H, Ar-CH2-N), 3.40 (s, 2H, Ar-CH2-N), 2.54 (d, J = 7.67 Hz, 1H, C6H6-N), 2.02 (d, J = 3.31 Hz, 2H, C6H6-N), 1.42 (m, 11H, C6H12-N and CH3-CH2Al), 0.43 (d, J = 7.23 Hz, 2H, CH2-Al).

2AlEt: ^{1}H-NMR (300 MHz, C_6D_6, ppm): δ_H 6.97 (s, 2H, Ar-H), 6.49 (d, J = 7.86 Hz, 2H, Ar-H), 3.47 (dd, J = 13.64, 42.81 Hz, 4H, Ar-CH2-N), 2.46 (s, 6H, p-CH3-Ar), 2.26 (s, 6H, o-CH3-Ar), 1.85 (d, J = 11.25 Hz, 2H, C6H6-N), 1.58 (m, 3H, CH3-CH2Al), 1.40 (d, J = 7.61 Hz, 2H, C6H12-N), 1.22 (m, 2H, C6H12-N), 0.72 (t, 2H, C6H12-N), 0.54 (q, 2H, C6H12-N), 0.34 (s, 2H, CH2-Al).

3AlEt: ^{1}H-NMR (300 MHz, C_6D_6, ppm): δ_H 6.97 (s, 2H, Ar-H), 6.44 (s, 2H, Ar-H), 3.28 (d, J = 13.14 Hz, 2H, Ar-CH2-N), 2.96 (d, J = 13.11 Hz, 2H, Ar-CH2-N), 2.34 (m, 12H, CH3-Ar), 1.67 (d, J = 9.26 Hz, 3H, CH3-N), 1.32 (m, 3H, CH3-CH2Al), 0.42 (m, 2H, CH2-Al).

2AlOiPr and **2AlOBz** complex formation

In a glove box, compound **2** (5.51 mg, 15 μmol) was dissolved in toluene (1 ml). Triethylaluminium (2.05 μl, 15 μmol) was added and stirred for 10 minutes to form complex **2AlEt**. Isopropanol (1.15 μl, 15 μmol) was added into **2AlEt** solution and stirred for 10 minutes to yield **2AlOiPr**. Furthermore, Complex **2AlOBz** was formed by adding benzyl alcohol (1.55 μl, 15 μmol) instead of isopropanol.

Table A1. Crystallographic details of **2AlEt**

Empirical formula	C26 H36 Al N O2
Formula weight	421.56
Temperature	100 K
Wavelength	0.71073 Å
Crystal system	Monoclinic
Space group	C2/c
Dimensions	$a = 34.3280(12)$ Å
	$b = 9.9232(6)$ Å
	$c = 15.9234(9)$ Å
	$\alpha = 90$ °.
	$\beta = 102.55(2)$ °.
	$\gamma = 90$ °.
Volume	5294.5(5) A^3
Z	8
Density (calculated)	1.06 mg/m^3
Absorption coefficient	0.096 mm^{-1}
F(000)	1824.00
Theta range for data collection	2.140 – 26.243 °
Reflections collected	9732
Independent reflections	5347 [R(int) = 0.036]
Data / restraints / parameters	4493 / 0 / 271
Goodness-of-fit on F^2	1.0870
Final R indices [I>2σ(I)]	R1 = 0.0374
	wR2 = 0.0392
R indices (all data)	R1 = 0.0434
	wR2 = 0.0542
Largest diff. peak and hole	0.25 and -0.23 e/A^3
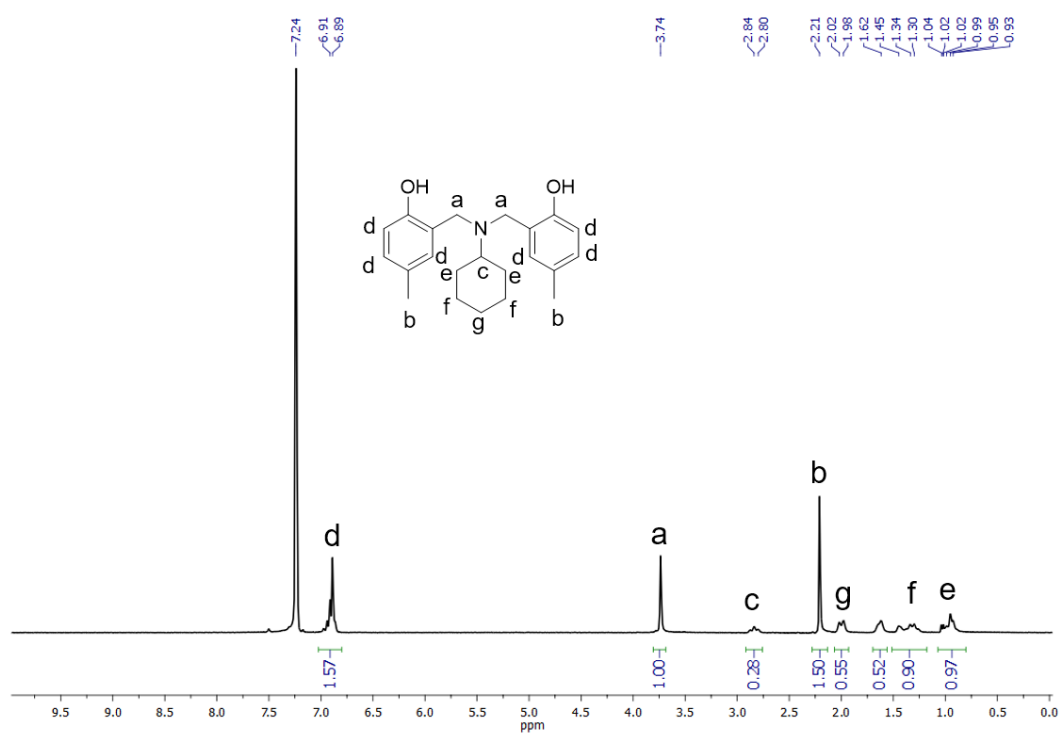
Figure A1. ^{1}H-NMR spectra of compound **1**.
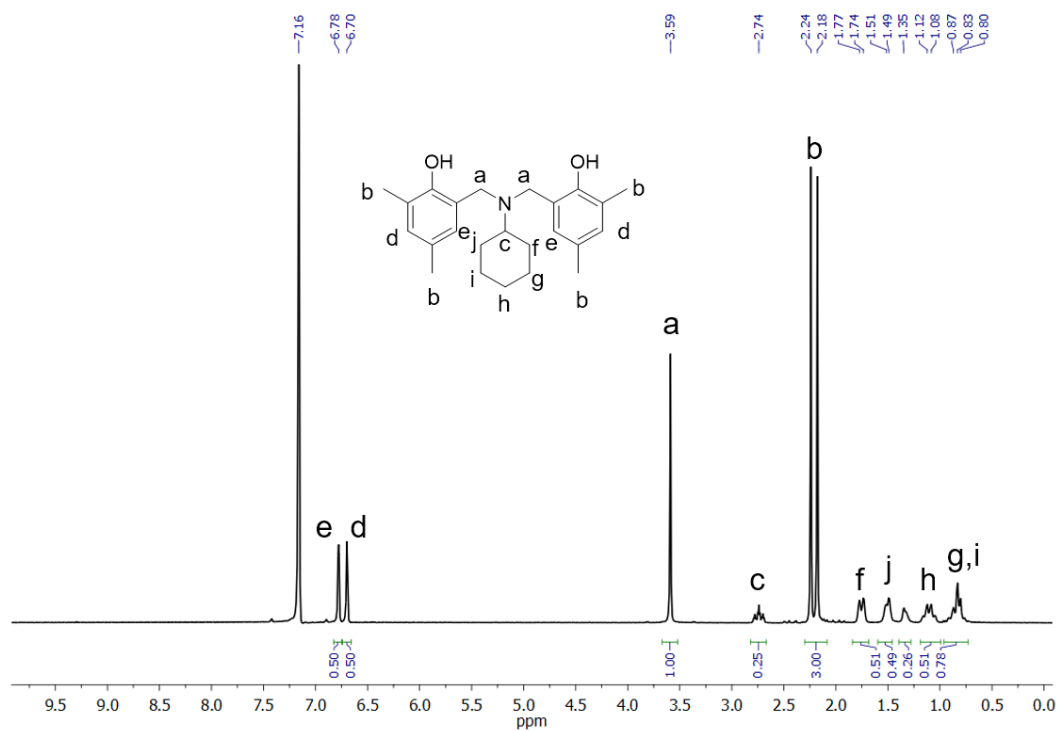
Figure A2. ^{1}H-NMR spectra of compound **2**.
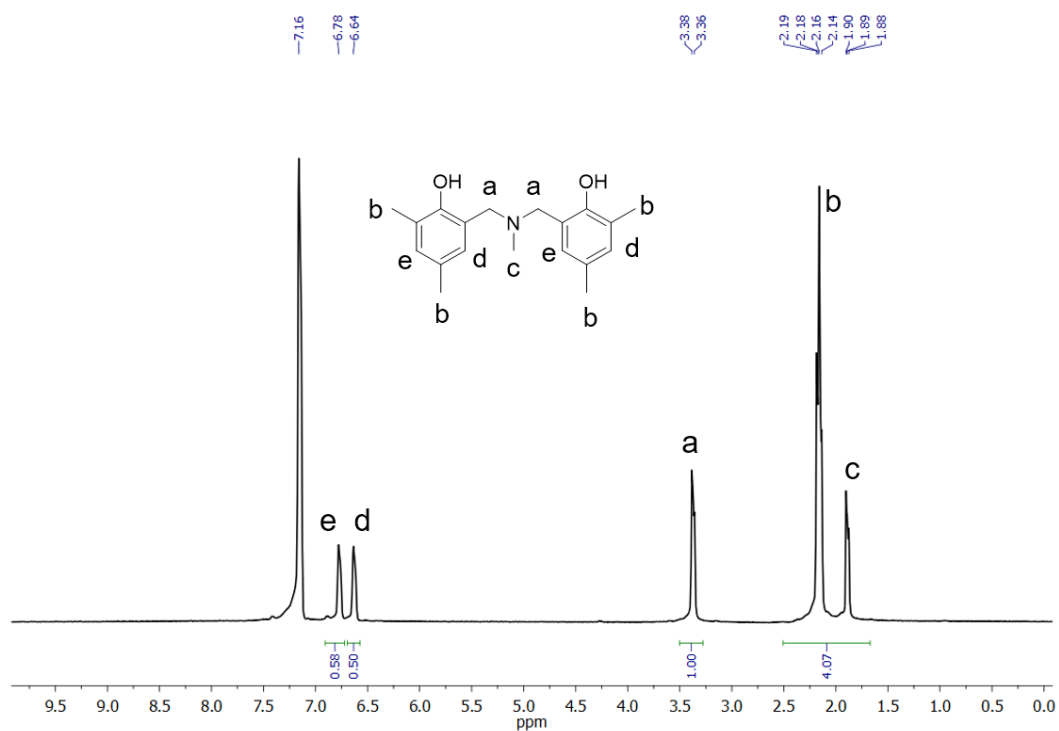
Figure A3. ^{1}H-NMR spectra of compound **3**.
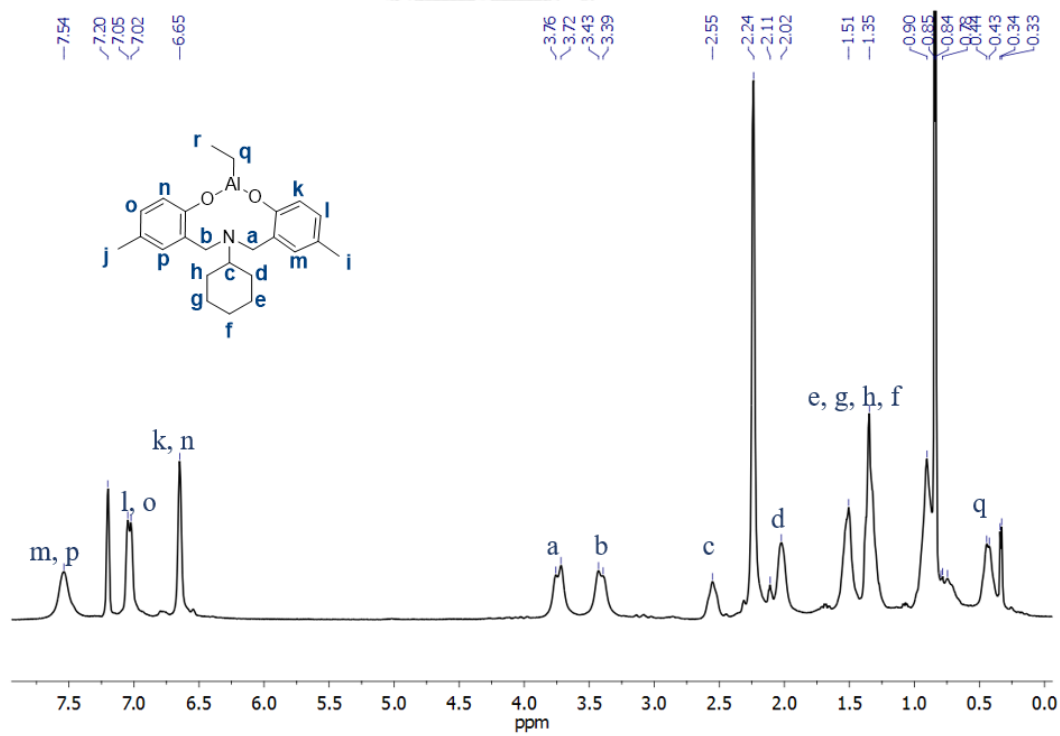
Figure A4. ^{1}H-NMR spectrum of complex **1AlEt**.
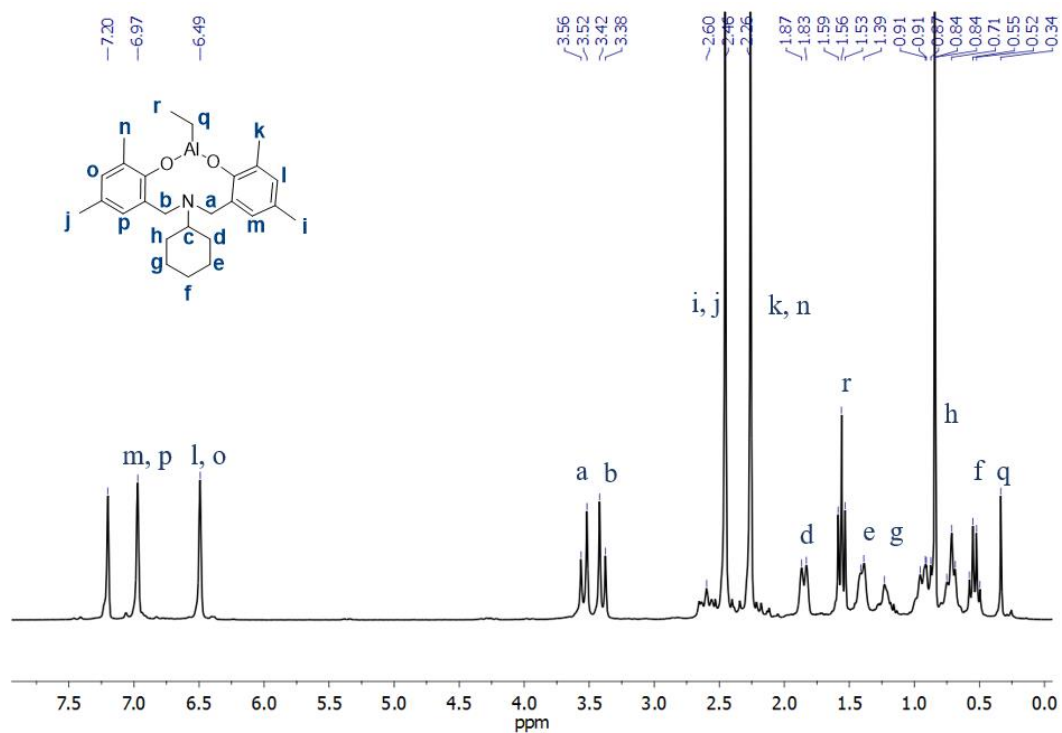
Figure A5. ^{1}H-NMR spectrum of complex **2AlEt**.
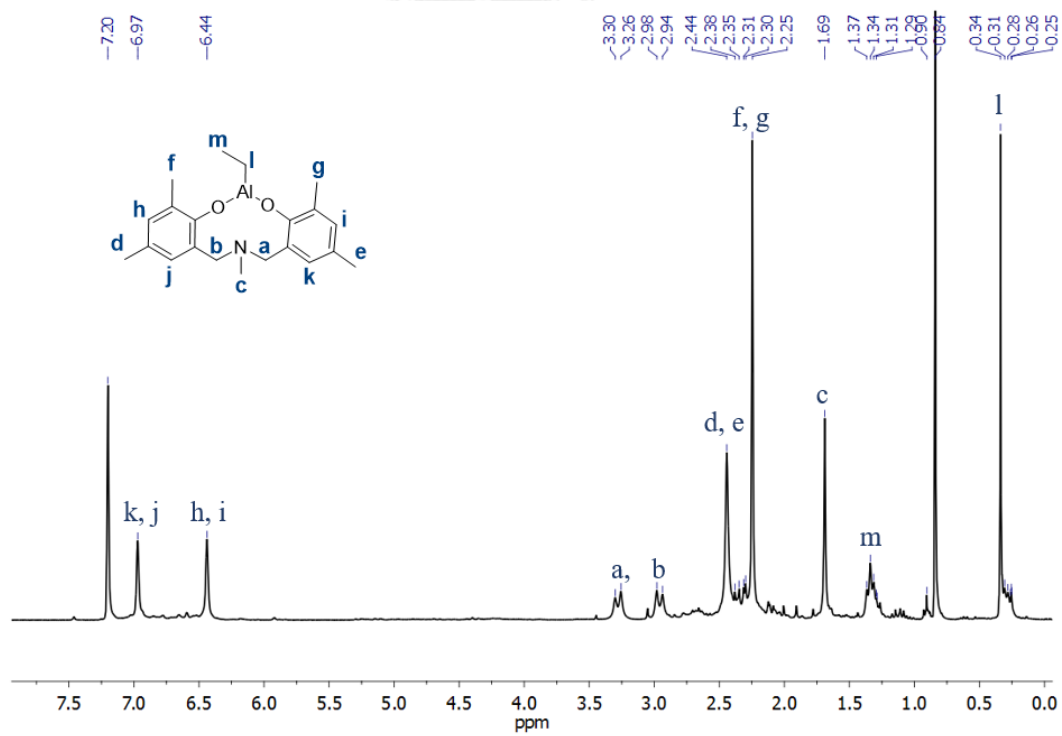
Figure A6. ^{1}H-NMR spectrum of complex **3AlEt**.

Table A2. Characterization of PLA obtained from various complex catalysts.

Ligand	Alcohol (equiv)	Conversion[a] (%)	M_n (calc)[b] (g/mol)	M_n (GPC)[c] (g/mol)	PDI
L1H2	--	41	11819	9048	1.15
L1H2	Isopropanol 1 eq.	82	--	--	--
L1H2	Benzyl Alcohol 1eq.	96	27670	18098	1.22
L2H2	--	75	21620	36870	1.18
L2H2	Isopropanol 1 eq.	100	28539	25520	1.16
L2H2	Benzyl Alcohol 1eq.	99	28828	27284	1.13

[a] Obtained by NMR of aliquot.

[b] M_n (calculated) = [*rac*-LA] / [Al] $\times$ 144.14 $\times$ conversion

[c] GPC results calibrated using polystyrene standards and corrected using the suggested Marke Houwink parameter of 0.58
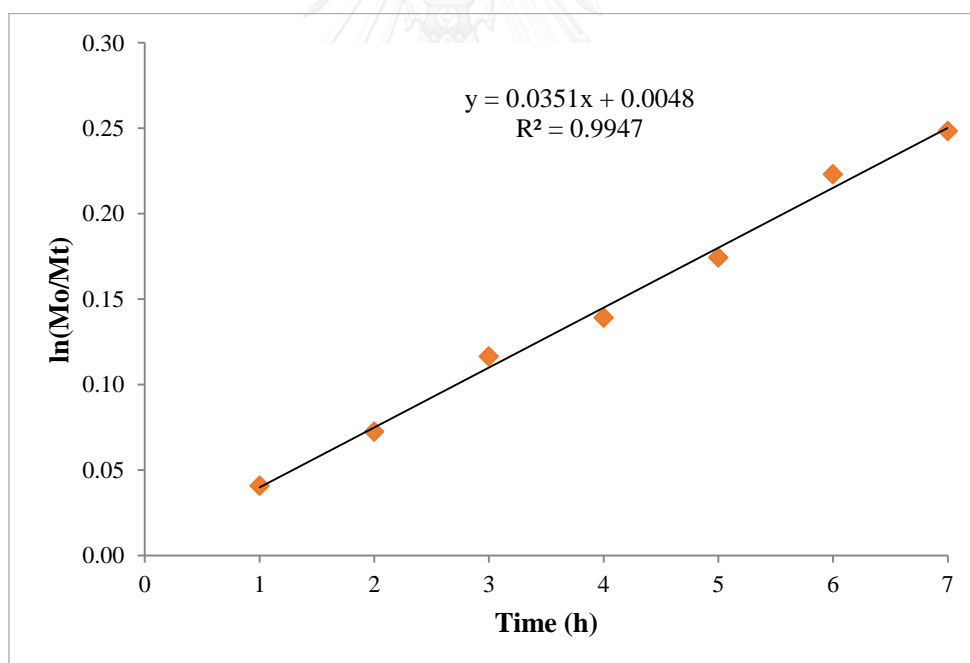
Figure A7. Kinetic plot of lactide ROP.
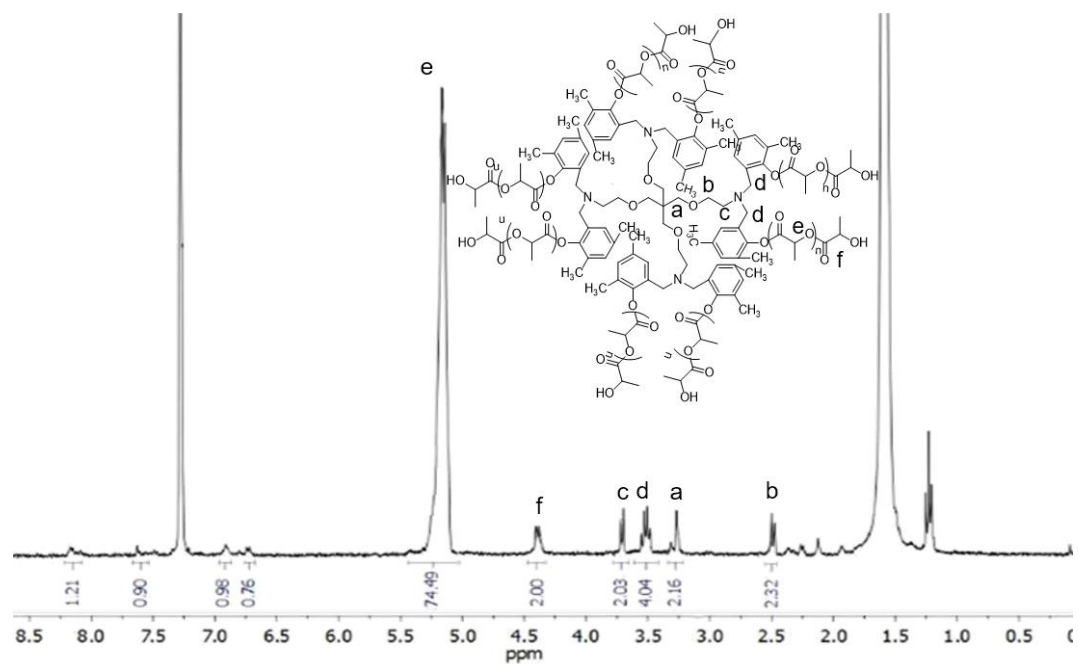
Figure A8. ^{1}H NMR of lactide ROP using tetra-branched benzoxazine dimers as an initiator.

CHAPTER VI

Synthesis of linear polylactide conjugated diacetylene (linear PLLA-DA)

Phenol (37.8 mg, 0.4 mmol), tin(II) 2-ethylhexanoate (40.5 mg, 0.1 mmol), and L-lactide (1441.4 mg, 10 mmol) were dried under vacuum for 3 hours. The ring opening polymerization was performed under N_2 at 120 °C in bulk state until it becomes a viscous. The product was precipitated in cold diethyl ether to obtain linear polylactide with 98 % conversion. ^{1}H NMR (500 MHz, $CDCl_3$, ppm): 7.36 (m, 2H, Ar-H), 7.07 (m, 1H, Ar-H), 6.90 (t, 1H, Ar-H), 6.80 (d, $J = 8.37$ Hz, 1H, Ar-H), 5.14 (dd, $J = 6.89, 13.97$ Hz, 39H, -OCH(CH3)C(O)- of PLLA), 4.33 (d, $J = 6.88$ Hz, 1H, terminal -OC(O)CH(CH3)-OH), 1.55 (t, 120H, OCH(CH3)C(O)- of PLLA). ^{1}H NMR analysis indicated a DP_n of 20 lactide units per chain. GPC analysis indicated $M_n = 2999$ g mol^{-1} and $M_w/M_n = 1.10$.

The conjugation reaction of linear polylactide with 10,12-pentacosadiynoic acid (149.8 mg, 0.4 mmol) was proceeded as the same procedure as 4BzD-8PLLA-8DA to obtain PLLA-DA with 92 % yield. ^{1}H NMR (500 MHz, $CDCl_3$, ppm): 7.36 (d, $J = 8.35$ Hz, 2H, Ar-H), 7.06 (d, $J = 7.50$ Hz, 1H, Ar-H), 6.89 (m, 1H, Ar-H), 6.79 (d, $J = 8.33$ Hz, 1H, Ar-H), 5.14 (dd, $J = 6.92, 14.01$ Hz, 36H, -OCH(CH3)C(O)- of PLLA), 4.34 (s, 1H, terminal -OC(O)CH(CH3)-OH), 2.51 (s, 2H, -OC(O)CH2- of DA), 2.22 (t, 4H, -(CH2)C≡C- of DA), 1.55 (t, 111H, OCH(CH3)C(O)- of PLLA), 1.25 (m, 32H, -CH2- of DA) 0.86 (t, 3H, -CH3 of DA). GPC analysis indicated $M_n = 3099$ g g mol^{-1} and $M_w/M_n = 1.00$.

Synthesis of 4 arms polylactide conjugated diacetylene (4PLLA-4DA)

Pentaerythritol (27.2 mg, 0.2 mmol) was used as initiator for ring opening polymerization of L-lactide (2882.8 mg, 20 mmol) in bulk at 120 °C with tin(II) 2-ethylhexanoate catalyst (81.0 mg, 0.2 mmol). At the end of the reaction, the medium was viscous. The product obtained was precipitated in cold diethyl ether and dried under vacuum to obtain 4 arms polylactide (4PLLA) with the yield of 95%. ^{1}H NMR (500 MHz, $CDCl_3$, ppm): 5.14 (d, $J = 7.11$ Hz, 44H, -OCH(CH3)C(O)- of PLLA), 4.34 (s, 1H, terminal -OC(O)CH(CH3)-OH), 3.51 (m, 2H, C(CH2)-O-PLLA), 1.56 (t, 135H,

OCH(CH3)C(O)- of PLLA). ^{1}H NMR analysis indicated a DP$_n$ of 22 lactide units per chain. GPC analysis indicated M_n = 19963 g mol^{-1} and M_w/ M_n = 1.21.

4PLLA and 10,12-pentacosadiynoic acid (149.8 mg, 0.4 mmol) was conjugated as the same procedure as 4BzD-8PLLA-8DA to obtain 4PLLA-4DA with 87 % yield. ^{1}H NMR (500 MHz, CDCl$_3$, ppm):), 5.14 (dd, J = 6.89, 13.89 Hz, 32H, -OCH(CH3)C(O)- of PLLA), 4.35 (s, 1H, terminal -OC(O)CH(CH3)-OH), 3.49 (m, 2H, C(CH2)-O-PLLA), 2.58 (s, 2H, -OC(O)CH2- of DA), 2.22 (s, 4H, -(CH2)C≡C- of DA), 1.48 (t, 131H, OCH(CH3)C(O)- of PLLA and -CH2- of DA) 0.86 (t, 3H, -CH3 of DA).

Synthesis of hyperbranched polylactide conjugated diacetylene (mPEI-PLLA-DA)

Ring opening polymerization of ʟ-lactide (4571.7 mg, 31.7 mmol) was proceeded in bulk at 120 °C with tin(II) 2-ethylhexanoate catalyst (81.0 mg, 0.2 mmol) by using branched polyethyleneimine (93.5 mg, 1.6 mmol) as an initiator. The crude product was precipitate in cold methanol to obtain hyperbranched polylactide (mPEI-PLLA) at 98 % yield. ^{1}H NMR (500 MHz, CDCl$_3$, ppm): 5.14 (dd, J = 6.81, 13.89 Hz, 1634H, -OCH(CH3)C(O)- of PLLA), 4.34 (s, 43H, terminal -OC(O)CH(CH3)-OH), 3.72 (dd, J = 8.65, 14.35 Hz, 172H, -NH- and –NH2 of mPEI), 1.54 (m, 5031H, OCH(CH3)C(O)- of PLLA). ^{1}H NMR spectrum suggested 43 polylactide chains with DP$_n$ of 19 lactide units per chain on PEI molecule.

10,12-pentacosadiynoic acid (50.0 mg, 0.13 mmol) was conjugated with -OH group of polylactide as the same procedure as 4BzD-8PLLA-8DA to obtain mPEI-PLLA-DA. ^{1}H NMR (500 MHz, CDCl$_3$, ppm): 5.14 (dd, J = 6.85, 13.89 Hz, 903H, -OCH(CH3)C(O)- of PLLA), 4.34 (s, 43H, terminal -OC(O)CH(CH3)-OH), 3.59 (d, J = 126.48 Hz, 172H, mPEI), 2.58 (t, 86H, -OC(O)CH2- of DA), 2.22 (t, 172H, -(CH2)C≡C- of DA), 1.54 (m, 4214H, OCH(CH3)C(O)- of PLLA and -CH2- of DA), 0.86 (t, 129H, -CH3 of DA).
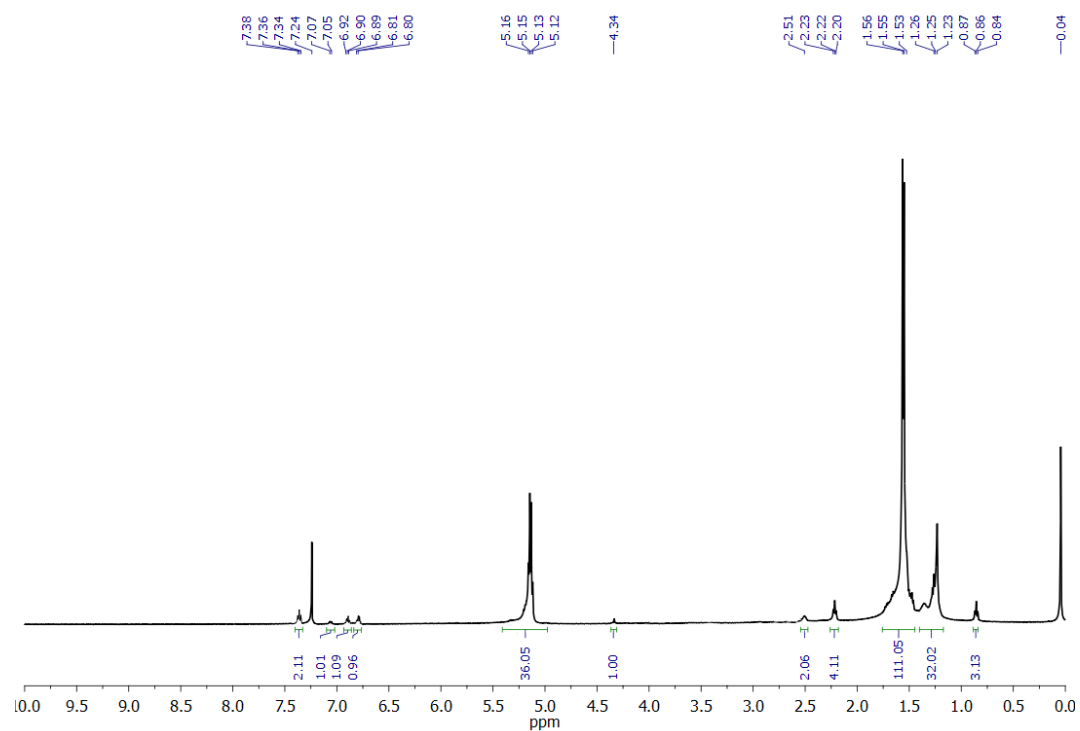
Figure B1. ^{1}H NMR of PLLA-DA.
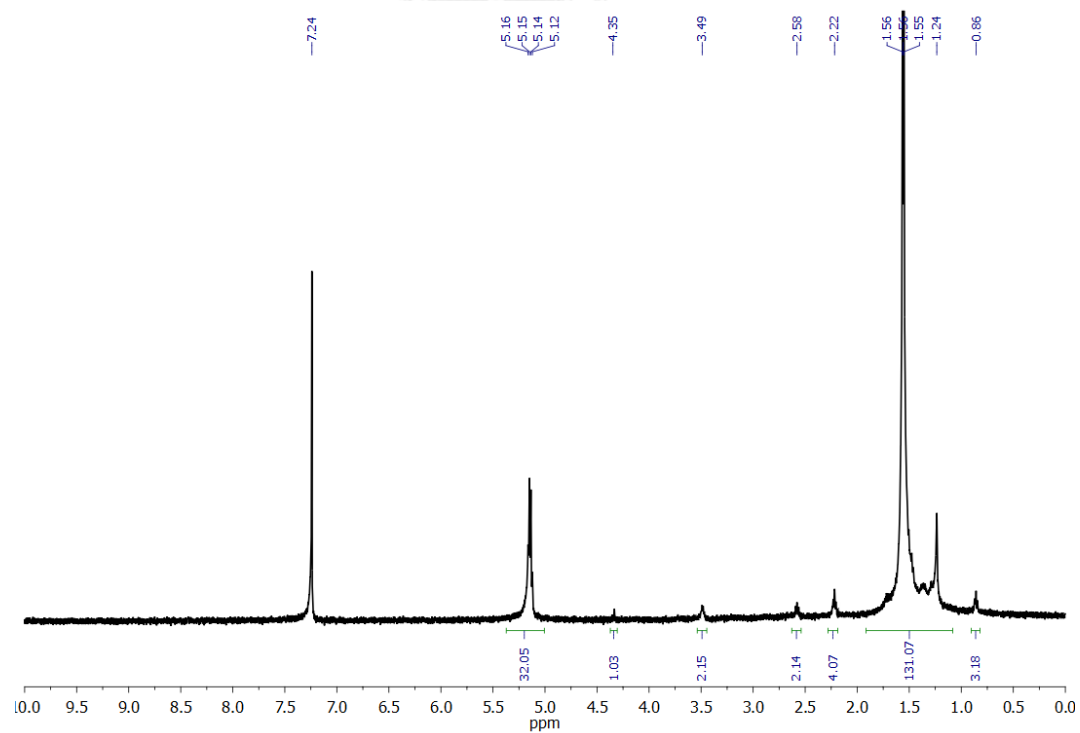
Figure B2. ^{1}H NMR of 4PLLA-4DA.
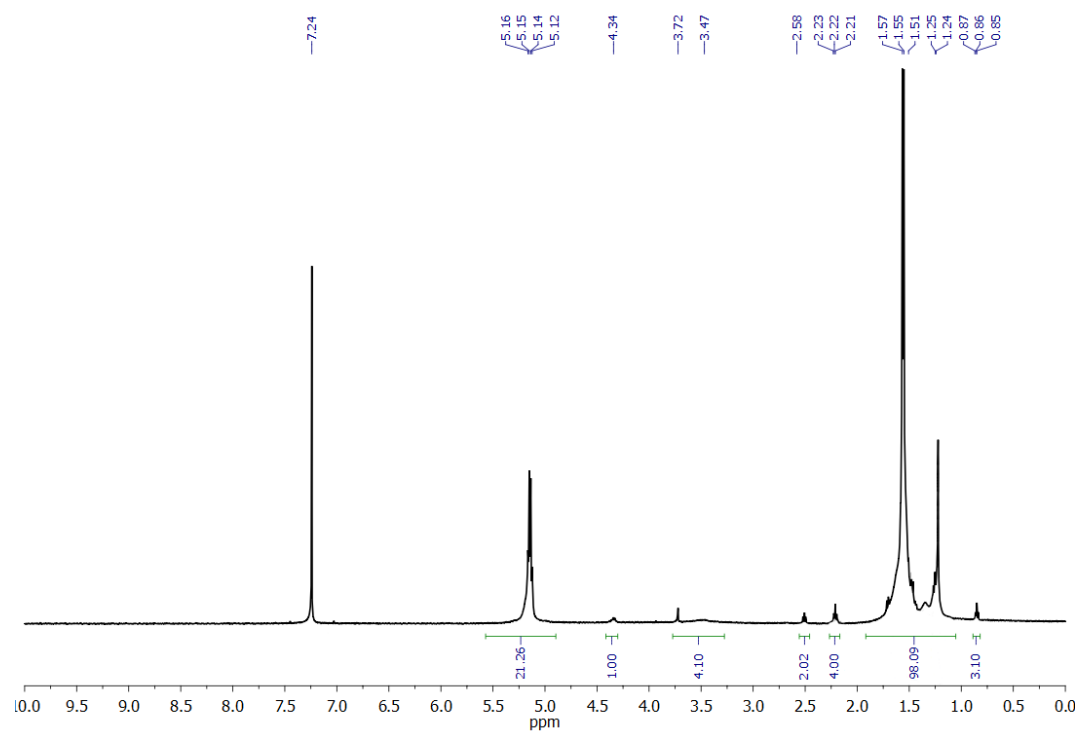
Figure B3. ^{1}H NMR of mPEI-PLLA-DA.
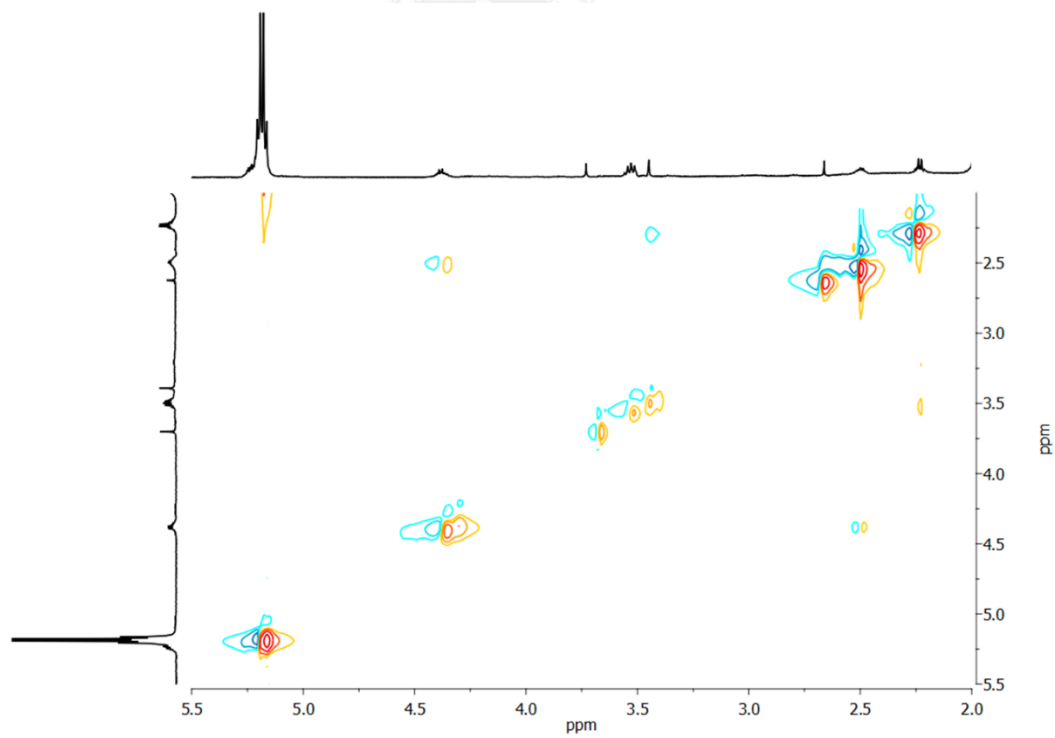
Figure B4. TOCSY NMR of 4BzD-8PLLA-8DA.
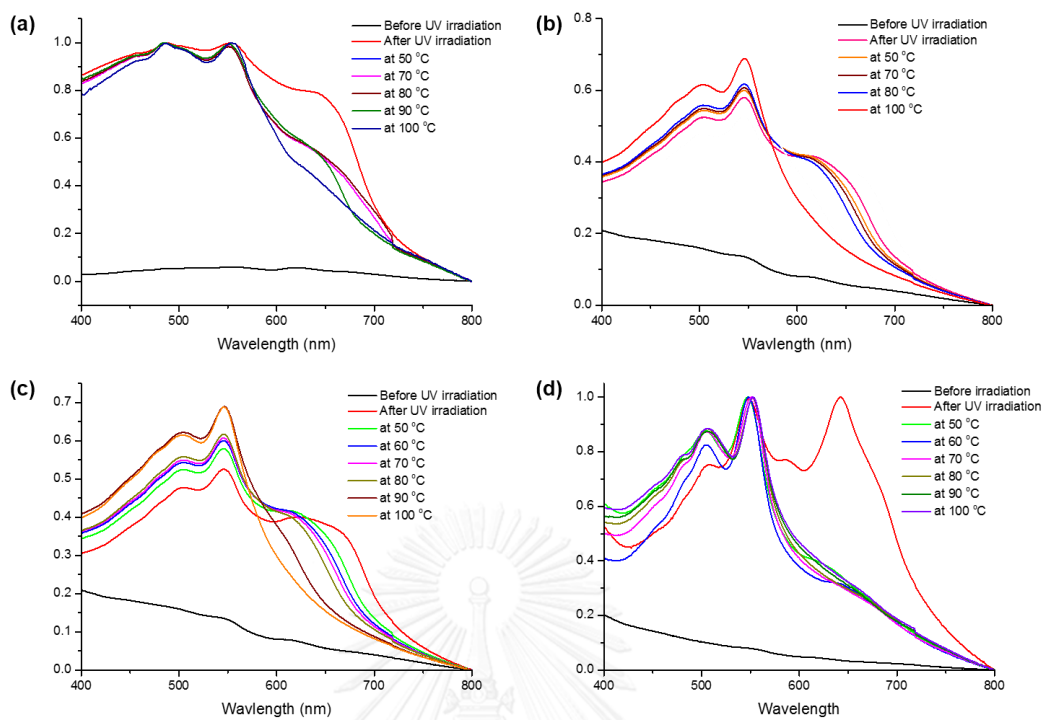
Figure B5. UV-Vis spectra of (a) DA, (b) PLLA-DA, (c) 4PLLA-4DA, and (d) mPEI-PLLA-DA.
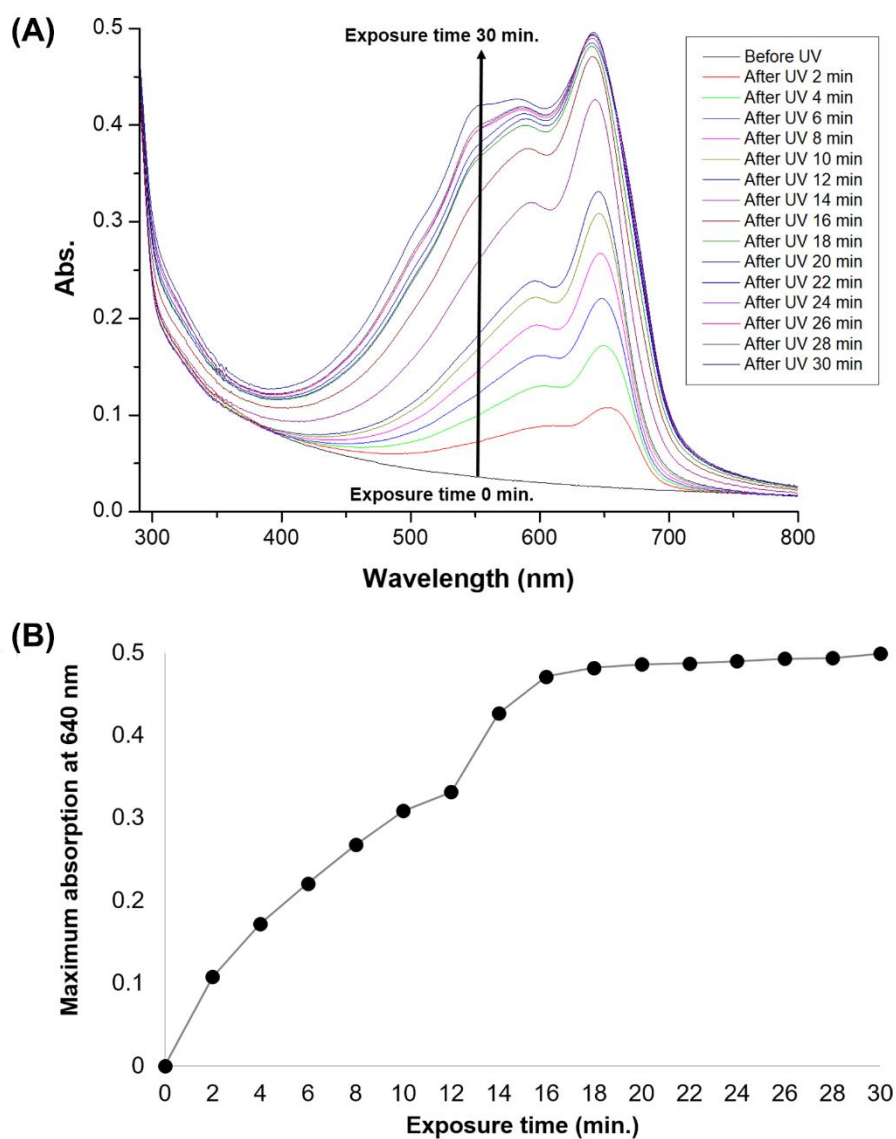
Figure B6. (a) UV-Vis spectra and (b) Time-resolved development of maximum absorption at 640 nm of kinetics of polymerization.
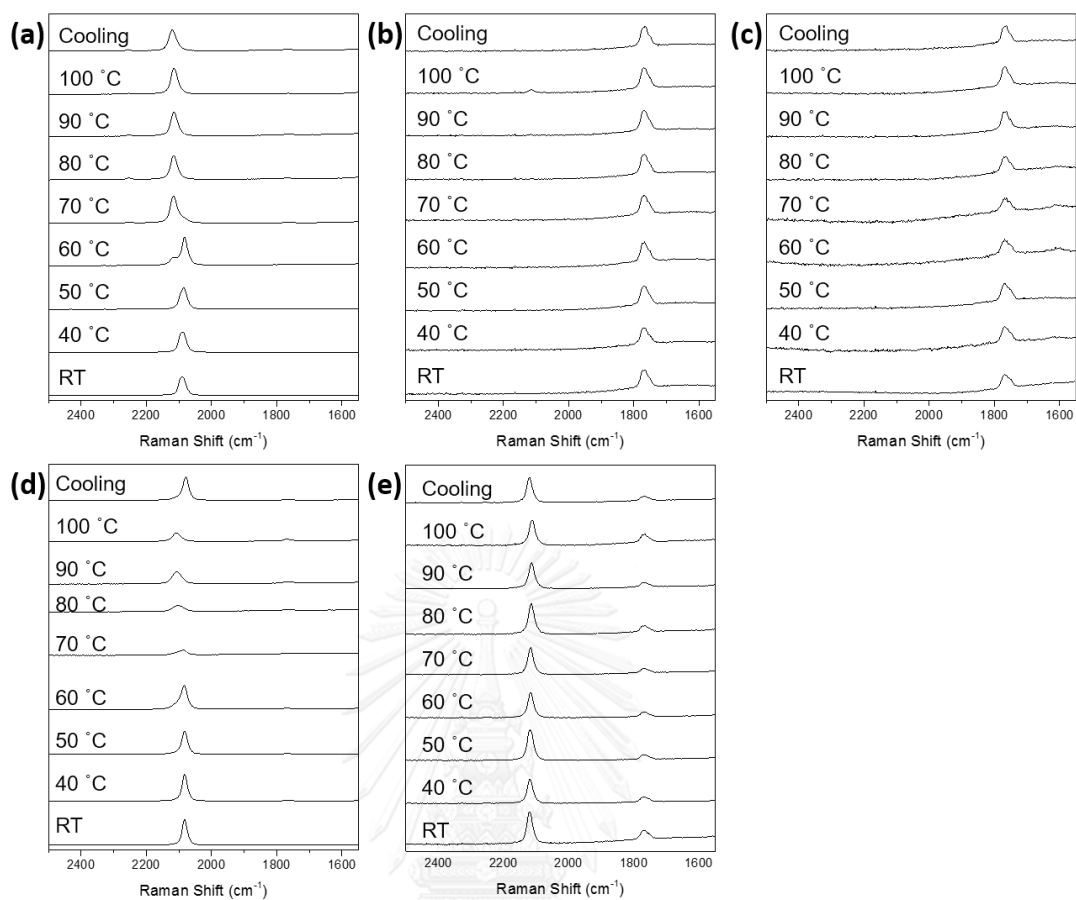
Figure B7. Temperature dependent Raman spectra of film (a) PDA/PLA, (b) PLLA-PDA/PLA, (c) 4PLLA-4PDA/PLA, (d) 4BzD-8PLLA-8PDA/PLA and (e) mPEI-PLLA-PDA/PLA.
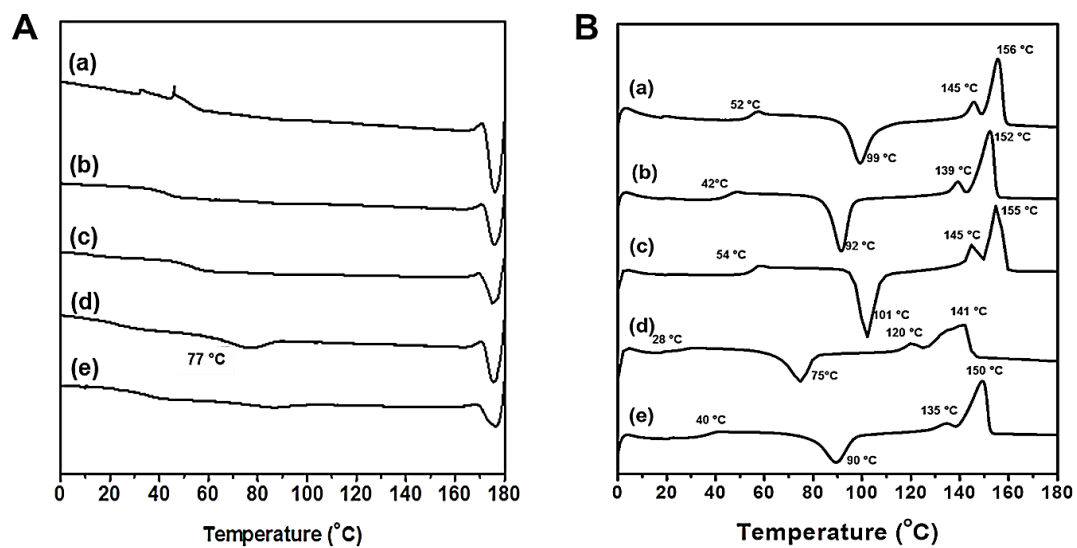
Figure B8. DSC thermogram of film (a) PDA/PLA, (b) PLLA-PDA/PLA, (c) 4PLLA-4PDA/PLA, (d) 4BzD-8PLLA-8PDA/PLA and (e) mPEI-PLLA-PDA/PLA at (A) cooling scan and (B) second heating scan.

CHAPTER V
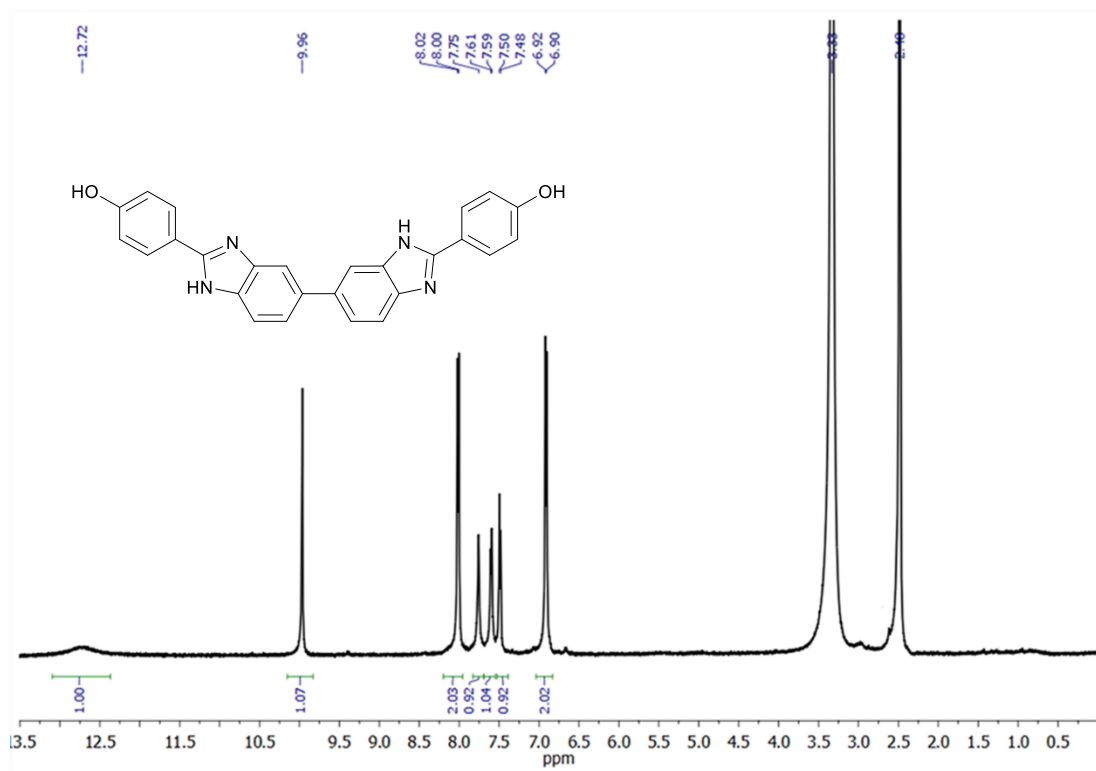
Figure C1. ^{1}H NMR of **b-Bm**.
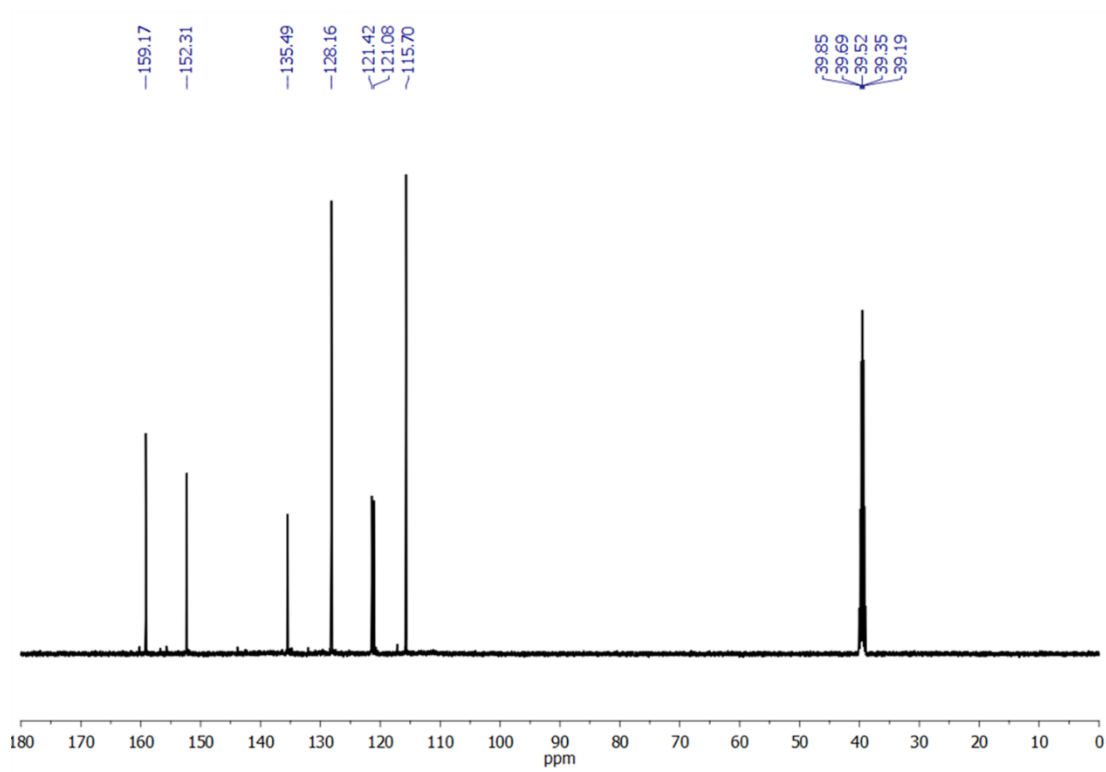
Figure C2. ^{13}C NMR of **b-Bm**.
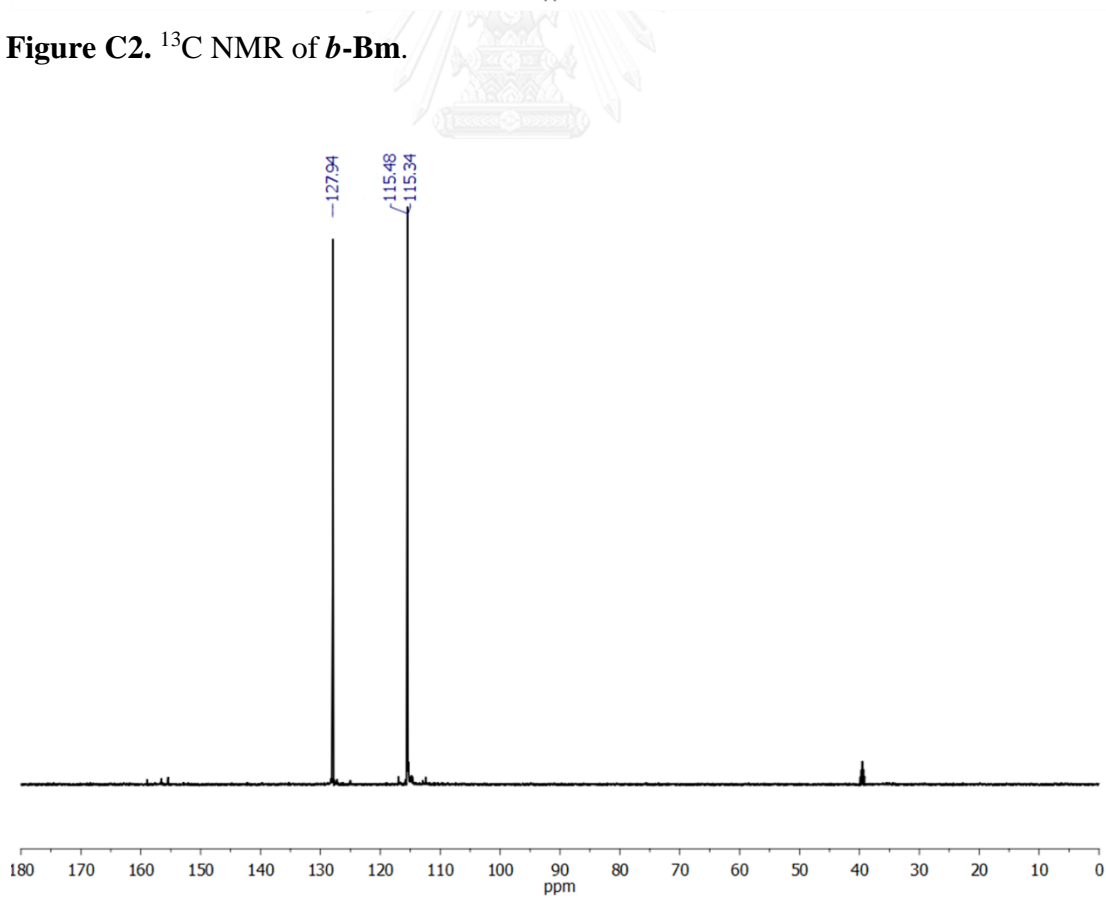
Figure C3. DEPT 90 of **b-Bm**.
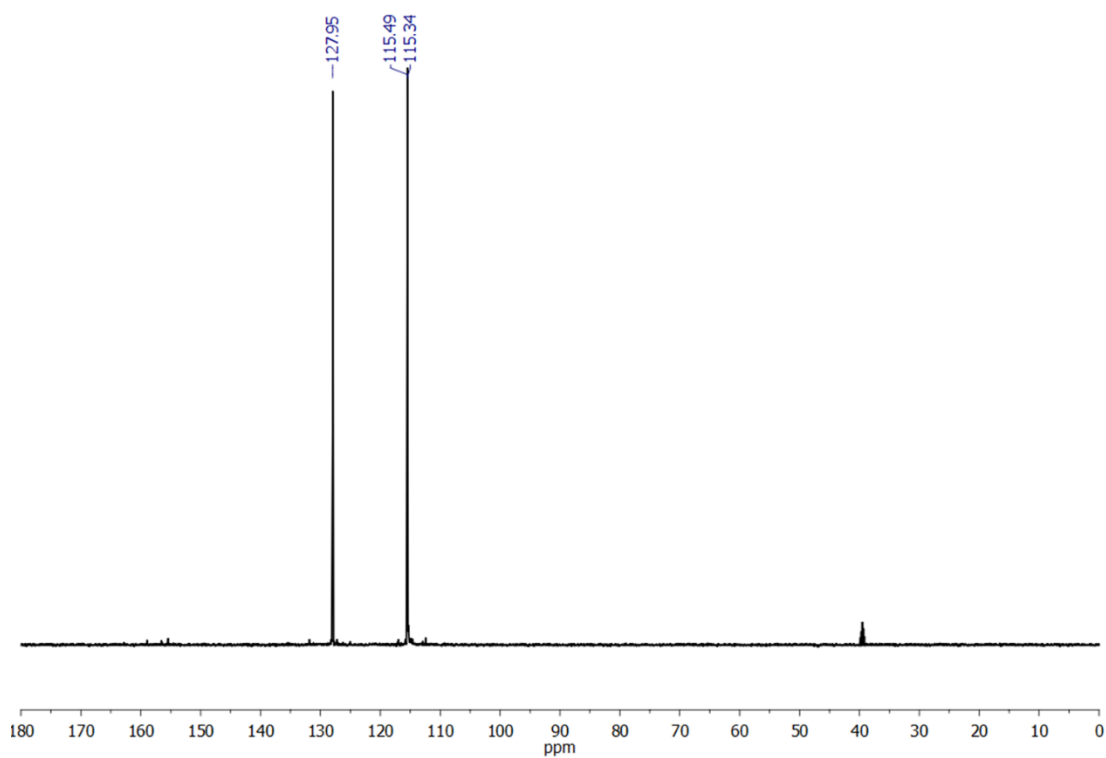
Figure C4. DEPT 135 of *b*-**Bm**.
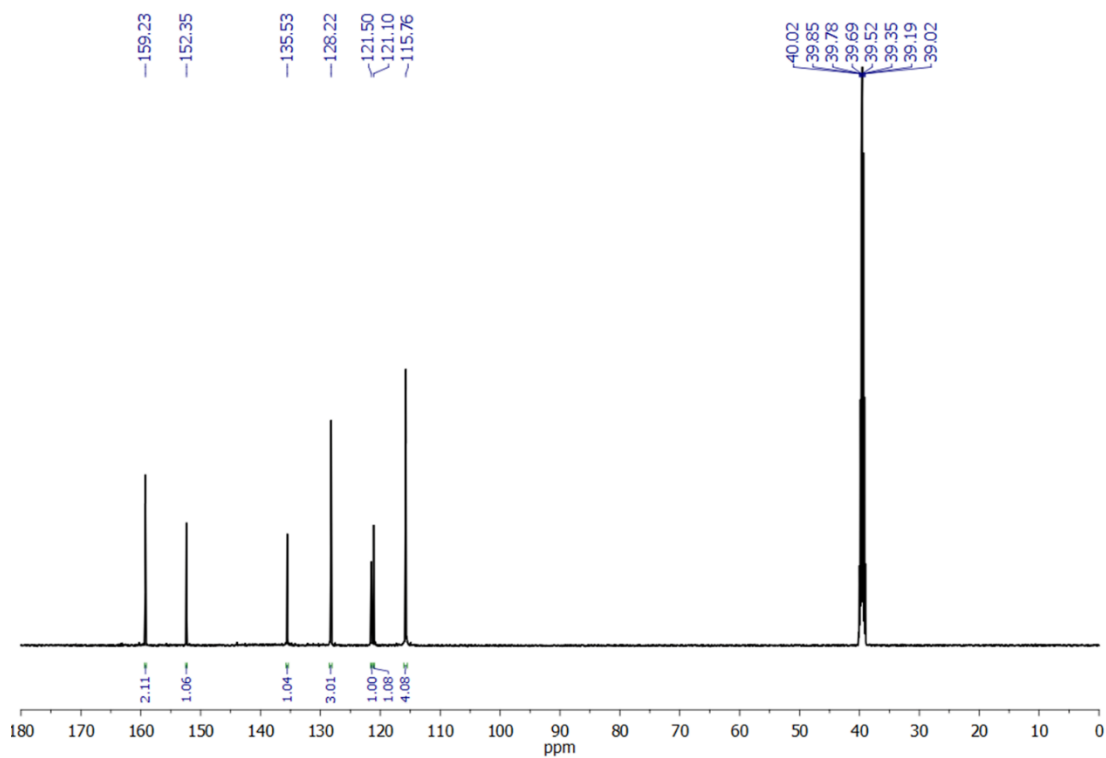
Figure C5. Quantitative ^{13}C NMR of *b*-**Bm**.
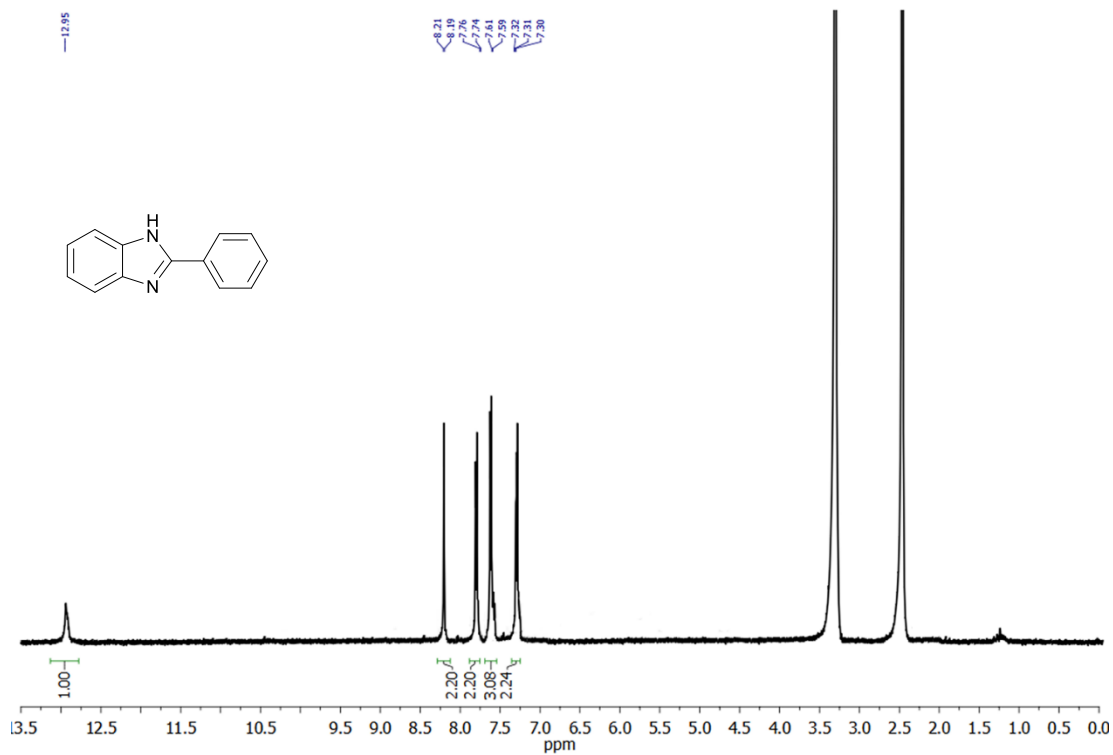
Figure C6. ^{1}H NMR of **Bm1**.
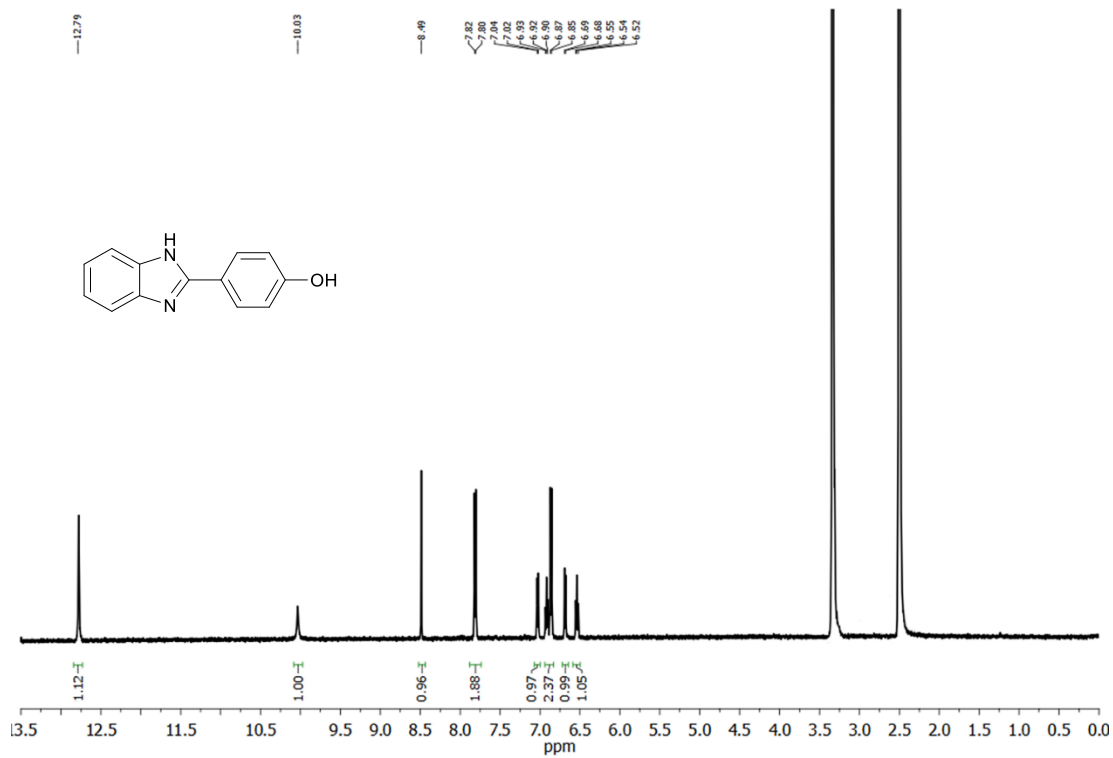
Figure C7. ^{1}H NMR of **Bm2**.
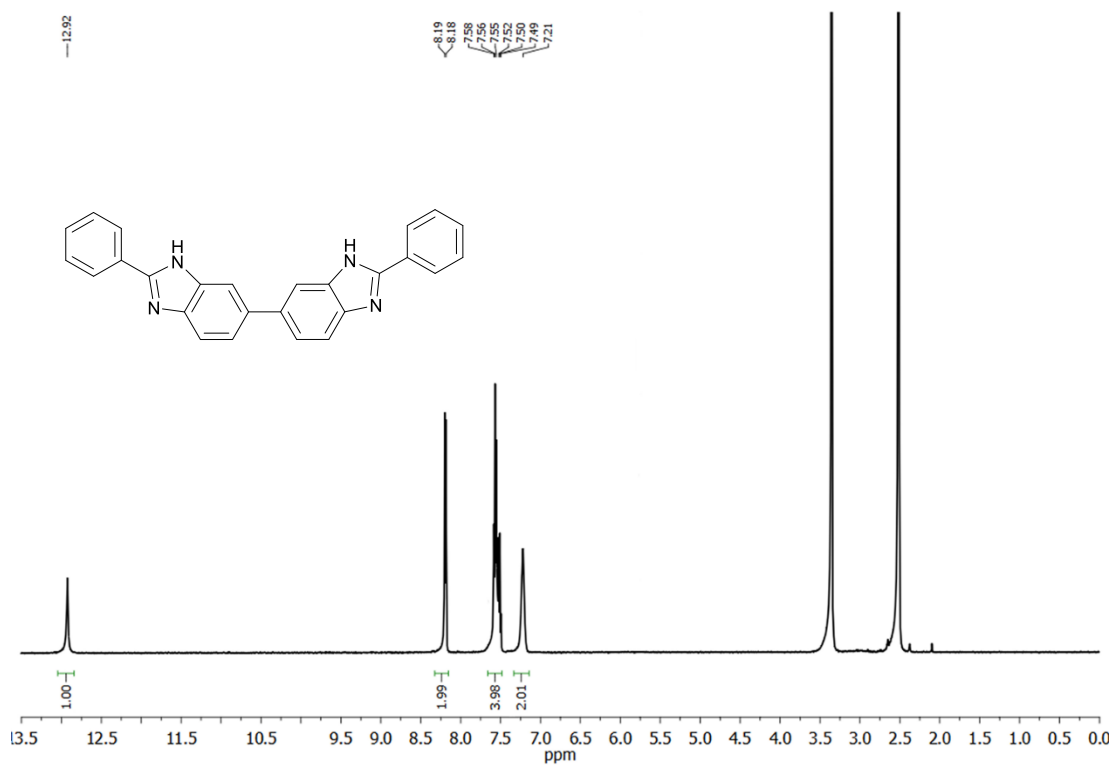
Figure C8. ^{1}H NMR of **Bm3**.
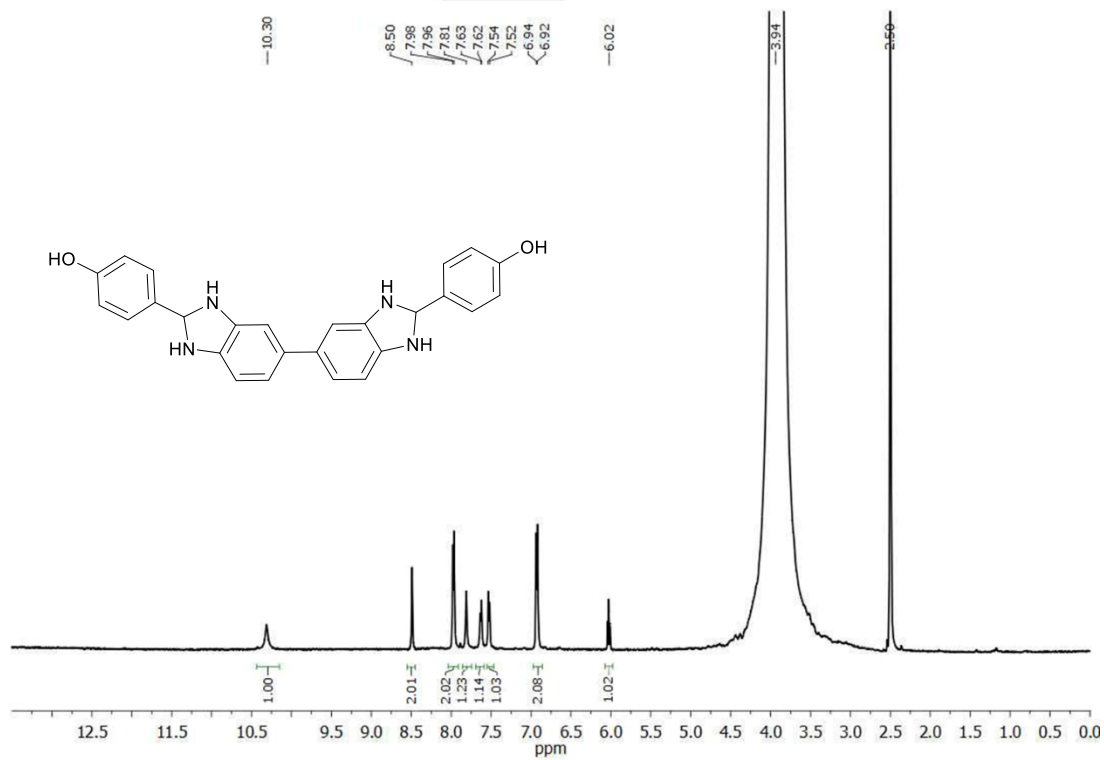
Figure C9. ^{1}H NMR of **Imz**.
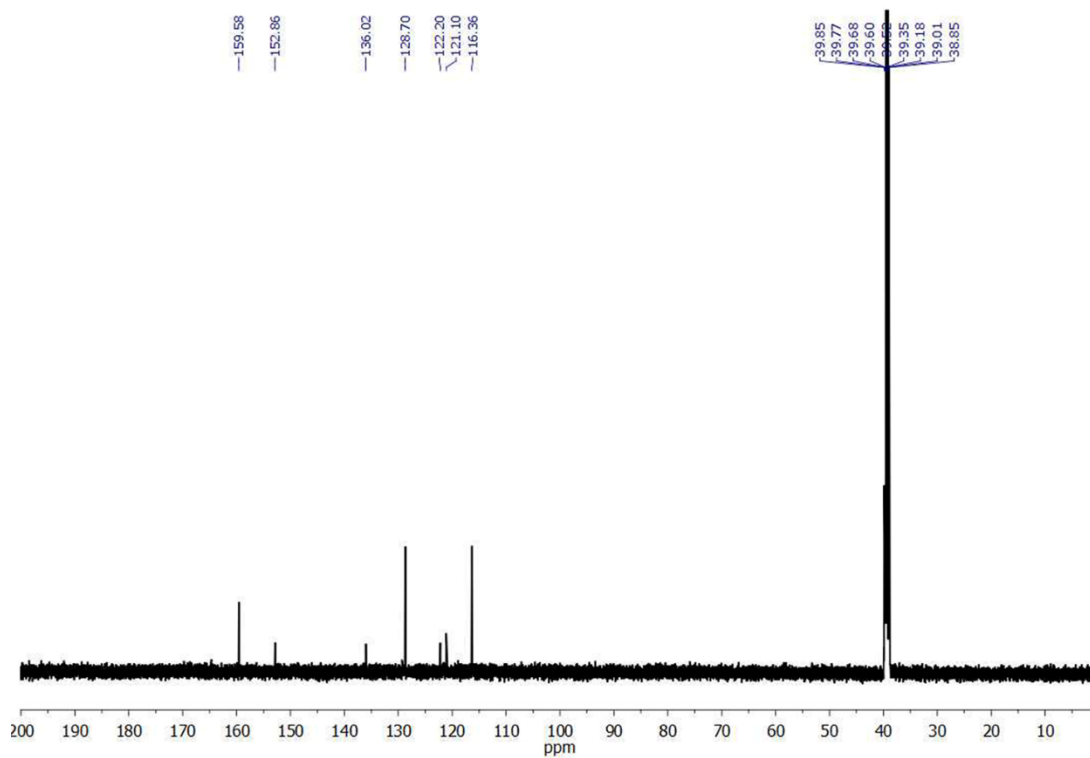
Figure C10. ^{13}C NMR of **Imz**.
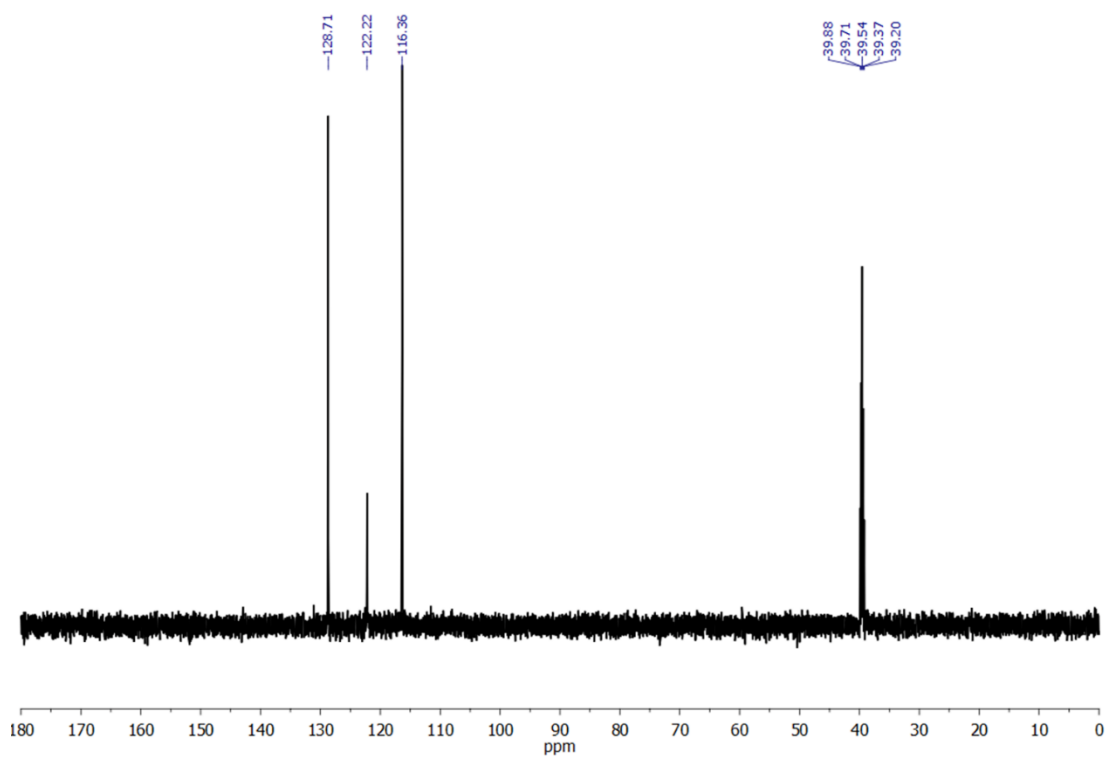
Figure C11. DEPT 90 NMR of **Imz**.
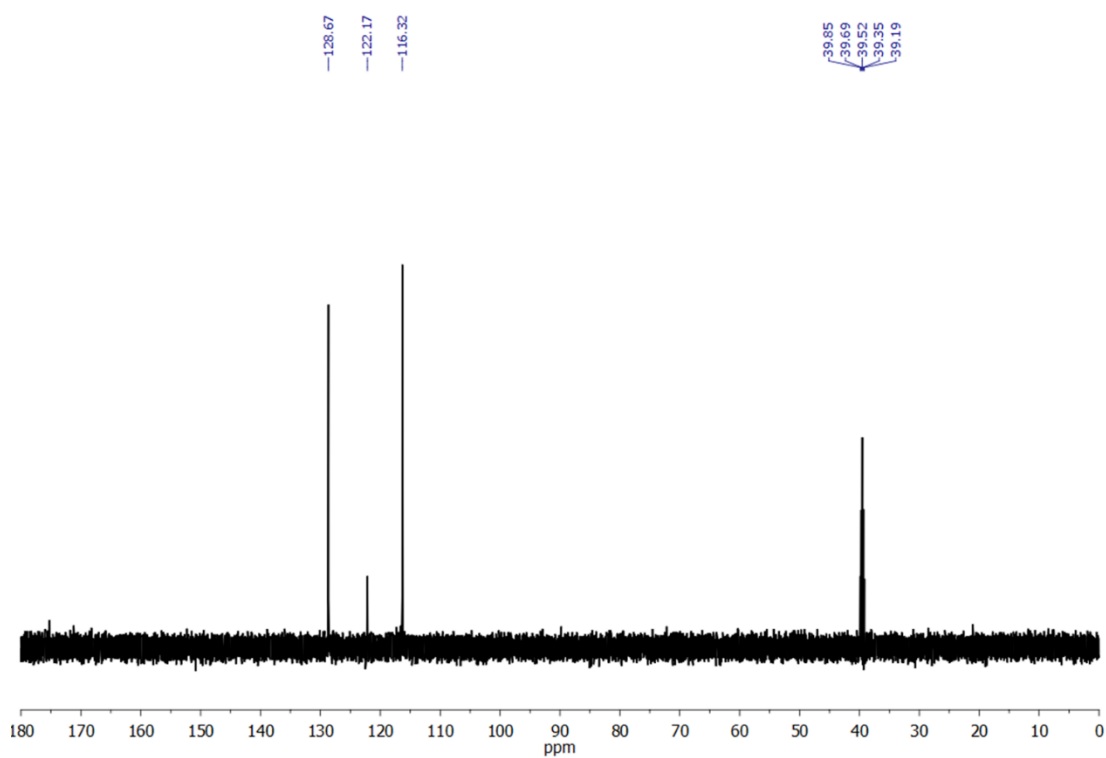
Figure C12. DEPT 135 NMR of **Imz**.
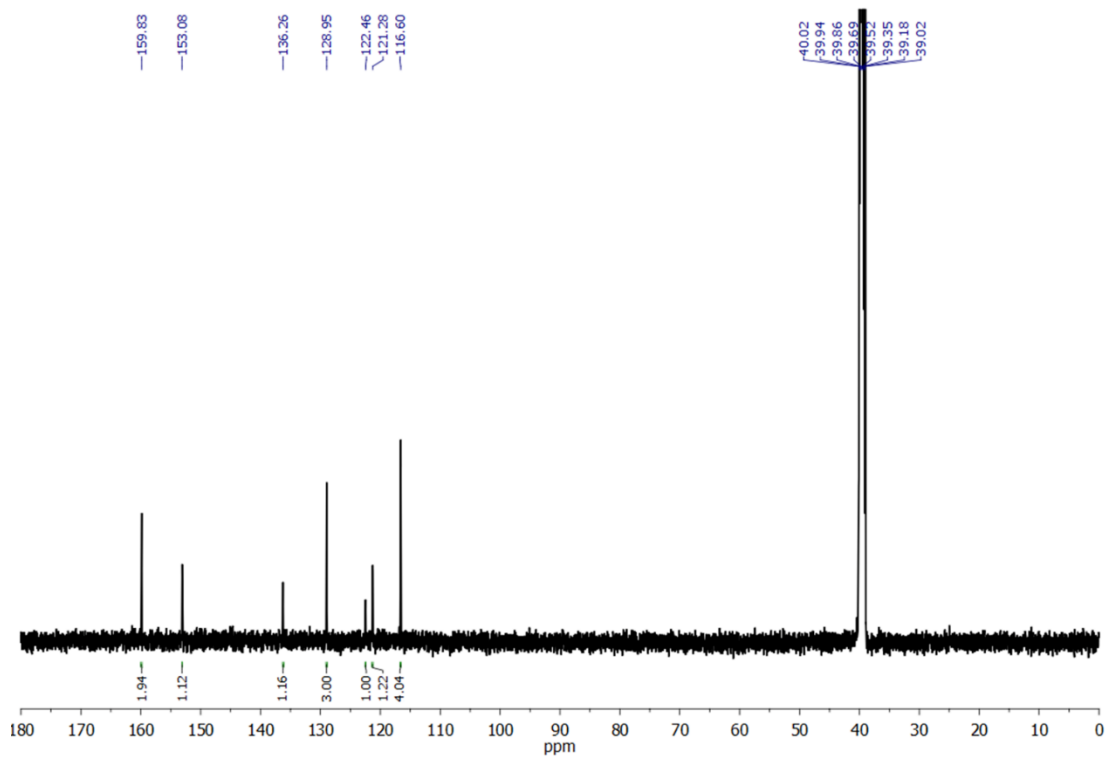
Figure C13. Quatitative ^{13}C NMR of **Imz**.
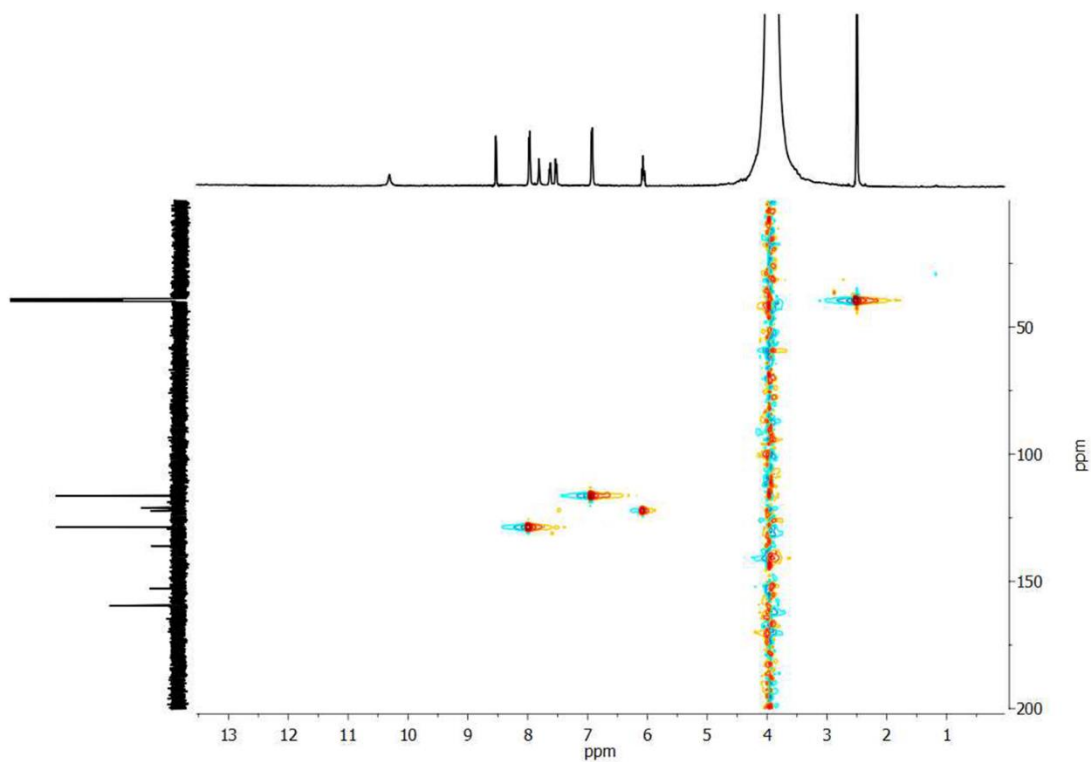
Figure C14. HSQC NMR of **Imz**.
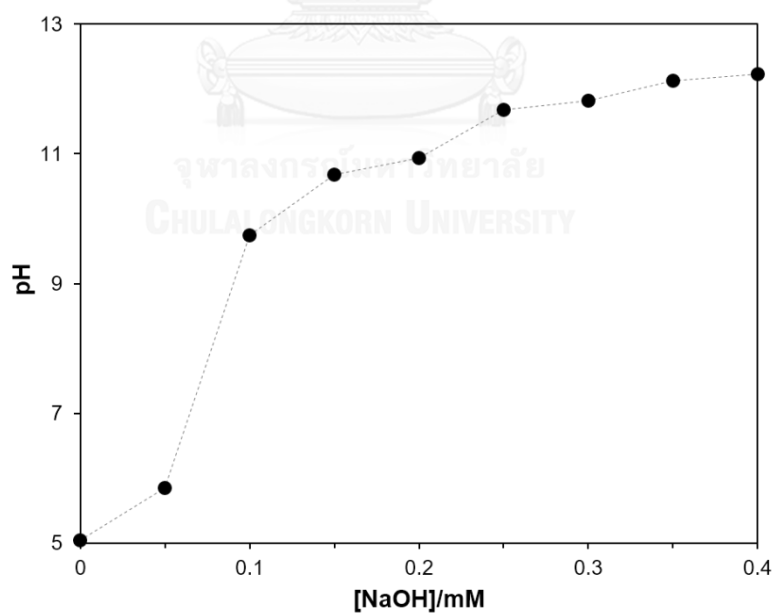
Figure C15. pH measurement of 0.1 mM **BmBz-1** with mole equivalent of NaOH.
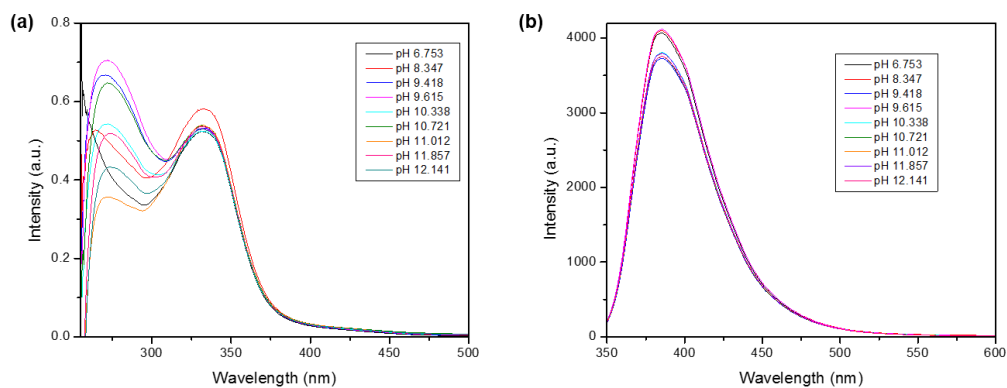
Figure C16. UV-Vis spectra and Fluorescent spectra of *b*-**Bm** upon addition of NaOH.
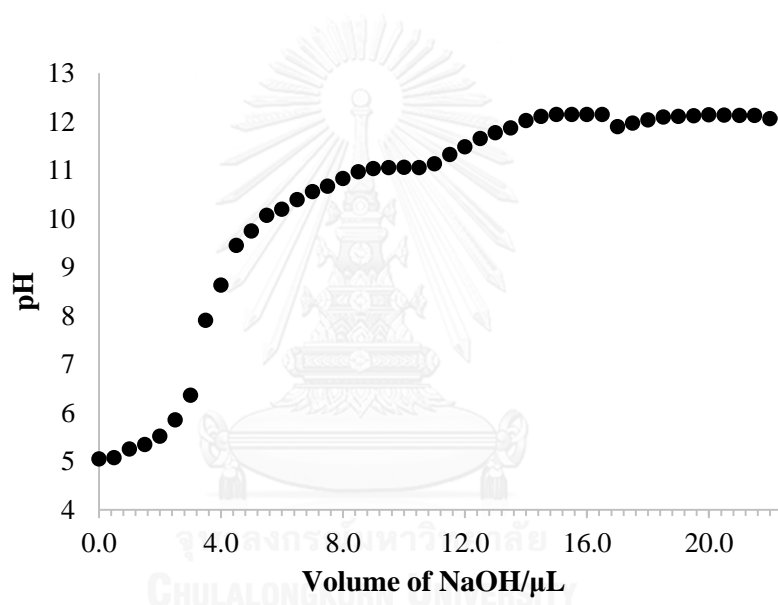

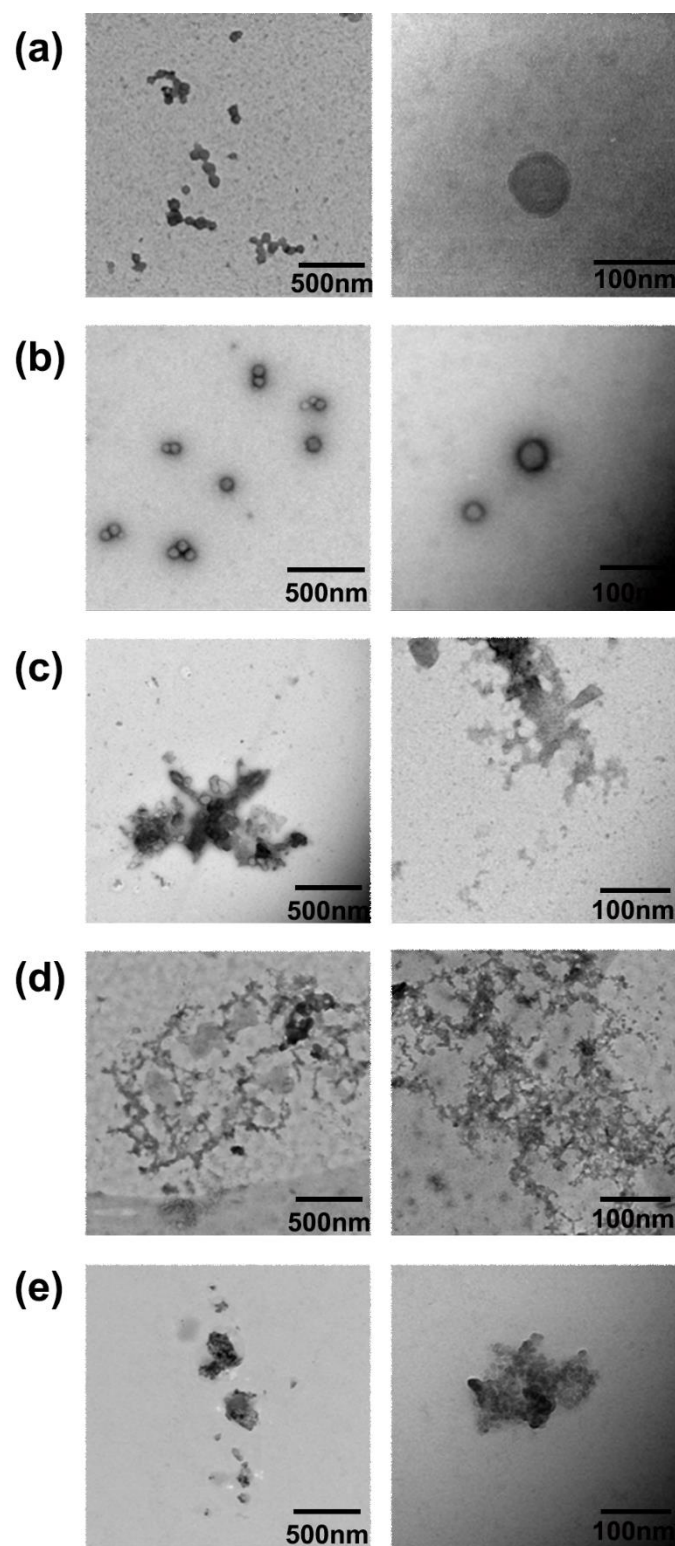**Figure C17.** pH titration curve of **BmBz-1** solution.

Figure C18. TEM micrographs of **BmBz-1** at (a) 0, (b) 1, (c) 2, (d) 3, and (e) 4 equivalent mole of NaOH.

VITA

Name: Ms.Choltirosn Sutapin

Gender: Female

Date of birth: November 7, 1986

Nationality: Thai

Telephone: +66809954192

E-mail: beoy_722@hotmail.com

Education:

2011 – 2016   Ph.D. candidate of Nano Science and Technology (Internatinal Program) Graduate School Chulalongkorn University, Bangkok, Thailand. (Dissertation: Development of supramolecular structured benzoxazine dimers and their potential applications)

2009 – 2010   Full time graduate of International Master's Degree of Science, Department of Polymer, The Petroleum and Petrochemical College, Chulalongkron University, Bangkok, Thailand. (Thesis: Development of star-shaped benzoxazine supramolecular)

2005 – 2008   Bachelor's Degree of Science, Department of Chemistry, Chiangmai University, Chiangmai, Thailand

Publications:

1.   Sutapin C., Mantranon, N. and and Chirachanchai, S. Eight-armed Polydiacetylene under Benzoxazine Dimer Branched Polylactide: A Structural Combination for Reversible Thermochromic Effect and Its Model Case for Free Standing Poly(lactic acid) Film, Journal of Materials Chemistry C 2017.

2.   Sutapin, C., and Chirachanchai, S. Cyclization through Aldehyde and Phenylenediamine under Pressure: a Convenient, Environmentally Friendly, and Simple Procedure for Benzimidazole Precursors (In submission).

3.   Sutapin, C., Bonnet, F., Zinck, P., and Chirachanchai S. Dual functions of N,N-bis(2-hydroxybenzyl)alkylamine as Initiator and Ligand for Lactide Ring-opening Polymerization (In preparation).